

Solar PV Plant Model Validation for Grid Integration Studies

by

Sachin Soni

A Thesis Presented in Partial Fulfillment  
of the Requirements for the Degree  
Master of Science

Approved April 2014 by the  
Graduate Supervisory Committee:

George G. Karady, Chair  
John Undrill  
Vijay Vittal

ARIZONA STATE UNIVERSITY

May 2014

## ABSTRACT

With the increased penetration of solar PV, it has become considerable for the system planners and operators to recognize the impact of PV plant on the power system stability and reliable operation of grid. This enforced the development of adequate PV system models for grid planning and interconnection studies. Western Electricity Coordinating Council (WECC) Renewable Energy Modeling Task Force has developed generator/converter, electrical controller and plant controller modules to represent positive sequence solar PV plant model for grid interconnection studies.

This work performs the validation of these PV plant models against the field measured data. Sheer purpose of this validation effort is to authenticate model accuracy and their capability to represent dynamics of a solar PV plant. Both steady state and dynamic models of PV plant are discussed in this work. An algorithm to fine tune and determine the electrical controller and plant controller module gains is developed. Controller gains as obtained from proposed algorithm is used in PV plant dynamic simulation model. Model is simulated for a capacitor bank switching event and simulated plant response is then compared with field measured data.

Validation results demonstrate that, the proposed algorithm is performing well to determine controller gains within the region of interest. Also, it concluded that developed PV plant models are adequate enough to capture PV plant dynamics.

## ACKNOWLEDGMENTS

I would like to express my profound gratitude to my research adviser Dr. George G. Karady for advising me and for the direction he has lent to this project. His expertise and insight have been influential in performing this research work. His teaching and work ethics are an inspiration. He has given me ample freedom during the entire Master tenure and it helped me in developing independent thinking ability. I would also like to thank the members of my supervisory committee, Dr. John Undrill and Dr. Vijay Vittal for their support.

I am very grateful to First Solar Inc., Tempe for providing me an opportunity to perform this research work. I appreciate the contribution of Vladimir Chadliev, Mahesh Morjaria and Dmitriy Anichkov at First Solar Inc. towards this research, especially Vladimir Chadliev, without his kind help, this work could not have been done successfully.

My sincere thanks also go to Abraham Ellis at Sandia National Laboratory, Albuquerque, New Mexico who continuously evaluated my work and gave directions and technical advice whenever I was in need. I would like to thank Juan Sanchez Gasca at General Electric Company and Western Electricity Coordinating Council Renewable Energy Modeling Task Force for providing me the solar plant model beta version to complete this work. I am also obliged to my parents and family members for their motivation, support and continuous encouragement throughout my research. Without you, I could not have gone that far.

## TABLE OF CONTENTS

	Page
LIST OF FIGURES .....	viii
LIST OF TABLES .....	xii
CHAPTER	
Chapter 1 .....	1
INTRODUCTION .....	1
Chapter 2 .....	5
LITERATURE REVIEW .....	5
2.1. Roadmap for PV Model Development .....	5
2.2. Mitigation Strategy for Controller Tuning.....	15
2.3. Summary .....	19
2.4. Objectives and Major Work.....	19
Chapter 3 .....	21
PV PLANT LOAD FLOW MODELING.....	21
Introduction.....	21
3.1. General Description of Solar PV System.....	21
3.2. Representation of PV Systems in Bulk System Studies .....	28
3.3. Single Machine Equivalencing Methodology.....	31
3.4. General Overview and Assumptions .....	32
3.4.1. Equivalent impedance for a group of inverters.....	32

CHAPTER	Page
3.4.2. Shunt representation.....	35
3.4.3. Pad-mounted transformer representation.....	36
3.5. Multiple Machine Representation.....	36
3.6. Case Study 1 – Comparison between Reduced Order and Full Scale Models in Multi-Machine Power System.....	37
3.7. Case Study 2 – PV Plant VAr Capability with Inverters.....	45
3.7.1. Transmission Line (Gen-tie).....	46
3.7.2. Main Step-up Transformer.....	46
3.7.3. Solar Inverters and Pad-mounted transformers.....	47
3.7.4. Capacitor Bank Sizing.....	47
3.7.5. Lagging Generation Condition.....	48
Conclusions.....	56
Chapter 4.....	58
PV PLANT DYNAMIC MODELING.....	58
Introduction.....	58
4.1. First Generation PV Plant Dynamic Model.....	59
4.1.1. Full Converter Generator / Converter Model (PV1G).....	59
4.1.2. Converter Control model (PV1E).....	61
4.2. Converter Control Modes.....	64

CHAPTER	Page
4.2.1. Reactive Power Control Mode.....	64
4.2.2 Power Factor Control Mode.....	64
4.2.3. Plant Level Reactive Compensation .....	65
4.2.4. Voltage Control Emulation for Plant Level Reactive Compensation Mode.....	65
4.3. Second Generation PV Plant Dynamic Models .....	66
4.3.1. Renewable Energy Generator Converter Model (REGC_A).....	67
4.3.2. Renewable Energy Electrical Controller Model (REEC_B) .....	68
4.3.2.1. Local Active Power Control (included in REEC_B model).....	68
4.3.2.2. Local Reactive Power Control (included in REEC_B model).....	68
4.3.3. Renewable Energy Plant controller model (REPC_A model).....	70
4.4. Active and Reactive Power Control Modes.....	71
4.5. Case Study – Validation of First and Second Generation Generic Models.....	72
4.5.1. System Description .....	72
Conclusions.....	78
Chapter 5.....	79
PROPOSED ALGORITHM AND ITS VALIDATION.....	79
Introduction.....	79
5.1. Performance Estimation of PI Controller .....	80
5.2. Linearization of REGC_A Model.....	80

CHAPTER	Page
5.3. Linearization of REEC_B Model.....	81
5.4. Linearization of REPC_A Model.....	83
5.5. Complete Structure of Solar PV plant Q-Controller.....	84
5.6. Overview of Particle Swarm Optimization (PSO) Technique.....	84
5.6.1. Parameter Selection .....	87
5.6.2. Fitness Function Definition.....	89
5.6.3. PSO flowchart to determine controller gain values .....	90
5.7. Algorithm for Proposed ZN-PSO Method.....	91
5.7.1. STEP A (Setting up GE PSLF model).....	91
5.7.2. STEP B (Finding Voltage Regulator Gains in REEC_B model).....	92
5.7.3. STEP C (Finding Q-Regulator Gains in REEC_B model).....	92
5.7.4. STEP D (Finding Power Plant Controller PPC Gains in REPC_A model).....	93
5.8.1. Case Study 1 – REEC_B model controller gain tuning with proposed algorithm.....	93
5.8.2. Case Study 2 – REPC_A model validation against field measured data.....	109
Conclusions.....	112
Chapter 6.....	113
CONCLUSIONS AND FUTURE WORK.....	113
Conclusions.....	113
Future work.....	113

CHAPTER	Page
REFERENCES .....	114
APPENDIX	
APPENDIX-A	
FIRST GENERATION MODEL DYNAMIC DATA FOR CASE STUDY .....	118
SECOND GENERATION MODEL DYNAMICS DATA FOR CASE STUDY .....	120
PSLF MODEL LOAD FLOW DATA FOR CASE STUDY IN SECTION 4.5 .....	122
APPENDIX-B	
MATLAB SUBROUTINE TO CONVERT GEN-TIE DATA TO PER UNIT .....	124
APPENDIX-C	
MATLAB SUBROUTINE FOR ZNPSO ALGORITHM .....	126
SUBROUTINE FOR FITNESS FUNCTION EVALUATION .....	131
APPENDIX-D	
REGC_A AND REEC_B MODEL PARAMETERS .....	133



## LIST OF FIGURES

Figure	Page
Fig. 2.1. PSO Search Process.....	17
Fig. 3.1. IV and PV characteristics of parallel connected strings at 1000 W/m <sup>2</sup> and T=45°C ....	23
Fig. 3.2. IV and PV characteristics of parallel connected strings at 500 W/m <sup>2</sup> and T=45°C .....	24
Fig. 3.3. IV and PV characteristics of parallel connected strings at 200 W/m <sup>2</sup> and T=45°C .....	24
Fig. 3.4. IV and PV characteristics under case 4 condition .....	25
Fig. 3.5. Grid connected three phase PV inverter topology [25] .....	26
Fig. 3.6. Generalized representation of PV plant medium voltage system [25] .....	28
Fig. 3.7. Single machine representation of solar PV plant [25] .....	30
Fig. 3.8. Daisy chain configuration of inverters and pad-mounted transformers .....	32
Fig. 3.9. Equivalent model representation .....	33
Fig. 3.10. Equivalent model of collector system line capacitance.....	35
Fig. 3.11. Medium and high voltage schematic of PV plant.....	38
Fig. 3.12. IEEE 39 bus test system [43].....	40
Fig. 3.13. PSLF model for IEEE 39 bus system with PV plant connected at bus 29 [43] .....	41
Fig. 3.14. Single machine equivalent model response to disturbance event.....	43
Fig. 3.15. Two machine equivalent model response to disturbance event .....	43
Fig. 3.16. Five machine equivalent model response to disturbance event.....	44
Fig. 3.17. Full scale model response to disturbance event.....	44
Fig. 3.18. Voltage response measured at POI bus .....	45
Fig. 3.19. Plant reactive power capability at POI at 0.95 p.u. voltage.....	55
Fig. 3.20. Plant reactive power capability at POI at 1.00 p.u. voltage.....	55

Figure	Page
Fig. 3.21. Plant reactive power capability at POI at 1.05 p.u. voltage.....	56
Fig. 4.1. PV1G model block diagram [26].....	59
Fig. 4.2. PV1E model block diagram [26].....	61
Fig. 4.3. Reactive Power Control Mode .....	64
Fig. 4.4. Power Factor Control Mode .....	65
Fig. 4.5. Plant Level Reactive Compensation Mode .....	65
Fig. 4.6. Voltage Control Emulation for Plant Level Reactive Compensation Mode .....	66
Fig. 4.7. Overall Model Structure for Central Station PV System [26].....	67
Fig. 4.8. REGC_A Model Block Diagram [26].....	67
Fig. 4.9. REEC_B Model Block Diagram [26].....	69
Fig. 4.10. REPC_A Model Block Diagram [26].....	70
Fig. 4.11. Voltage response of all three test models to 9-cycles LLLG fault .....	76
Fig. 4.12. Active power at inverter terminals .....	77
Fig. 4.13. Reactive power response at inverter terminals .....	77
Fig. 5.1. PV plant generator model in MATLAB Simulink .....	81
Fig. 5.2. Simplified REGC_A and REEC_B with local V and Q-control loops .....	82
Fig. 5.3. Plant model with REEC_B block in MATLAB Simulink .....	83
Fig. 5.4. Simplified REPC_A Q-Control model block diagram .....	83
Fig. 5.5. Plant model with REPC_A block in MATLAB Simulink .....	84
Fig. 5.6. Simplified overall solar PV plant Q-Control model block diagram .....	84
Fig. 5.7. General Concept of modification of search point by PSO .....	85
Fig. 5.8. Algorithm for PSO method.....	90

Figure	Page
Fig. 5.9. Work flow model of proposed methodology.....	91
Fig. 5.10. WTGM V1 model validation process.....	94
Fig. 5.11. WTGMV model validation using user-written inverter model .....	96
Fig. 5.12. ZN-PSO method to find V and Q-controller gains in REEC_B model.....	96
Fig. 5.13. PSLF load flow model of PV plant under test.....	97
Fig. 5.14. Voltage support during grid fault according to grid codes .....	98
Fig. 5.15. Dynamic data input parameters of EPCL model .....	98
Fig. 5.16. Voltage at inverter terminal in response to 18cycles LLLG grid fault.....	99
Fig. 5.17. Active Power at inverter terminal in response to 18cycles LLLG grid fault .....	99
Fig. 5.18. Reactive power at inverter terminal in response to 18cycles LLLG grid fault .....	100
Fig. 5.19. Measured and optimized response for EPCL model in WTGMV tool .....	100
Fig. 5.20. WTGMV parameters input window with EPCL model variables.....	101
Fig. 5.21. Dynamic data input parameters for WECC generic format .....	102
Fig. 5.22. Reactive power output at different Kvp gains .....	103
Fig. 5.23. Search process in two-dimensional Kqp-Kqi solution space .....	104
Fig. 5.24. PV plant step response at different Kqp and Kqi gains.....	105
Fig. 5.25. Different Kqp and Kqi gains at any iteration .....	105
Fig. 5.26. Voltage dips at inverter terminals during LLLG fault at POI .....	107
Fig. 5.27. Reactive power contribution to support voltage during LLLG fault at POI .....	107
Fig. 5.28. Active power dip during LLLG fault at POI.....	108
Fig. 5.29. Swarm trajectory and movement in Kp and Ki search space .....	109
Fig. 5.30. Commanded reactive power (Qcmd) – field test vs. simulation .....	111

Figure

Page

Fig. 5.31. Inverter reactive power contribution during 12 MVar capacitor engagement test... 111

## LIST OF TABLES

Table	Page
Table 1. Electrical characteristics of STP 245-20/Wd.....	22
Table 2. Temperature characteristics of STP245-20/Wd.....	23
Table 3. IEEE 1547 protection threshold <sup>‡</sup> .....	27
Table 4. Inverter and pad-mounted transformer equivalencing.....	39
Table 5. Collector System Equivalence impedance.....	39
Table 6. Steady State Parameters Measured at POI.....	42
Table 7. Plant Gen-tie Data.....	46
Table 8. Inverter specifications.....	47
Table 9. Medium Voltage pad-mounted transformer specifications .....	47
Table 10. Load flow study results with voltage at POI = 0.95 per unit (Lagging p.f. case).....	49
Table 11. Load flow study results with voltage at POI = 0.95 per unit (Leading p.f. case) .....	50
Table 12. Load flow study results with voltage at POI = 1.00 per unit (Lagging p.f. case).....	51
Table 13. Load flow study results with voltage at POI = 1.00 per unit (Leading p.f. case).....	52
Table 14. Load flow study results with voltage at POI = 1.05 per unit (Lagging p.f. case).....	53
Table 15. Load flow study results with voltage at POI = 1.05 per unit (Leading p.f. case) .....	54
Table 16. PV1G variables description .....	60
Table 17. PV1E variables description.....	62
Table 18. Active Power Control Options.....	71
Table 19. Reactive Power Control Options .....	71
Table 20. Inverter and pad mounted transformer data.....	73
Table 21. Station step-up transformer data.....	73
Table 22. Collection system equivalent impedance.....	74

Table	Page
Table 23. Gen-tie positive sequence Impedance data in p.u. on 100 MVA and 500 kV base.....	74
Table 24. Parameter values for PV1G and REGC_A for model simulation .....	74
Table 25. Parameter values for PV1E and REEC_B in simulation model .....	75
Table 26. ZN controller gain calculation table .....	92
Table 27. Estimated optimal gain values for using WTGMV tool .....	102
Table 28. PSO parameter settings .....	103
Table 29. Time domain performance criteria measures.....	104
Table 30. Estimated optimal gain values using ZNPSO method.....	106
Table 31. Estimated optimal gain values by WTGMV and ZNPSO method .....	108

## **Chapter 1**

### **INTRODUCTION**

Photovoltaic (PV) electric power generation has been proven a significant source of energy for harnessing the power available from Sun. To achieve higher level of penetration of renewable energy, US Department of Energy (DOE) has targeted 20% of electricity from renewable sources by 2030. Federal and state governments have set their portfolios of energy production capacity by means of solar energy.

Power system is a complex network of thousands of buses with generators, transformers, transmission lines, compensating devices, and other auxiliary equipment's required to assure its safe and reliable operation. The overall system thus consists of multiple generating sources and several layers of transmission networks. This provides a high degree of structural redundancy that enables the system to withstand unusual contingencies without service disruption to the consumers. Power system planners and operators require wide-ranging data analysis and computer model simulation to understand; the behavior of complex power system under contingency situations to avoid cascaded outages and; to evaluate the ability of power system to withstand such events. Computer simulation helps system planners and/or operators to develop strategies to mitigate the potential problem. The response obtained from the model simulation studies indicates the vulnerability of the system against the potential power system threats. In general a system model is needed to reasonably represent the actual equipment performance in simulations.

With the increased penetration of solar PV, it has become considerable for the system planners and operators to recognize the impact of PV plant on the stability and reliable operation of grid. This enforces the development of adequate PV system models for grid planning and

interconnection studies. Western Electricity Coordinating Council's (WECC) task force on modeling on renewable energy, also called Renewable Energy Modeling Task Force (REMTF) gives the specifications for the development of generic PV system positive-sequence dynamic model for use in bulk system dynamic simulations in accordance with North American Electric Reliability Corporation (NERC) Modeling and Data Analysis (MOD) standards. NREC MOD standards states that "the generic model shall be non-proprietary, shall provide a reasonably good representation of dynamic electrical performance of solar photovoltaic power plants at the point of interconnection with the bulk electric system, and not necessarily within the solar PV power plant itself". As a technical specification and limitation to model development, it is recommended by NERC that- "models shall be suitable for studying system response to electrical disturbances, not solar irradiance transients and electrical disturbances of interest are primarily balanced transmission grid faults (external to the solar PV power plant), typically 3 - 9 cycles in duration". As a member of WECC, First Solar shared this responsibility with Sandia National Laboratory, Albuquerque to validate these generic models.

Development of generic PV plant model and its controllers is still in evolving phase. For the development of generic PV plant model WECC working groups, as a starting point, propose the use of Type 4 Wind Turbine Generator (WTG) model for the grid side structure as both PV plant and Wind Power Plant (WPP) uses a converter interface to the power grid. Like WPP, large PV plants are also spread over a large area with several PV units that interface with the AC system through numerous identical inverters. Inverters are then aggregated and injected into the transmission system at a single point. This representation is considered adequate for positive sequence transient stability simulations at the bulk system level. However, there are some limitations to this representation; with this model it is not possible to analyze the disturbances



within the local collector grid. It is assumed that power outputs of all inverters will be the same at a given instant of time. It is assumed that all PV arrays receives uniform solar irradiation and have similar array orientation shading and array temperature.

WECC data preparation manual states that “single generating units 10 MVA or higher or aggregated capacity of 20 MVA connected to the transmission system (60kV and above) through a step-up transformer(s) should be modeled as distinct generators in WECC base cases”. It also states that “collector-based system such as wind or solar plants connected to the transmission grid may be represented as an equivalent generator, low voltage to intermediate voltage transformer, equivalent collector circuit, and transformer”. WECC proposed single machine equivalent load flow model would be used for PV plant modeling. PV plant model must meet the performance criteria, such as voltage regulation, reactive power control and under-voltage tripping. Interconnection requirements and performance standards addressing reactive power capability from large PV systems are still evolving.

A general description of model for the proposed study needs two parts: plant part such as modeling PV arrays, PV inverters, filters and grid utility; and the control part which includes algorithms such as Maximum-Power-Point-Tracking (MPPT) to adjust the PV output voltage for maximum power point tracing, phase-locked loop (PLL) to detect the grid voltage for d-q axis transformations and it synchronizes the frequency and phase angle of inverter output current and grid voltage, dc voltage controller, current controller etc. Modeling of local active and reactive plant controller and a plant level controller to allow plant level active and reactive power control as per WECC REMTF recommendations will be the focus of this work. To meet the voltage requirements at the POI, power factor of individual inverters can be adjusted via plant-level reactive controller. Several possible control modes will be analyzed: closed-loop voltage control

to maintain voltage schedule within the reactive power capability of the PV plant, voltage droop control to increase or decrease reactive power output linearly as a function of voltage, power factor control to maintain the power factor at the interconnection point close to a specified level, and reactive power control to maintain reactive power flow within some specified limits.

One of the objectives of this thesis work is to validate these generic models of large scale solar PV plant connected to transmission system at point of interconnection (POI) developed by WECC. In this work, validation is performed by simulating these models for test plants and validating the results against the recorded system events in Supervisory Control and Data Acquisition (SCADA) system. All simulations are performed in General Electric Positive Sequence Load Flow (GE PSLF®) program. A rational agreement between recorded field measurement and simulated results will be the measure of success. Important characteristics that are used to determine reasonable agreement includes general shape of the measured and simulated curves (including magnitude and rate of response), Rise time, overshoot and bandwidth, Dead-bands and delays, Initial and final values. For time domain response studies rapid slope in the simulated response compared with actual plant response must be within 10%. Taking into account the voltage at the point of interconnection, the deviation of the plant model from the actual plant response for active and reactive power must not exceed 10% of the total change in the quantity.

## **Chapter 2**

### **LITERATURE REVIEW**

This chapter gives a comprehensive summary on the previous work that has been done by researchers on the solar photovoltaic (PV) plant modeling and model validation for power system planning studies.

#### **2.1. Roadmap for PV Model Development**

The influx of variable generation technologies, particularly solar generation, into the bulk transmission grid in United States has been significant in this decade. Report on Energy Efficiency & Renewable Energy [1, 2] from US Department of Energy states in its key finding that renewable electricity represented nearly 13% of total installed capacity and more than 12% of total electricity generation in United States in 2011. In 2011, in United States wind and solar photovoltaic (PV) were two of the fastest growing electric generation technologies. Report also concludes that in 2011, cumulative installed solar photovoltaic capacity grew more than 86% from the previous year. Although solar electricity represents a very small part of overall U.S. electricity generation (0.2%), but it has grown by a factor of more than 9 between 2000 and 2011. Same inclination exists in other countries around the world with either rich solar availability or extensive solar policies or both - such as Germany, Spain, Japan, and Italy. This trend will most likely to continue in light of national and state renewable portfolio standards. Thus, there is at present a need for generic, standard and publicly available models for variable generation technologies for the purpose of power system planning studies.

Development of generic model for solar PV plants has been hot topic since 2010, when the North American Electric Reliability Corporation (NERC), Integration of Variable Generation Task Force (IVGTF) Task 1-1 published a report [3] that outlines the need for such generic

models for variable generation technologies such as wind and solar-photovoltaic (PV). The NERC IVGTF Task 1-1 document explains that the term “generic” refers to a model that is standard, public and not specific to any vendor, so that it can be parameterized in order to reasonably emulate the dynamic behavior of a wide range of equipment. Furthermore, the NERC document, as well as working drafts of the documents from Western Electricity Coordinating Council (WECC) Renewable Energy Modeling Task Force (REMTF) and IEC TC88 WG27, explains that the intended usage of these models is primarily for power system stability analysis. Those documents also discuss the range in which these “generic” models are expected to be valid. There are presently two major industry groups working towards the development of generic models for use in power system simulations for solar PV plants – the WECC REMTF and the International Electrotechnical Commission (IEC) Technical Committee (TC) 88, Working Group (WG) 27.

Several papers has been published on solar PV modeling considering variety of issues related to solar PV plants like penetration, grid stability, economic operation, effect of weather and geographical location of PV plant on grid security and stability, power quality, voltage and frequency ride through capability of solar PV plants etc. PV plant model development started with detailed modeling including, PV cell models, DC-to-DC stage, DC-to-AC stages, DC-link capacitor, Phase-locked loop, and grid model represented by a single-phase or a three-phase source based on specific studies.

The development of dynamic models of PV generation has been the subject of only a few scientific publications in last two decades. In [4], O. Wasynczuk and N. Anwah modeled PV inverter using self-commutation for dynamic performance of photovoltaic inverter system while in [5] and [6] inverter is line-commutated. In all these references, the voltage reference signal of

the inverter is assumed to be equal at all times to the value needed to achieve the maximum power point for the current irradiance level. The operation of the Maximum Power Point Tracking (MPPT) controller is therefore not represented in these models. Hence it was decided to develop an empirical model based on experimental results rather than on analytical manipulations.

Most common MPPT techniques are open circuit voltage method, incremental conductance method, ripple-based method and perturb & observe (P&O) method. These MPPT algorithms have been described in the literature [7–9]. D. Kirschen and N. Jenkins et al. [10] first proposed a model of photovoltaic (PV) generation suitable for studying its interactions with the power system in 2004. The model used algebraic and differential equations like classical models of conventional generating units to express the relationship between variables. It used modern software for power system stability analysis [11] to combine discrete time domain model with conventional time models. This model reflected accurately the dynamic behavior of the PV generating unit following small or slow changes in irradiance, sudden large increases and decreases in irradiance, as well as sudden changes in ac grid voltage. During experimental analysis it was concluded that MPPT controller plays a critical role in the dynamic response of the PV system.

M. Piazza and M Pucci, et al. [12] presented a grid-connected PV system where the PV source was replaced by a real time emulator. The PV emulator was based on a DC/DC converter controlled by the pole placement technique according to PV current-voltage characteristics. These characteristics were obtained by an analytical model whose parameters were identified on the basis of an actual PV installation. In the proposed plant model the power conditioning system was given by a boost converter whose control was based on a fuzzified PI regulator. The DC bus

was connected to the grid by a three phase voltage oriented controlled (VOC) active rectifier. The use of the emulator allowed accurate investigation of the whole PV system behavior, in every potential working condition, without the use of a real outdoor installation. This paper presented a novel power conditioning method but, issues related to PV penetration were not discussed.

A. Wandhare and V. Agarwal then proposed control schemes for active and reactive power control to overcome penetration issues [13]. This paper proposed the essential operating modes and control scheme for large capacity, centralized PV-grid systems to overcome these challenges related to penetration. Various control techniques were proposed to achieve full flexibility of operating mode selection by the operator/Load Dispatch Center (LDC) to overcome major PV penetration problems of active power sharing, voltage fluctuation, reactive power support and system instability. A major outcome of this work was that it empowered the operator to deal with these complex PV penetration issues by facilitating precise active power control, reactive power control, AC bus voltage regulation, active power sharing and economical load dispatching. New control philosophy for the boost converter and the voltage source inverter (VSI), which constitutes the conventional PV-grid interface, was proposed under different operating modes. Major and essential modifications in the conventional power and control circuits and need for additional bi-directional control signals were highlighted and incorporated. These advance control features allowed the utility to interface huge capacity PV plants with the power grid and reduce the burden on conventional power plants, without causing system malfunction on account of voltage variation, impact of passing clouds, reactive power demand, intermittent active power, etc.

Another similar paper by H. Choi and V. Agelidis et al. [14] with high gain DC/DC converter was published in 2012. This paper focused on the upcoming challenges on the existing PV plant architectures by requiring power converters with a higher power rating and a higher voltage level at the point of common coupling (PCC), which can lead to higher ratio transformers or more transformation stages to be used for the connection with the electricity grid. This paper proposed a solution to minimize the number of transformation stages or the transformer turns ratio of a grid-connected PV plant without changing the standard configuration of the system. The paper introduced a multistring PV system architecture based on a high voltage gain DC/DC converter. A 1-MW PV plant has been modeled and simulated using MATLAB/Simulink and PLECS block-set in this paper. Model was tested under three different scenarios- constant solar irradiation, fast changing solar irradiation and grid voltage sag condition.

H. Wang et al. [15] discussed about possible impacts of variable PV generation on local grid in terms of grid security, stability and economic operation and power quality, when the installed capacity of PV power plants reaches a comparable order of magnitude to the local grid. The paper discussed about technology of grid-connected inverter that can participate in power dispatching, low-voltage tolerance of grid-connected inverters, PV inverter group control technology, power management and dispatching automation of PV power plant.

Utility-scale PV plants are now being developed and installed for the purpose of wholesale power generation, with maximum capacity ranging from a few MW to a few hundred MW. These larger-scale PV facilities are interconnected to the grid at the transmission level, via dedicated feeders at the distribution voltage level, or sometimes directly connected to ordinary distribution feeders. At the transmission level, it is routinely required that interconnected generation provide grid support functions including voltage regulation and fault ride-through.

Utility customers will not be exposed to an islanding situation if the dedicated feeder is tripped at the substation. The small-scale PV applications are by nature distributed generation (DG), and their interconnection to the grid at the distribution level poses a number of possible challenges.

These challenges and its mitigation plans were well addressed by R. Walling and K. Clark [16] in their paper stating that “it is both practical and desirable to consider inclusion of grid support functionality in utility-scale PV plants; even if that functionality conflicts with IEEE-1547 standards [17] which does not allow distributed generation to regulate grid voltage, and thus does not allow the distributed generator the ability to self-correct voltage variations caused by the inherent power variations of PV”. This research paper addressed three major issues: effect of PV variability on local grid, augmentation of voltage regulation capability with grid connected PV plants and enhancement of grid security in presence of high PV penetration. Discussing about consequences of solar variability, this paper mentioned that with the penetration of many PV plants and small PV installations in a control area, the aggregate PV generation variability is substantially mitigated by geographic dispersion of the PV facilities; as rapid power variations due to cloud passage will not be synchronized over many plants extended over a wide area. Paper conferred that the consequences of either a variable generation source or a variable load have both a local dimension and a different dimension of impact to the power grid control area. The local impact of variable generation (or load) is due to the variations in current, which interact with the impedance of the system, to result in voltage magnitude variations. Voltage phase angle variations also occur, but these generally are relatively inconsequential except in the rare case where there are electro-mechanical oscillations in a nearby synchronous machine. Finally it was concluded that, injection of reactive power can be used to nullify the voltage magnitude variations caused by the variable source. Paper also



described how a plant level control can coordinate the reactive power output of all inverters to regulate the voltage at the point of interconnection to the utility grid, or regulate the voltage of a remote location using line drop compensation. While talking about grid security, a hypothetical future scenario of high PV penetration (about 20%) in the WECC base case was modeled with PV plants sensitive to under-voltage trip threshold set at 0.9 p.u. and a fault sequence was initiated resulting in complete blackout of WECC grid. Other two scenarios with no PV tripping and reduced PV plant sensitivities to under-voltage condition were also modeled and it was concluded that with major PV penetration, the disturbance sensitivity of the inverters could pose a threat to bulk power system security.

To maintain the grid stability due to the huge penetration of photovoltaic power to the grid, much stricter grid codes are being imposed by the energy regulatory bodies. G. Islam and A. Durra et al. [18] in their paper discussed about the detailed PV plant modeling and a novel control strategy by controlling boost converter (MPPT control) was proposed for overvoltage protection of a large scale grid connected photovoltaic system that can help to augment the low voltage ride through capability of PV plant. Study attempt to incorporate DC link over and under voltage protection in the control loop without increasing overall cost of protective device, which was another salient feature of the study.

With all these studies and research led by various researchers, objective was to develop a generic full-featured model to represent a utility scale solar PV plant, fit for load flow as well as dynamic modeling. Since the size of solar PV plant was not limited to 10's of MW but has gone as high as 550 MW in 2012, a model suitable for system planning and system impact studies was demanded by utilities and transmission planners, that can simplify all power electronics included in PV systems and can be incorporated in system planning tools used by system operators and

planners in real time. Interest in positive-sequence power flow and dynamic models has also increased due to both commissioning and interconnection applications, and interest in understanding the possible impacts of high PV penetration levels on grid performance.

In September of 2010, Electric Power Research Institute (EPRI) held a workshop in Charlotte, NC where many of the key organization and individuals involved in this work made presentations on the latest developments and some of the outstanding issues related to modeling of variable generation – primarily focused on wind and solar PV. Presentations were given by ABB, Enernex, EPRI, General Electric (GE), Hydro-Quebec, National Renewable Energy Laboratory (NREL), Siemens PTI and Sandia National Laboratory (SNL). Some of the results presented at that workshop are reported in an IEEE Task Force publication [19, 20].

Solar plant has many similarities to a wind plant that uses full converter wind turbine generators (type 4). Both use a converter interface to the power grid. Both consist of multiple small sources of electrical power that rely on inverters to interface with the AC system and which are aggregated and injected into the transmission system at a single point. Both must meet system performance criteria, such as voltage regulation, reactive power control, and under-voltage tripping. Thus modified version of full-converter model for wind power plant was therefore adopted by WECC REMTF to describe solar plant model, except the drive train which is not present in PV systems [21].

K. Clark and R. Walling from General Electric Inc. proposed one such model in 2011 in their paper [22] to give realistic and correct results when used for bulk system performance studies. This model for solar PV plant was based on full-converter wind turbine model and was implemented in GE Positive Sequence Load flow (PSLF) tool which is widely used in western United States for load flow and dynamic modeling of power plants. The control of active and

reactive power was handled by fast, high bandwidth regulators within the converter controls, and was greatly simplified for simulation of bulk power system dynamic performance. Two device models, a converter model and an electrical control model, were used to construct a solar plant model. The control model include closed loop reactive power controls, and voltage regulation with either a simplified emulator of GE's SunIQ® solar plant supervisory control system or a separate, detailed control model as described in [23]. The control model sends a reactive command to the converter model. Zero-power operation, i.e., the ability to inject or absorb reactive power and regulate voltage at zero real power, was also included. A 10MW solar PV plant model implemented with proposed design was tested for a bolted three-phase fault at 34.5 kV Point of Interconnection (POI).

In 2011, A. Ellis and M. Behnke et al. [24] wrote a classical paper on load flow modeling and dynamic modeling method of solar PV plants connected to grid or distribution level feeder. This paper described advances in power flow and dynamic modeling of PV systems for grid planning studies based on on-going efforts by the Western Electricity Coordinating Council (WECC) Renewable Energy Modeling Task Force (REMTF). The goal of REMTF is to improve the adequacy, availability and accessibility of PV system models for grid planning and interconnection studies. Method proposed in the paper to calculate the collection system impedance (typically 34.5 kV cable) is recommended by WECC for impedance and susceptance calculations of medium voltage collection feeders for solar PV plants and was presented in WECC PV plant power flow modeling guide [25].

In 2012, WECC released a guide for solar PV system dynamic simulation models [26]. This document is intended to serve as a specification for generic solar photovoltaic (PV) system positive-sequence dynamic models to be implemented by software developers and approved by

the WECC Modeling and Validation Workgroup (MVWG) for use in bulk system dynamic simulations in accordance with NERC MOD standards. Two specific dynamic models are included in the scope of this document. The first, a Central Station PV System model, intended to capture the most important dynamic characteristics of large scale (> 10 MW) PV systems with a central Point of Interconnection (POI) at the transmission level. The second, a distributed PV system model, intended to represent an aggregation of smaller, distribution-connected systems that comprise a portion of a composite load that might be modeled at a transmission load bus.

Solar PV model is still under development and testing phase, Electric Power Research Institute (EPRI) along with WECC is working on developing and testing solar PV models for positive sequence load flow and dynamic stability studies. Article on technical update on these models is documented by EPRI [20]. Prior to release of any PV plant model for dynamic study of solar PV plants, plant owner's used to submit user-written EPCL model files written in GE PSLF or Siemens PSSE to WECC data base. Those models are highly based on inverter technology and require specific code to simulate inverter response. These models are no more accepted by WECC. First generation solar PV models named PV1G for generator converter model; PV1E for electrical control model was released in 2012 and are available in GE PSLF 18.1, where PV stands for Photovoltaic and numeric 1 indicates that this is first generation model. Second generation models called Renewable Energy model, REGC\_A for Generator/converter, REEC\_B for Electrical controller and REPC\_A for plant controller are under development for implementation in GE PSLF or Siemens PSSE versions.

To study inverter behavior and centralized plant controller (also known as smart grid interface), REGC\_A, REEC\_B and REPC\_A models are currently under development by WECC for System Impact Studies (SIS) while submitting an interconnection request by local control

area or Independent System Operator's (ISO's). These models need a rigorous tuning of controller gains, time constants, and other control parameters based on plant design. P. Pourbeik from EPRI developed a tool called Wind Turbine Generator Model and Validation (WTGMV 1.0) tool [27] using MATLAB® Simulink to tune REGC\_A and REEC\_B models. This tool was primarily developed to tune wind turbine models, but since the architecture of solar PV model is derived from full-converter type-4 wind machine, therefore same tool is used in practice for solar PV model tuning as well. This tool has a shortcoming that it does not implement an auto-tuning algorithm to find the various proportional-integral (PI) controller gains and time constants. It requires a lot of manual adjustment till the operator hits the right gain values and hence requires a lot of time. Also, for PPC tuning no tool is yet developed.

## **2.2. Mitigation Strategy for Controller Tuning**

The proportional-integral (PI) controllers are widely used in feedback control of industrial processes [28, 29]. PI control algorithm is even used at the lowest level of hierarchical sophisticated control strategies [30]. So the design of PI controller is important to satisfy the need of good robustness and near-optimal performance in industrial processes. Many tuning methods for PI controllers exist with difference in flexibility, complexity, and performance. The widely accepted Ziegler-Nichols (ZN) tuning method [31] is simple and easy-to-use. The Ziegler-Nichols tuning method is a heuristic method of tuning a PID controller. It is performed by setting the integral ( $K_i$ ) and derivative ( $K_d$ ) gains to zero. The proportional gain,  $K_p$  is then increased (from zero) until it reaches the ultimate gain  $K_u$ , at which the output of the control loop oscillates with a constant amplitude.  $K_u$  and the oscillation period  $T_u$  are used to set the P, I, and D gains depending on the type of controller used. But this method fails to work well when the processes are high-order and nonlinear [32]. Many improved and well-known methods

are also available, including the Cohen-Coon (CC) method, the ITSE (Integral of Time weighted Squared Error) optimum, ITAE (Integral of Time and Absolute Error) optimum, the IAE (Integral of Absolute Error) optimum, ISE (Integral of Squared Error) optimum, gain and phase margin design method [33]. The design of PI controllers is considered as a constrained nonlinear optimization problem, because the design objective is to achieve the near-optimal performance subject to a series of constraints.

In order to solve this problem, many researchers introduce different intelligent optimization algorithms into PI controller design, such as Genetic Algorithm (GA) [34], Particle Swarm Optimization [35, 36], and Simulated Annealing [37]. Genetic algorithm (GA) is a heuristic method that belongs to family of evolutionary algorithms (EA). It generates solutions to optimization problems using techniques inspired by natural evolution, such as inheritance, mutation, selection, and crossover. Simulated annealing (SA) is a probabilistic method to find the global optimum of a given function in a large search space. It is often used when the search space is discrete. Some simplify it to an unconstrained single-objective optimization problem by adding a penalty item to the objective function, which needs the careful tuned penalty parameters. Others convert it to a multi-objective optimization problem (MOP), which needs the careful selection of optimum objectives and is more complicated and time-consuming than the single objective optimization. Thus, it is necessary to develop an effective and simple method for tuning PI controllers in the industrial practice.

Particle Swarm Optimization (PSO) is a powerful stochastic evolutionary algorithm that is used to find the global optimum solution in an X-Y search plane.

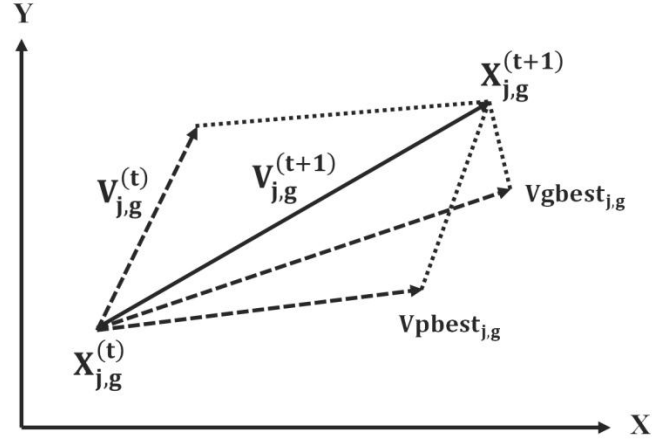


**Fig. 2.1. PSO Search Process**

It solves an optimization problem by iteratively improving a solution. PSO optimizes a problem with the help of a population of candidate solutions, also called particles, and moving these particles around in the search-space according to simple mathematical formulae shown below over the particle's position and velocity.

$$V_{j,g}^{(t+1)} = \omega \cdot V_{j,g}^{(t)} + C_1 \text{rand} (pbest_{j,g} - x_{j,g}^{(t)}) + C_2 \text{rand} (gbest_g - x_{j,g}^{(t)})$$

$$x_{j,g}^{(t+1)} = x_{j,g}^{(t)} + V_{j,g}^{(t+1)} \quad \forall \quad j = 1,2 \dots \dots n \text{ and } g = 1,2 \dots \dots m$$

Where,

$n$  = number of particles in a group &  $m$  = number of members in a particle;

$t$  = number of iterations (generations);

$V_{j,g}^{(t)}$  = velocity of particle  $j$  at iteration  $t$ ,  $V_g^{\min} \leq V_{j,g}^{(t+1)} \leq V_g^{\max}$ ;

$\omega$  = Inertia weight factor;

$C_1, C_2$  = Acceleration constant;

rand = Random number between 0 and 1;

$x_{j,g}^{(t)}$  = Current position of particle  $j$ ;

$pbest_{j,g}$  = personal best of particle  $j$ ;

$gbest_g$  = global best of the group  $g$ .

Z. L. Gaing [38] proposed a novel design method for determining the optimal proportional-integral-derivative (PI) controller parameters of an Automatic Voltage Regulator (AVR) system using the particle swarm optimization (PSO) algorithm. This paper demonstrated in detail how to employ the PSO method to search efficiently the optimal PID controller parameters of an AVR system. Paper compared the proposed approach with the genetic algorithm and had shown superior features, including stable convergence characteristic, and good computational efficiency.

Problem of falling into local optimum in PSO was addressed in [39-40], [39] suggested that if the proportion factor of multi-optimum programming cannot be dynamically adjusted in the optimization process, the performance of the algorithm will be limited. This paper proposed a modified adaptive particle swarm optimization algorithm based on fuzzy and adaptive programming of multi-optimum to adjust proportion factor of multi- optimum programming in the optimization process. In [40] an advanced PSO scheme by adaptively changing parameters was proposed to increase the convergence rate.

An improved particle swarm optimization algorithm (IPSO) applied on optimal reactive power dispatch and voltage control of power systems was proposed by B. Zhao and C. Guo et al. [41] using particles information to control the mutation operation. The proposed IPSO algorithm was also extended to handle mixed variables, such as transformer taps and the reactive power source installation, using a simple scheme.

In order to deal with the time-varying, nonlinear, and large-lagging problems in control process, a self-tuning PID controller with variable parameters based on PSO was proposed in [42]. By finding the relationship between  $K_p$ ,  $K_i$ ,  $K_d$  and the deviation, the s-functions are



written to complete the design of self-tuning PID controller with variable parameters. Then, particle swarm optimization is used for achieving the correction coefficient values of deviation which are sent to the controller so that the control effect is improved.

### **2.3. Summary**

For solar PV plant modeling, efforts placed down by EPRI and WECC [20, 25, and 26] to study inverter behavior and centralized power plant controller resulted in development of second generation plant models derived from full-converter wind models. These models were deemed fit and approved by WECC for positive sequence power system studies. Although these models are under trial and test phase but are widely used in industry for system impact studies, load flow modeling, fault analysis, online and offline operations and planning studies by utilities and ISO's across the nation. To validate these models, tool developed by P. Pourbeik for wind systems WTGMV 1.0 [27] is capable of determining controller gains and time constants for voltage regulator and Q-control loop in REEC\_B and REGC models for solar PV plants as well, but it requires lot of manual efforts because it uses hit-and-trial method to find the controller parameters. Also, it is identified that no tool is available till date to validate the centralized power plant controller model. One reason behind this is the lack of real-time data available from solar industry to tune power plant controller and converter models, as discussed in previous WECC meeting held in March 2013 and June 2013.

### **2.4. Objectives and Major Work**

On the basis of identified areas in system modeling and model validation, following items would be the major objectives of this research work-

- (1) Implementation of correct positive sequence load flow representation of solar PV plant in GE PSLF to compare reduced scale one machine, two machine and five machine

equivalent models with full scale detailed representation. The purpose of this study would be to validate that, an equivalent PV plant load flow model is adequate to study the full plant behavior at grid interconnection point with increased computational efficiency without any loss of significant plant information.

- (2) To validate and support the fact that with inverter reactive power contribution within plant, it is possible to obtain an optimal capacitor bank size to meet the grid interconnection requirements of 0.95 power factor leading and lagging under  $1\pm 0.05$  per unit voltage conditions at plant interconnection point, as mandated by transmission owners/utilities in their control area.
- (3) Comparison of dynamics between user-written inverter models provided by inverter manufacturer with first and second generation generic models developed by WECC to validate their performance under different test scenarios.
- (4) Development of novel auto-tuning algorithm to determine the electrical (REEC\_B) and plant controller (REPC\_A) module controller gains and validate simulation results against the field measured data for a utility scale grid-connected solar PV plant.
- (5) Finally, to identify and report any inadequacies or deviation from expected behavior of these proposed models during test runs to WECC for further review.

## Chapter 3

### PV PLANT LOAD FLOW MODELING

#### Introduction

With the rapid increase in the installation of solar PV generation in United States, specifically in the western states, accurate representation of solar PV plants in both steady and dynamic state for power system stability studies has gained attention of grid researchers. Large scale solar PV plant connected to transmission system is similar in many aspects with a wind power plant that uses full converter wind turbine generators. Both are spread over a large land area consisting of multiple small sources of power interfaced with the AC system through inverters (or power converters), medium voltage transformers, collection system and step-up transformers, and finally connected to grid at a single interconnection point. Like wind power plant, a solar PV plant must meet the grid requirements for interconnect including voltage ride-through, reactive power capability support and frequency response. The Modeling and Validation Work Group (MVWG) of the Western Electricity Coordinating Council (WECC) recently expanded the scope of its Renewable Energy Modeling Task Force (REMTF) to address modeling of PV systems. This chapter includes two case studies- First study focuses on correct positive sequence load flow model representation in GE PSLF to compare the reduced scale solar PV plant models with full scale model representation. Second study validates that with inverter reactive power contribution to grid, an optimal capacitor bank size can be obtained to meet the grid interconnection requirements as mandated by transmission owners/utilities.

#### 3.1. General Description of Solar PV System

In a PV system, the PV array converts solar radiation directly into direct current (DC) electricity. At a given solar irradiance and cell temperature, the current and power output of the

array is a function of terminal voltage. The voltage vs. current characteristic (or IV curve) is nonlinear in nature and is related by (1) – (4).

$$I_o = \frac{I_{sc}}{e^{\left(\frac{V_{oc}}{V_T}\right)} - 1} \quad (1)$$

$$V_T = \frac{aN_s kT}{q} \quad (2)$$

$$R_s = -\left.\frac{dV}{dI}\right|_{V=V_{oc}} - \frac{V_T}{I_{sc}} \quad (3)$$

$$I_{ph} = (I_{ph_{nom}} + K_I \Delta T) \frac{G}{G_{nom}} \quad (4)$$

A circuit model for PV array designed using detailed design equations for SUNTECH 245 W module using datasheet of STP245-20/Wd polycrystalline PV module is calculated [47]. This is a single diode model, however two-diode model is also possible but to limit the complexity a single-diode model is preferred. Detailed electrical characteristics of the module at Standard Test Conditions (STC) are shown in Table 1. At STC Irradiance is 1000 W/m<sup>2</sup>, module temperature is 25°C and Air mass (AM) is 1.5.

**Table 1. Electrical characteristics of STP 245-20/Wd**

STC	STP245-20/Wd
Optimum operating Voltage (Vmp)	30.5 V
Optimum operating Current (Imp)	8.04A
Open Circuit voltage (Voc)	37.3V
Short Circuit Current (Isc)	8.52A
Maximum power at STC (Pmax)	245W
Module Efficiency	15.1%
Operating Module Temperature	-40°C to +85°C
Maximum System Voltage	1000V DC(IEC)/600 VDC (UL)
Maximum Series Fuse Rating	20A
Power Tolerance	0/+5%

Detailed temperature characteristics of the module are shown in Table 2. PV model is designed for Nominal Operating Cell Temperature (NOCT) of 45°C.

**Table 2. Temperature characteristics of STP245-20/Wd**

Nominal Operating Cell Temperature	45±2 °C
Temperature Coefficient of Pmax	-0.44% / °C
Temperature Coefficient of Voc	-0.33% / °C
Temperature Coefficient of Isc	-0.055% / °C

Four different test cases are considered to study the PV and IV characteristics –

Case 1: A constant irradiation intensity of 1000 W/m<sup>2</sup> is assumed for all modules i.e., both strings with 12 panels in each string. Simulation is run at temperature equal to NOCT (45°C).

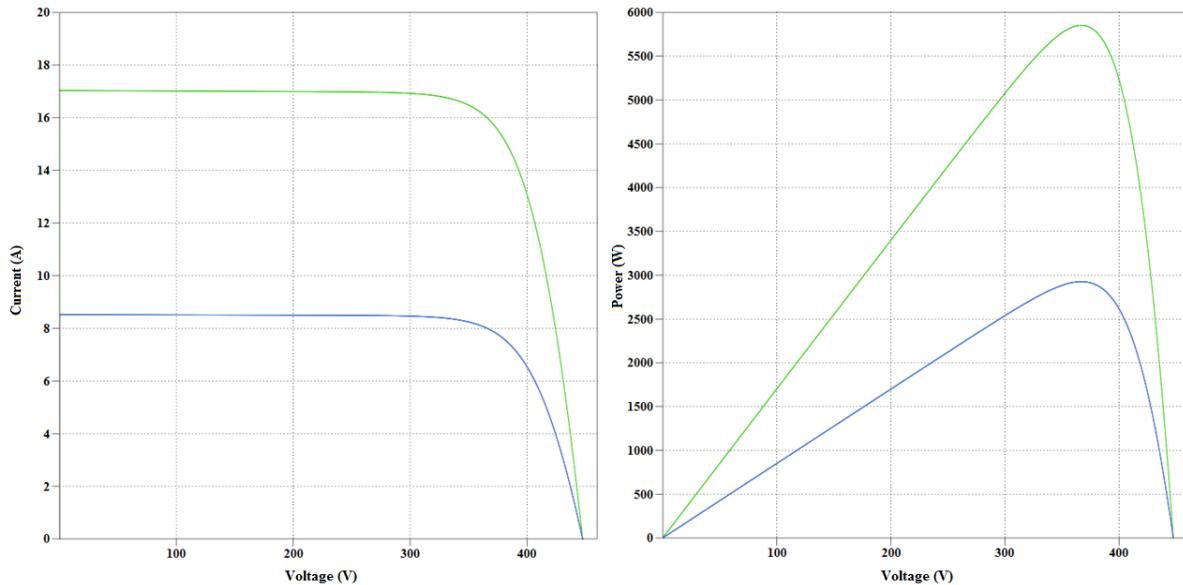


**Fig. 3.1. IV and PV characteristics of parallel connected strings at 1000 W/m<sup>2</sup> and T=45°C**

Case 2: A constant irradiation intensity of 500 W/m<sup>2</sup> is assumed for all modules i.e., both strings with 12 panels in each string. Simulation is run at T= NOCT (45°C).

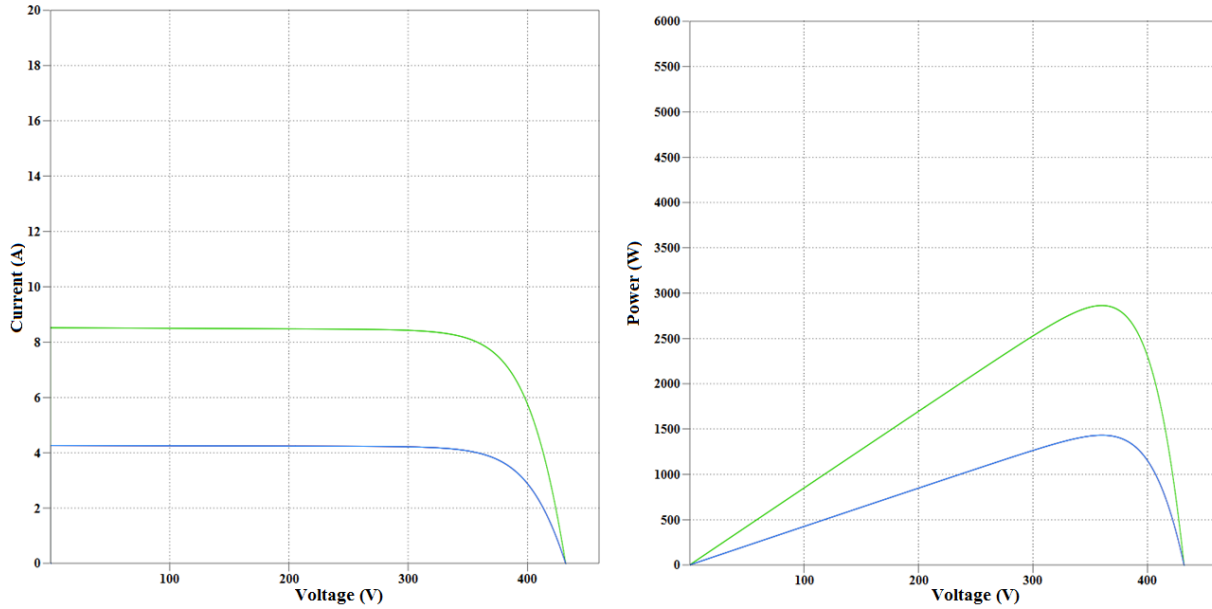


**Fig. 3.2. IV and PV characteristics of parallel connected strings at  $500 \text{ W/m}^2$  and  $T=45^\circ\text{C}$**

Case 3: A constant irradiation intensity of  $200 \text{ W/m}^2$  is assumed for all modules i.e., both strings with 12 panels in each string. Simulation is run at  $T = \text{NOCT}$  ( $45^\circ\text{C}$ ).

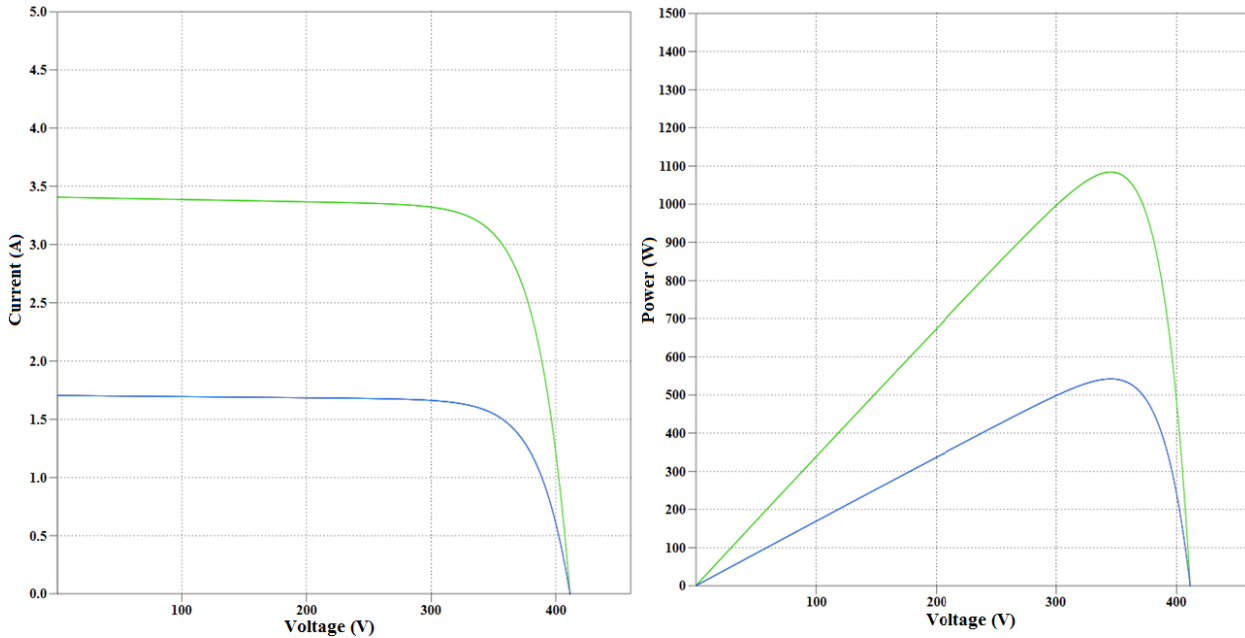


**Fig. 3.3. IV and PV characteristics of parallel connected strings at  $200 \text{ W/m}^2$  and  $T=45^\circ\text{C}$**

Case 4: A constant irradiation intensity of  $500 \text{ W/m}^2$  for 6 modules of string 1 and  $800 \text{ W/m}^2$  for rest of the string 1. For string-2 a constant irradiation of  $1000 \text{ W/m}^2$  is assumed.

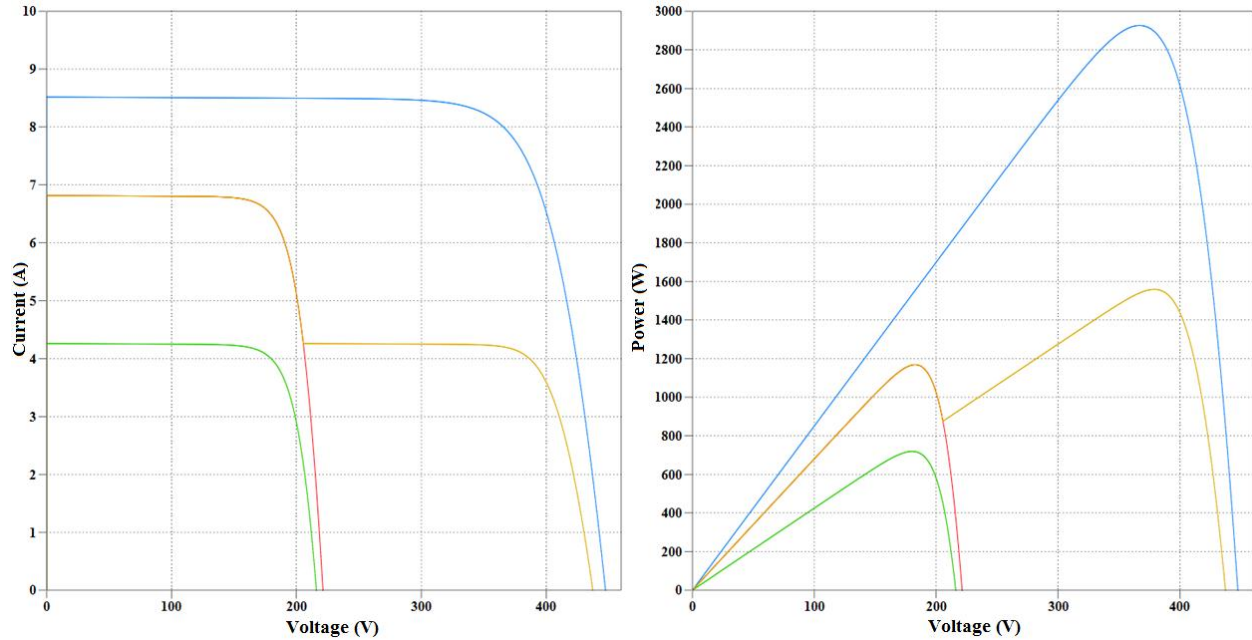


***Fig. 3.4. IV and PV characteristics under case 4 condition***

The maximum power is extracted at a voltage level for a given irradiance level. The available current and power from PV array varies in proportion to the effective irradiance falling on the plane of the PV array as shown in the test cases above. Temperature also affects the performance but it is secondary compared to irradiance, lower operating temperature results in better performance and higher efficiency. Wind speed around the array compensates for cell temperature to some extent. Thus irradiance level, ambient temperature and wind speed affect cell temperature. To maximize energy capture, some PV arrays are mounted on sun-tracking structures. In flat-panel photovoltaic (PV) applications, trackers are used to minimize the angle of incidence between the incoming sunlight and a photovoltaic panel. This increases the amount of energy produced from a fixed amount of installed power generating capacity.

An inverter is used to connect the PV array to an AC network. Fig. 3.5 shows the topology of a specific type of grid connected three phase PV inverter. Control system is embedded with control algorithms which take care of maximum power point tracking and controls the voltage across the DC link capacitor to maintain maximum power tracking point.

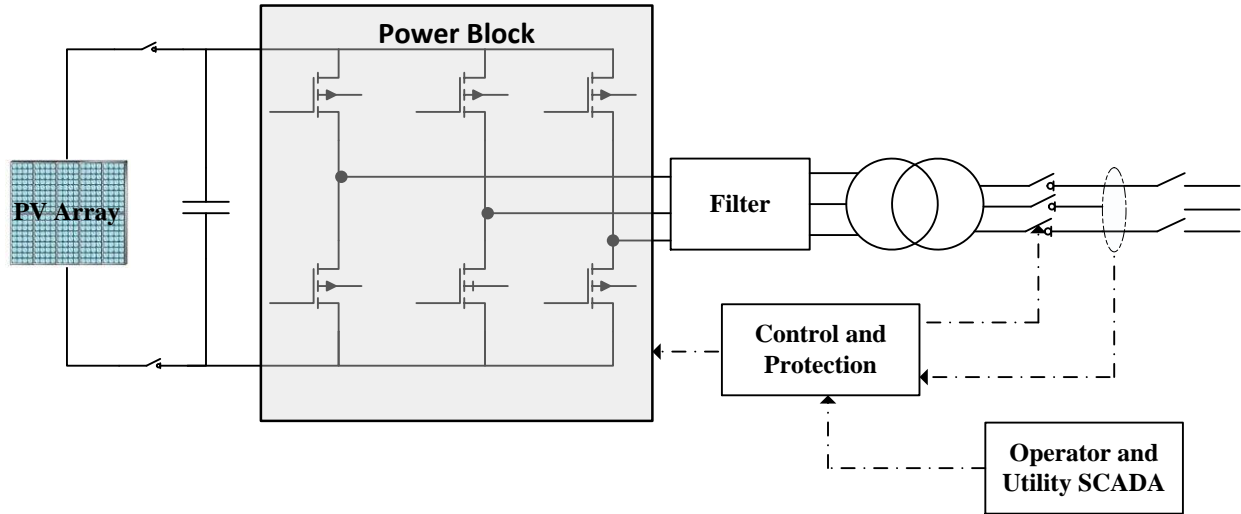


**Fig. 3.5. Grid connected three phase PV inverter topology [25]**

PV inverters are classified as high-frequency, pulse-width modulated, current-regulated devices. They operate to regulate their respective AC output currents in response to a current command through high carrier frequency pulse width modulation (PWM) of the connected DC source. This provides a high fidelity sinusoidal output current waveform that is synchronized to the grid voltage waveform (i.e., it follows the grid frequency). The photovoltaic modules that serve as input sources to the inverters consist of solid state semiconductor cells that produce direct current as a function of the irradiance and voltage to which they are subjected on an essentially instantaneous basis. Thus it is the inverter characteristics and controls that dominate the dynamic behavior of the plant and its interaction with the grid.

During event disturbance within the plant or close to point of interconnect (POI), inverter rapidly regulates ac current magnitude ensuring that current and temperature limits of the switching elements in the power block are not exceeded. Recent advances in the inverter technology have enabled inverters to change power factor within the current magnitude limits. Some inverters are capable of operating with 0.9 power factor limits in both lagging and leading regions at full active power output levels. This improvement contributed to reactive power



support from the inverter apart from static VAR compensation devices in the megawatt level solar PV plants, where a significant amount of reactive power is lost in feeders within the plant itself. With appropriate controls implemented, inverter-based reactive power capability could be used to achieve reactive power control objectives at the plant level. The integrated isolation transformer and LC filter circuit on AC side reduce harmonic injection into the grid and reduce high frequency electromagnetic emissions. Ripple effects on the DC side of inverter are generally reduced by applying additional filtering.

Low voltage and frequency issues are handled by grid converter which monitors the AC voltage and frequency to modulate converter behavior and disconnect the inverter from the grid in case of any such event. The IEEE 1547-2003 [17] standards define voltage and frequency thresholds for residential and commercial PV systems and other distributed energy resources, as shown in Table 3. IEEE 1547 requires that distribution-connected PV inverters also known as Distributed Energy Resource (DER) to de-energize after faults and prior to circuit reclosure. Inverters must “cease to energize” within 2 seconds of the formation of an electrical island (i.e., when a portion of the grid disconnects from the bulk system). This feature is commonly referred to as “anti-islanding”. PV inverters connected to the customer side of the meter are required to have certification that they comply with these and other safety and grid compatibility requirements.

**Table 3. IEEE 1547 protection threshold<sup>‡</sup>**

Voltage Range (% Nominal)	Max. Clearing Time (sec)*	Frequency Range (Hz)	Max. Clearing Time (sec)
$V < 50\%$	0.16	$f > 60.5$	0.16
$50\% \leq V < 88\%$	2.0	$f < 57.0^{**}$	0.16
$110\% < V < 120\%$	1.0	$58.8 < f < 57.0^{***}$	Adjustable (0.16 and 300)
$V \geq 120\%$	0.16		

‡From WECC Load Flow modeling guide for Solar PV plant

\*Maximum clearing time for DER  $\leq 30$  kW; Default clearing times for DER  $> 30$  kW

\*\* 59.3 Hz if DER  $\leq 30$  kW

\*\*\* For DER  $> 30$  kW

### 3.2. Representation of PV Systems in Bulk System Studies

A typical central-station PV plant consists of several individual PV inverters tied to a medium voltage collector system as shown in Fig. 3.6. Inverters are typically integrated with an array of PV modules on DC side, step-up transformers and other balance-of-system (BOS) components.

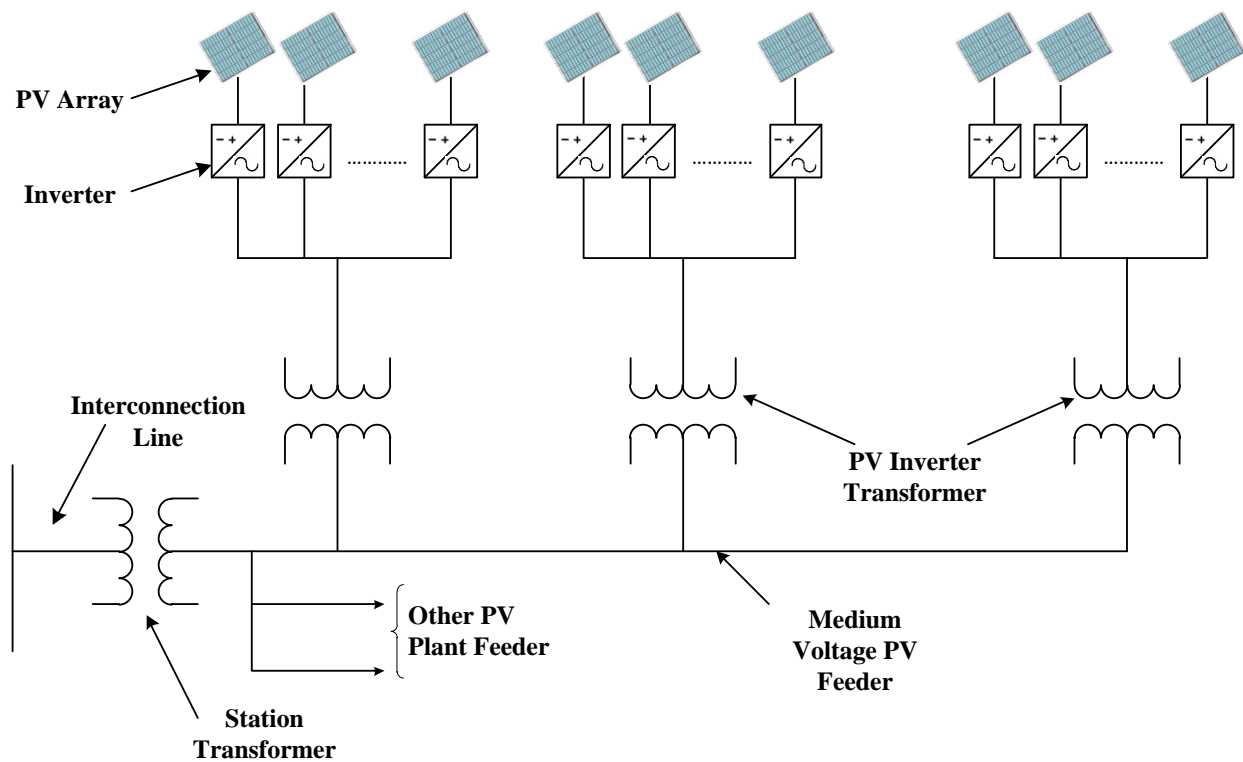


**Fig. 3.6. Generalized representation of PV plant medium voltage system [25]**

Large scale PV power plant typically consists of hundreds of inverters coupled to a single point of interconnection. Full scale modeling of such a large scale system would lead to extensive computational time during power flow and dynamic runs. Therefore it is recommended

by WECC REMTF to use “equivalenced” power flow and dynamics models to reduce data assimilation and computational time in interconnection studies [26]. WECC proposed an equivalent single generation representation of large scale PV plants, in which all converter units and pad-mounted step-up transformers are approximated by connecting them in parallel into a single equivalent large converter and a low voltage to medium voltage step-up transformer. All overhead and underground medium voltage collection system lines are equivalenced by method proposed in [25], and station step-up transformers are represented explicitly. An equivalenced model aggregates the multiple generators (inverters) within the plant into one or more larger generators that are integral multiples of the individual units. Similarly, step-up transformers and collection system feeders are equivalenced in a manner that results in terminal voltages at the equivalenced generators that are near the mean terminal voltages of the individual generators in a full plant model. This is a reasonable approximation in a well-designed plant where the terminal voltages from generator to generator do not vary by more than a few percent. However, certain limitations to this are as follows -

- Local disturbances within the PV plant at medium voltage feeders, on station step-up transformer, or close to VAR compensation device cannot be analyzed.
- Due to huge size of PV plant partial clouding on certain set of arrays is most common phenomenon to occur. Effect of partial clouding and its impact on power output of converters cannot be modeled.

For system impact studies these limitations are acceptable because these studies are typically performed at full plant power output. WECC REMTF recommends the use of the single-machine equivalent model representation shown in Fig. 3.7 to represent a central-station

PV plant in WECC base case. This representation is also considered adequate for positive-sequence transient stability simulations at the bulk system level.

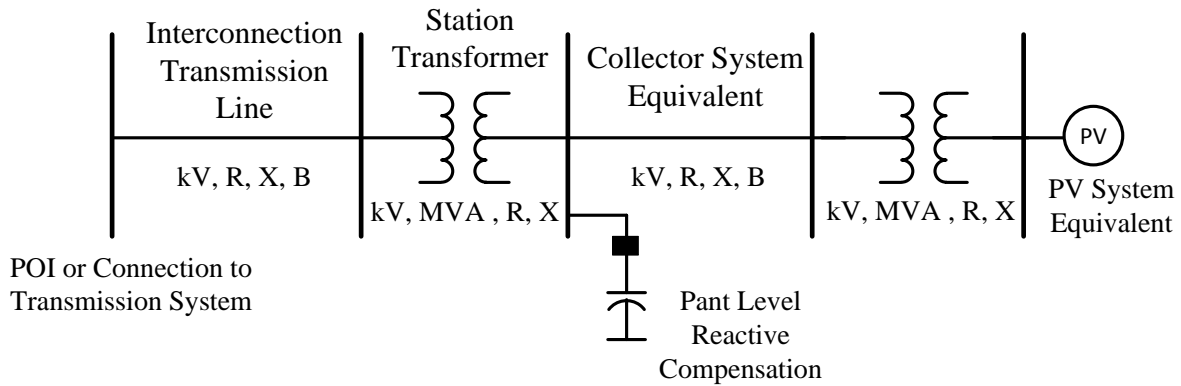


**Fig. 3.7. Single machine representation of solar PV plant [25]**

The Power Plant Controller (PPC) also known as Smart Grid Interface (SGI) if present at a particular plant, works in conjunction with the inverters to achieve the interconnection requirements for reactive power support as specified in a given project's Interconnection Agreement (IA). The PPC continuously monitors the control bus, which is in common practice a POI bus, and generates real and reactive power commands that are communicated to the inverters via the plant's local area communications network. Communications cycle times vary from project to project based upon plant size and location of PPC with respect to individual inverter. Inverters located closer to PPC sees lesser communication lag time compared to inverters at the far end of plant. Communications cycle time are on the order of several seconds. Thus, the PPC is designed to compensate for pseudo steady-state changes in voltage that occur as the result of the plant output power changing over the course of the day, and not for dynamic voltage support during grid faults. Depending on PPC field application and control strategy, it can also control additional reactive devices such as switched capacitors and reactors.

### 3.3. Single Machine Equivalencing Methodology

A typical modern solar power plant consists of hundreds of inverters. An inverter is usually rated at low three phase voltage output (315 V – 690 V). A pad mounted transformer at the inverter AC side step-up the voltage to medium voltage (12 kV – 34.5 kV). To collect the power output from individual inverters, several inverters are connected in a daisy chain to form a group. Several of these groups are finally connected to medium voltage 34.5 kV photovoltaic combiner switchgear (PVCS) bus. These feeders are connected to the substation where the substation transformer steps up the voltage to a desired transmission level from 69 kV to 500 kV depending on interconnection voltage of plant. These plant substations are connected with an interconnection transmission line to a larger substation.

Within a solar PV plant, there are a lot of diversities in the line feeder and the solar irradiance at each set of inverters. Line impedance in the line feeder connecting each inverter group to the POI differs from each other. The solar irradiance experienced by one inverter can be different from another located at another part of the plant, but not significant enough. The diversity of a solar PV plant is a good attribute in many ways. For example, the interaction between PV plant with the grid is determined by the collective behavior of the overall plant. In contrast, a conventional power plant interacts with the grid as a single large generator. During disturbances, a conventional power plant may be disconnected from the grid and it may lead to a cascading effect. On the other hand, a solar PV plant may lose a small percentage of the total generation, depending on the location of each inverter group with respect to the fault origin. All of the components shown in Fig. 3.7 should be represented in a power flow calculation. It is important to understand the significance of compatibility of power flow input data (sav files in PSLF or raw files in PSSE) and the dynamic data file (dyd file in PSLF and dyr files in PSSE).

### 3.4. General Overview and Assumptions

In the following derivation, equivalent circuit is based on apparent power losses. Following assumptions were made to derive general equation for a circuit within solar PV plant-

- The current injection from all inverters is assumed to be identical in magnitude and angle assuming uniform solar irradiance.
- Reactive power generated by the line capacitive shunts is based on the assumption that the voltage at the buses is one per unit.

#### 3.4.1. Equivalent impedance for a group of inverters

To derive the generalized equation for equivalent impedance of collection system for solar PV plant, an example of six PV inverters followed by their respective pad-mounted transformers connected in daisy chain configuration is considered. Fig. 3.8 shows this configuration of PV inverters and connected pad-mounted transformers. First step is to determine the equivalent of this daisy chain network.

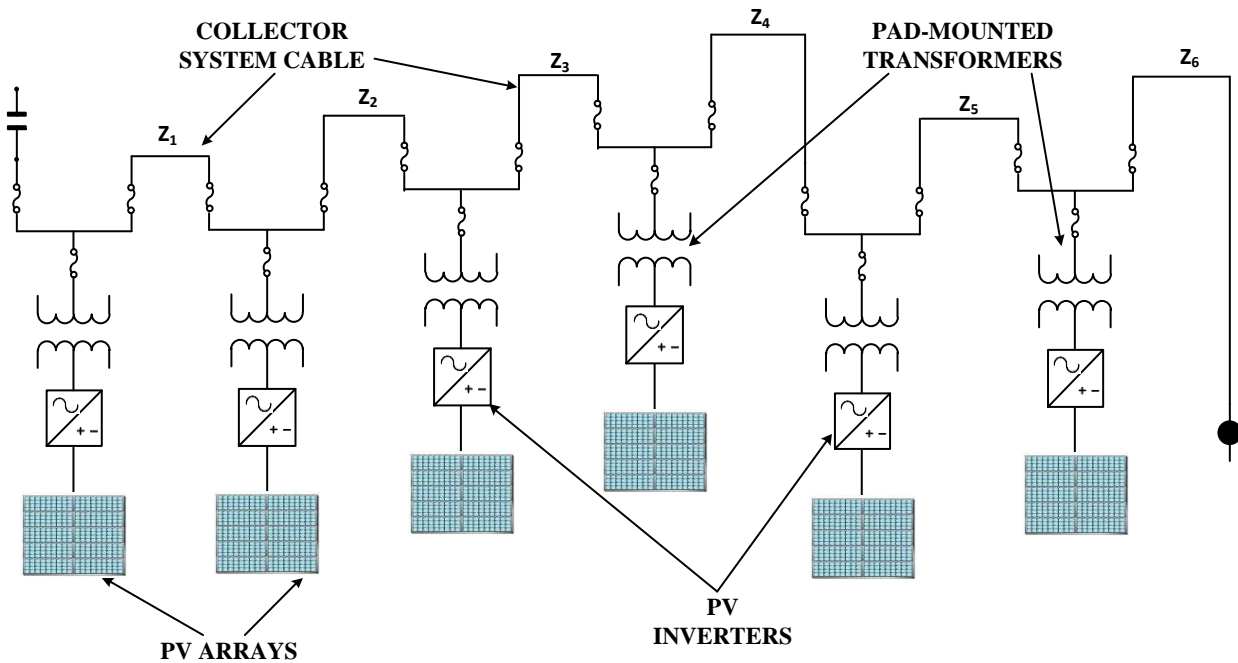


*Fig. 3.8. Daisy chain configuration of inverters and pad-mounted transformers*

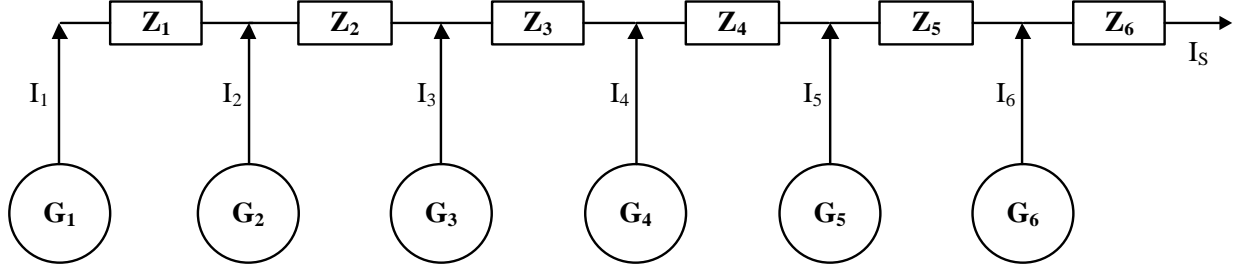


**Fig. 3.9. Equivalent model representation**

Fig. 3.9 is drawn as equivalent of the above shown network where pad-mounted transformer is considered as part of generator itself.

Current flowing out of each inverter unit is a phasor quantity and is represented as -

$$\mathbf{I}_m = I_m \angle \theta_m \quad (5)$$

All phasor quantities are represented in boldface. For example,  $\mathbf{I}_1$  signifies the output current of the inverter unit 1 and,  $I_1$  represents the magnitude and  $\theta_1$  represents angle of  $\mathbf{I}_1$ . Since the irradiation falling on each inverter is assumed similar neglecting solar variability, therefore current output of each inverter is equal. We obtain the following -

$$\mathbf{I}_1 = \mathbf{I}_2 = \mathbf{I}_3 = \mathbf{I}_4 = \mathbf{I}_5 = \mathbf{I}_6 = \mathbf{I} \quad (6)$$

Total current in the equivalent representation can be written as-

$$\mathbf{I}_s = n\mathbf{I} \quad (7)$$

Voltage drop across impedance  $Z_1$  connected to inverter 1 can be written as -

$$\Delta V_{Z_1} = \mathbf{I}_1 Z_1 = \mathbf{I} Z_1 \quad (8)$$

Similarly

$$\Delta V_{Z_2} = (\mathbf{I}_1 + \mathbf{I}_2) Z_2 = 2 \mathbf{I} Z_2 \quad (9)$$

And so on

$$\Delta V_{Z_6} = (\mathbf{I}_1 + \mathbf{I}_2 + \mathbf{I}_3 + \mathbf{I}_4 + \mathbf{I}_5 + \mathbf{I}_6) Z_6 = 6 \mathbf{I} Z_6 \quad (10)$$

The apparent power loss across individual impedance can simply be written as -

$$S_{Z1} = \Delta V_{Z1} I_1^* = I_1 I_1^* Z_1 = I^2 Z_1 \quad (11)$$

$$S_{Z2} = \Delta V_{Z2} I_2^* = (I_1 + I_2)(I_1 + I_2)^* Z_2 = (2I)^2 Z_2 \quad (12)$$

$$S_{Z3} = \Delta V_{Z3} I_3^* = (I_1 + I_2 + I_3)(I_1 + I_2 + I_3)^* Z_3 = (3I)^2 Z_3 \quad (13)$$

$$S_{Z4} = \Delta V_{Z4} I_4^* = (I_1 + I_2 + I_3 + I_4)(I_1 + I_2 + I_3 + I_4)^* Z_4 = (4I)^2 Z_4 \quad (14)$$

$$S_{Z5} = \Delta V_{Z5} I_5^* = (I_1 + I_2 + I_3 + I_4 + I_5)(I_1 + I_2 + I_3 + I_4 + I_5)^* Z_5 = (5I)^2 Z_5 \quad (15)$$

$$S_{Z6} = \Delta V_{Z6} I_6^* = (I_1 + I_2 + I_3 + I_4 + I_5 + I_6)(I_1 + I_2 + I_3 + I_4 + I_5 + I_6)^* Z_6 = (6I)^2 Z_6 \quad (16)$$

Since  $I_s = nI$ , the power loss equation can be simplified as follows -

$$S_{\text{Tot\_loss}} = I^2 (Z_1 + 2^2 Z_2 + 3^2 Z_3 + 4^2 Z_4 + 5^2 Z_5 + 6^2 Z_6) \quad (17)$$

Thus a generalized equation for loss can be written as -

$$S_{\text{Tot\_loss}} = I^2 \sum_{m=1}^n m^2 Z_m \quad (18)$$

Where,

$I$  = output current of a single inverter

$m$  = index

$n$  = number of inverters in a daisy-chain string

The equations for the simplified equivalent circuit can be written as follows -

$$S_{\text{Tot\_loss}} = I_s^2 Z_s \quad (19)$$

$$Z_s = \frac{\sum_{m=1}^n m^2 Z_m}{n^2} \quad (20)$$

Eq. 20 can be expanded further to determine the equivalent impedance of overall medium voltage collection system as -

$$Z_{\text{EQ}} = \frac{\sum_{k=1}^l \sum_{m=1}^{n_k} m^2 Z_m}{n_{\text{inv}}^2} \quad (21)$$

where

$n_k$  = the number of inverters in line  $k$



$m$  = an index of the branch within a line

$k$  = an index of the line considered

$l$  = the total number of lines considered

$n_{inv}$  = number of the inverters considered

$Z_m$  = the impedance of a branch

### 3.4.2. Shunt representation

Fig. 3.10 shows typical illustration of the collector system equivalent represented as a pi-circuit. This equivalent representation is based on the assumption that under normal conditions, bus voltage will remain close to unity, and reactive power produced or absorbed by a capacitor is proportional to square of voltage across it. Therefore the plant susceptance  $B$  can be considered as sum of all shunts in the power system network.

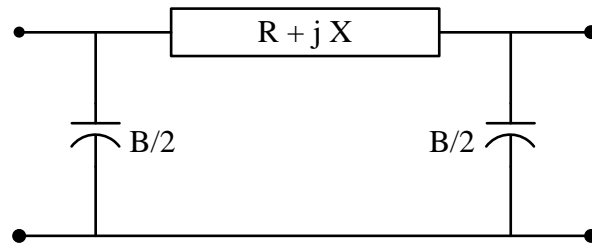


**Fig. 3.10. Equivalent model of collector system line capacitance**

This assumption is close to reality under normal condition. Therefore total shunt capacitance within the PV plant is as follows:

$$B_{tot} = \sum_{i=1}^n B_i \quad (22)$$

Where,  $B_i$  = the capacitance of individual branch (in p.u. system base,  $S_{base}$ )

$n$  = the number of branches

### 3.4.3. Pad-mounted transformer representation

The pad-mounted transformer must be represented to process the entire solar PV plant. The equivalent circuit can be scaled so that the resulting voltage drop across the impedances (leakage) and the reactive and real power losses are equal to the sum of individual reactive and real losses of the inverters. The equivalent representation for the entire plant can be computed as the impedance of a single transformer divided by the number of the inverters. Note, that the

$$Z_{eq} = Z/n_{inv} \quad (23)$$

Where

$Z_{eq}$  = the equivalent impedance of pad mounted transformer (in p.u. system base,  $S_{base}$ )

$Z$  = the impedance of a single pad mounted transformer (in p.u. system base,  $S_{base}$ )

$n_{inv}$  = the number of inverters connected to pad mounted transformer

Note, that this equation is valid using the actual values of the impedance (ohms) or using the system base value. WECC however recommended to use the system base value for the pad mounted transformer to prepare the input for power flow modeling.

### 3.5. Multiple Machine Representation

In certain cases, solar PV plants are built with different types of PV inverters for several reasons -

- Mixing inverter types to achieve more economic plant cost
- Meet reactive power requirements at POI as mandated by utility or control area
- Raise plant capacity of an already built plant, by adding more number of inverters

For any of the above mentioned reason, plant collection system equivalent impedance must not be the same. If any change in inverter technology is proposed then each inverter types must be grouped together and represented as a separate generator in solar PV plant aggregated

model. Based on inverter type and topology, its dynamic response to any system transient event may vary. In common practice more than two inverter types are not proposed to use in any plant design. However, if two or more different inverter types are present, then they must be represented as separate generators and collection system and connected pad-mounted transformer equivalent will then be calculated separately.

### **3.6. Case Study 1 – Comparison between Reduced Order and Full Scale Models in**

#### **Multi-Machine Power System**

In this study, time-domain dynamic simulations in Positive Sequence Load Flow (PSLF) tool are used to compare collector system equivalencing method for a one-machine equivalent model, to multiple-machine reduced order model and full scale model to account for diversity in collector line impedance. A comparison of both steady state and dynamic behavior of a 147-MW solar PV plant modeled with and without collector system equivalencing is performed under different scenarios. In first scenario complete plant is modeled as a single generator, in second scenario plant is modeled as two separate generators considering the presence of a tie-breaker switch at 34.5 kV bus and collection system equivalencing is applied to each generation side, in third scenario five generators are used with collector system equivalencing applied at 34.5 kV PVCS bus, and finally a full scale model of the PV plant containing all 117 inverters modeled as individual generators is used. Full scale model comprises of 117 inverters, with each inverter rated at 1260 kW/1350 kVA with power factor operating range from 0.93 lead to 0.93 lag. In all scenarios PV plant is connected to bus 29 of modified IEEE 39-bus system. A single line diagram of PV plant is shown in Fig. 3.11. Due to large number of inverters and proportional numbers of pad mounted transformers, low voltage buses are not shown in this single line.

**Fig. 3.11. Medium and high voltage schematic of PV plant**

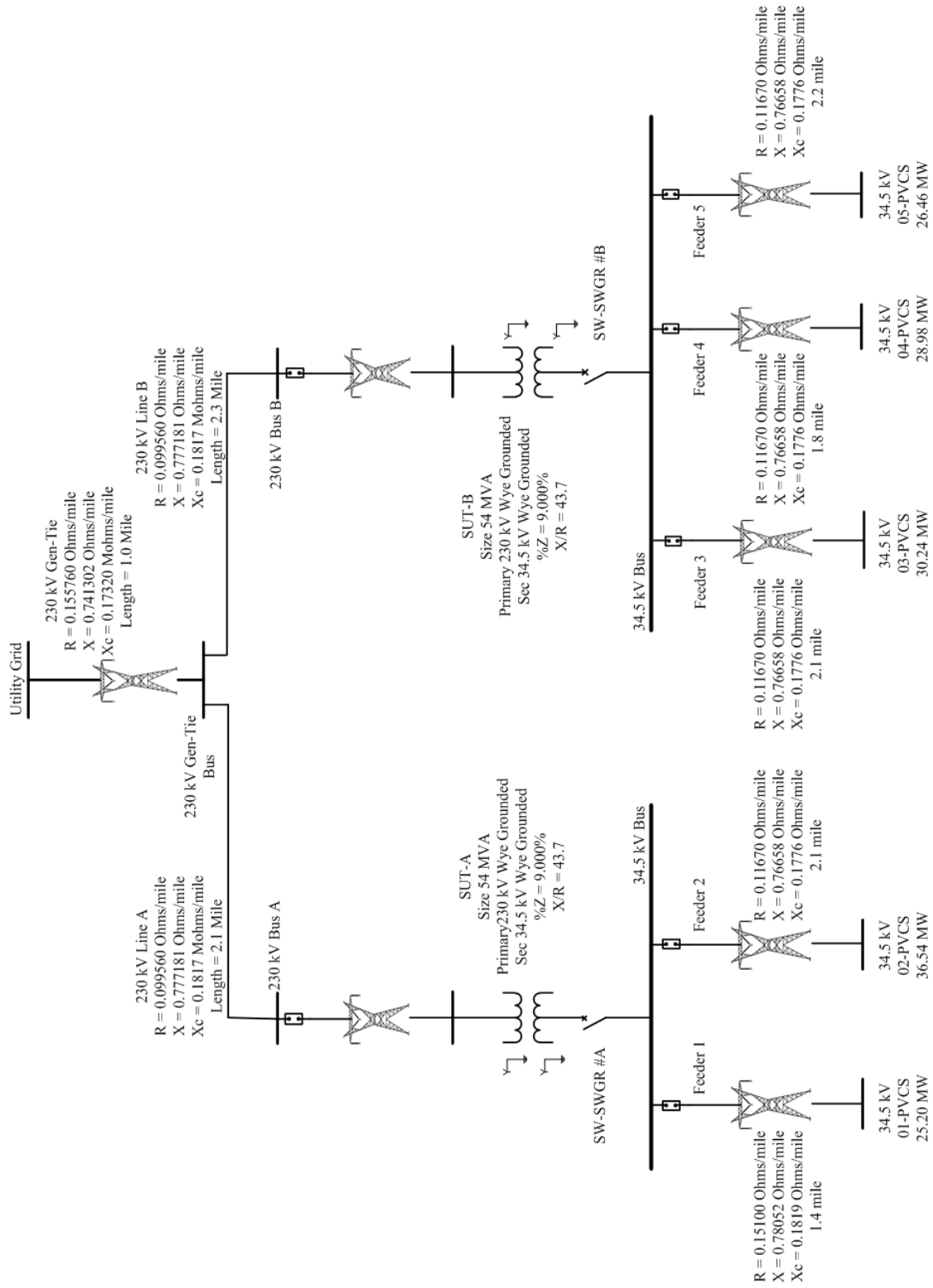


Table 4 indicates the total number of connected inverters, their capacity, and pad-mounted transformer equivalent impedance on 34.5 kV, 100 MVA base connected to each PVCS bus in five machine model.

**Table 4. Inverter and pad-mounted transformer equivalencing**

Model	Number of PVCS buses	Inverter			Pad Mounted Transformer		
		Number of inverters	Generator Rating		Equivalent impedance on Transformer Equivalent MVA		
			MVA	MW	MVA	R (p.u.)	X (p.u.)
Five Machine	01-PVCS	20	27.00	25.19	27.20	0.1881	1.1851
	02-PVCS	29	39.15	36.53	39.44	0.2727	1.7184
	03-PVCS	24	32.40	30.23	32.64	0.2257	1.4221
	04-PVCS	23	31.05	28.97	31.28	0.2163	1.3629
	05-PVCS	21	28.36	26.45	28.56	0.1975	1.2444
Two Machine	01-PVCS	49	66.15	85.65	66.64	0.4608	2.9036
	02-PVCS	68	91.80	61.71	92.48	0.6396	4.0295
One Machine	01-PVCS	1	157.95	147.36	159.12	1.1005	6.9332
Full Scale	117-PVCS	117	1.35	1.259	1.36	0.0094	0.0592

Collection system equivalent impedance for each scenario (except for full scale model) on 34.5 kV & 100 MVA base calculated using equivalencing method is given in Table 5.

**Table 5. Collector System Equivalence impedance**

Test Scenarios	Section	R (p.u.)	X (p.u.)	B (p.u.)
Full Scale Model	All Sections	0.00504	0.00201	0.00022
One Machine model	Full feeder	0.00493	0.02681	0.03261
Two Machines model	Section-I	0.01226	0.06558	0.01432
	Section-II	0.00812	0.04488	0.01829
Five Machines model	Section-I	0.02189	0.09342	0.00534
	Section-II	0.02382	0.13667	0.00898
	Section-III	0.02314	0.13641	0.00692
	Section-IV	0.00327	0.12009	0.00602
	Section-V	0.02841	0.14302	0.00565

The IEEE 39-bus system data was taken from [43] and [44]. Modifications done to IEEE 39 bus system to accommodate complete PV plant are as follows -

- Power output of generator 9 connected at Bus 38 is reduced to 100 MW.

- In order to maintain same power injection at Bus 29 as in actual system the load at Bus 29 is disconnected.
- Voltage regulator and power system stabilizer of generator 9 were disconnected to expose connected solar PV plant to more severe conditions during transient event.

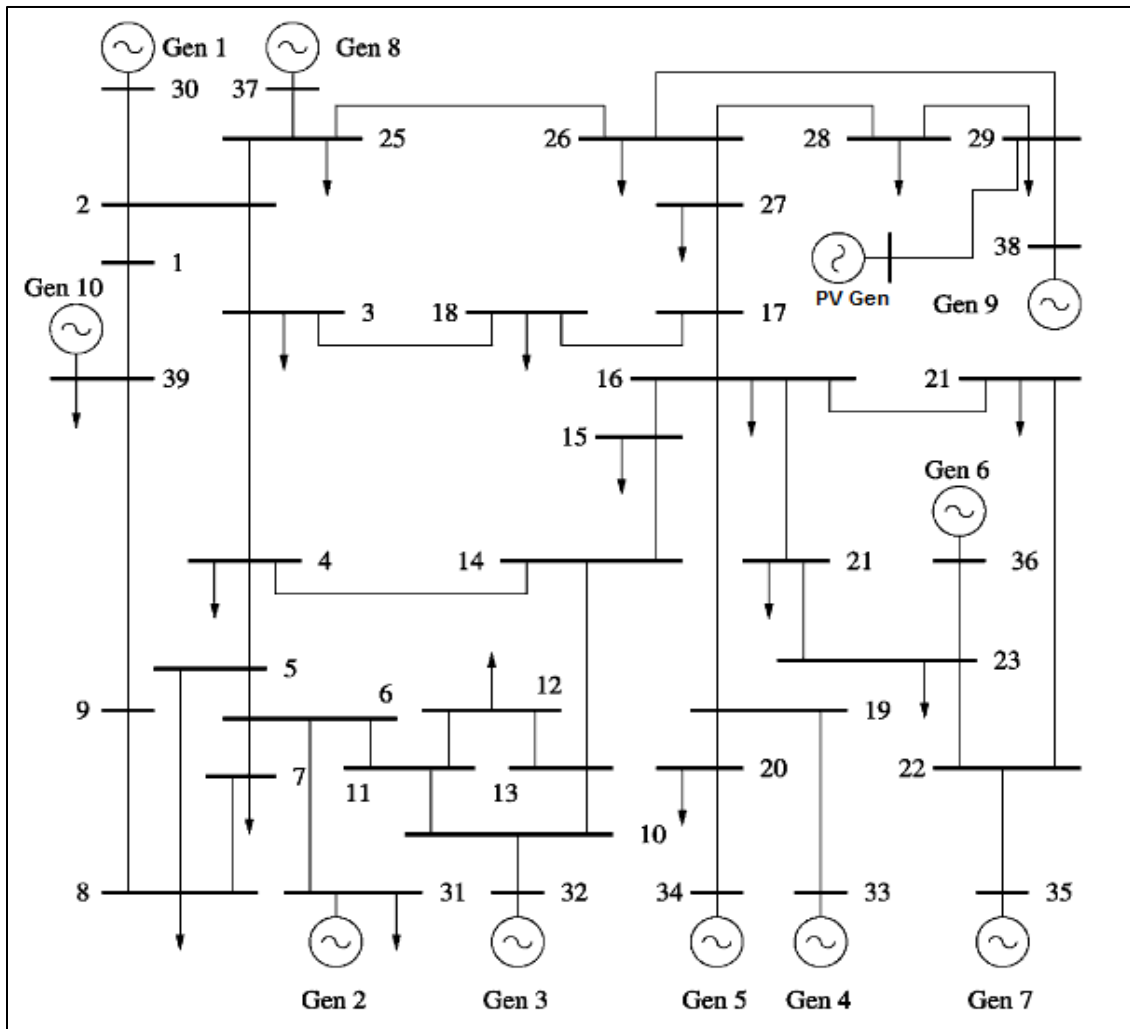


*Fig. 3.12. IEEE 39 bus test system [43]*

Fig. 3.12 above shows the IEEE 39 bus test system. For all test cases PV plant is connected to Bus 29. A detailed load flow model of test system with PV plant is shown in Fig.3.13.



To compare the performance of full scale and all reduced scale models, a short-circuit fault is applied at Bus 26. Fault duration in all case is 9-cycles and duration of simulation is kept same. Traces of voltage, active power and reactive power measured at POI during steady-state analysis for full scale model compared to single-machine, two-machines, and five-machines reduced scale models are shown in Table 6.

**Table 6. Steady State Parameters Measured at POI**

Simulated Cases	Measured Parameters at POI		
	Active Power (MW)	Reactive Power (MVAR)	Voltage (p.u.)
Single Machine Equivalent	144.8	-23.5	1.062
Two Machines Equivalent	144.8	-23.7	1.061
Five Machines Equivalent	144.9	-23.7	1.061
Full Scale Model	144.9	-23.7	1.061

Fig. (3.14)- (3.17) shows the response of single-machine, two-machine, five-machine and full scale models respectively to grid disturbance. Voltage measured in per unit (p.u) at inverter terminals and POI is shown in voltage plots followed by active and reactive power respectively in their actual units. In all cases, the regulated bus was the 315V low voltage terminal bus and the solar control system was active. When a 3-phase fault to ground is applied at 230 kV interconnection bus at t =1 second, the reactive power output of the solar plant was at its maximum in an effort to support voltage. After the fault was cleared by protection devices at 1.15 seconds, electrical controller quickly restores the voltage at the POI and terminal bus to its initial value. The effect of low voltage power logic can be seen in the post-fault real power recovery over 250 milliseconds. Reactive power requirements as defined by the transmission owner normally specifies the power factor requirements at the point of interconnection between certain levels, typical range is between 0.95 leading to 0.95 lagging. Steady state results



illustrates that this particular plant is operating within these typical limits by maintaining 0.985 lagging power factor at POI.

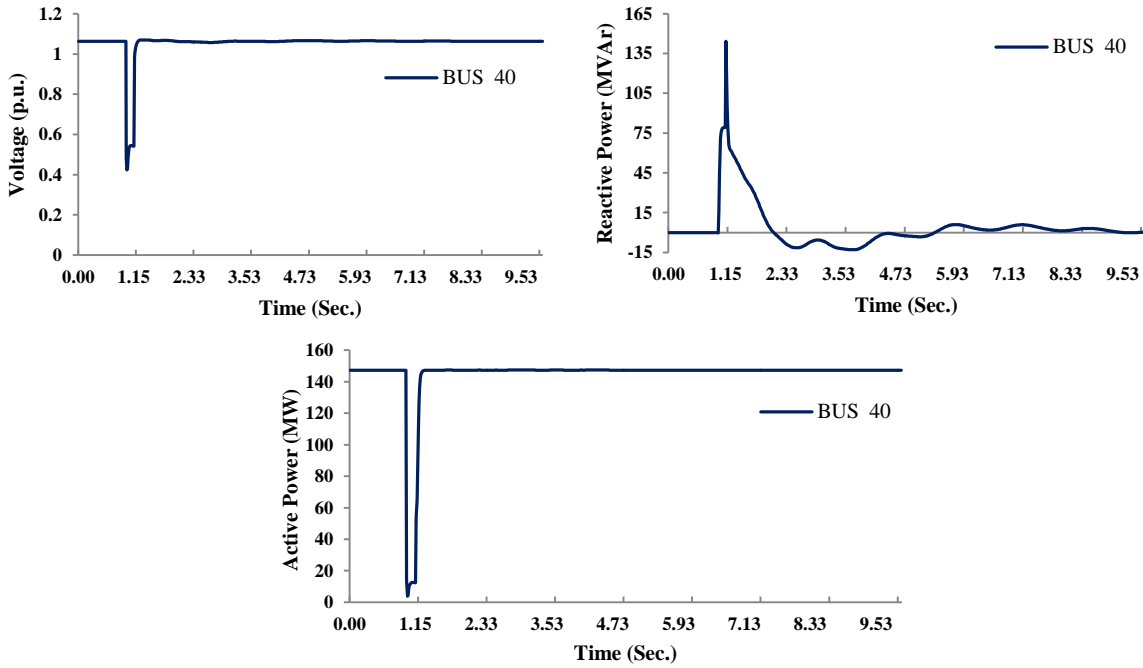


**Fig. 3.14.** Single machine equivalent model response to disturbance event

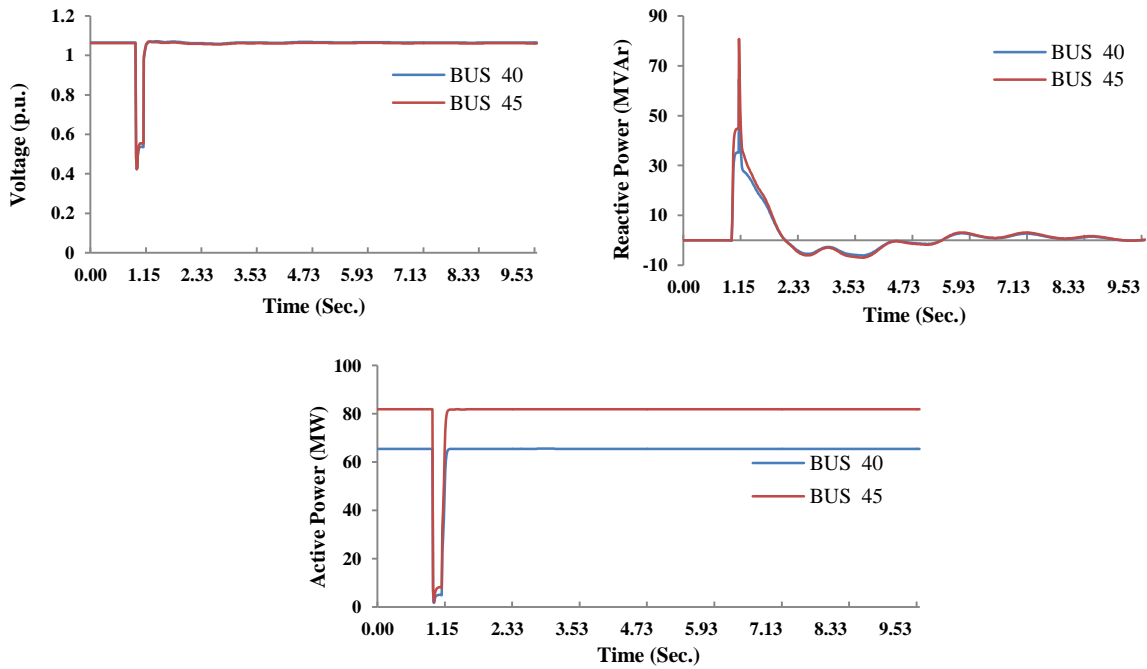


**Fig. 3.15.** Two machine equivalent model response to disturbance event

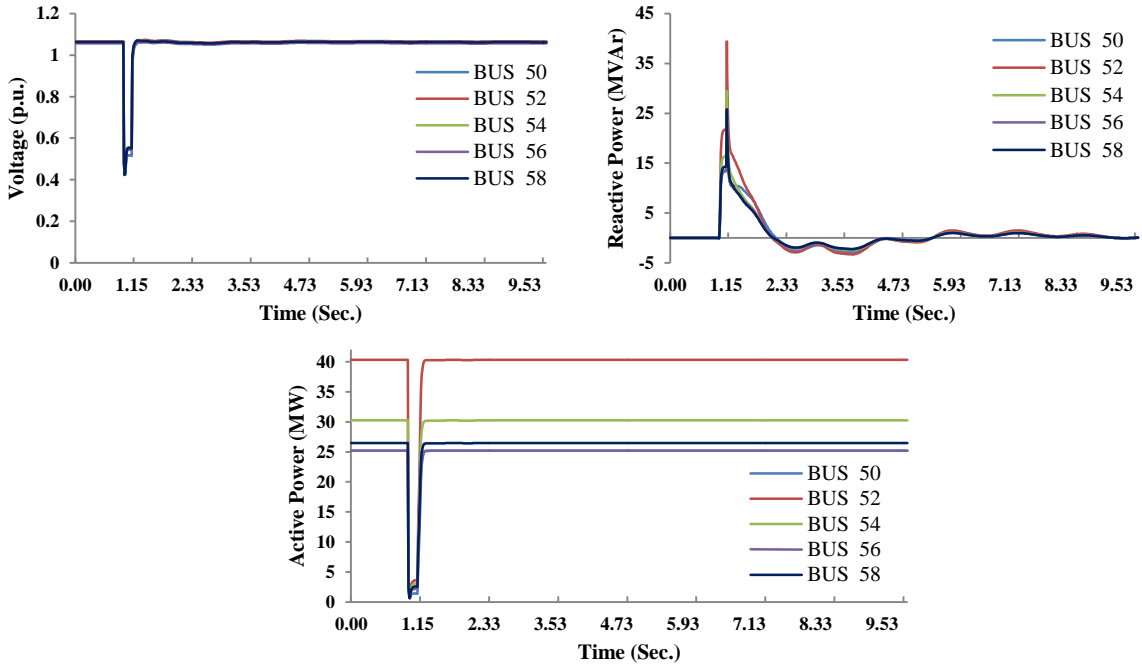


**Fig. 3.16. Five machine equivalent model response to disturbance event**

In Fig. (3.14)- (3.16) bus number indicates the actual buses to which solar PV generator models are connected in modified IEEE 39 bus system.

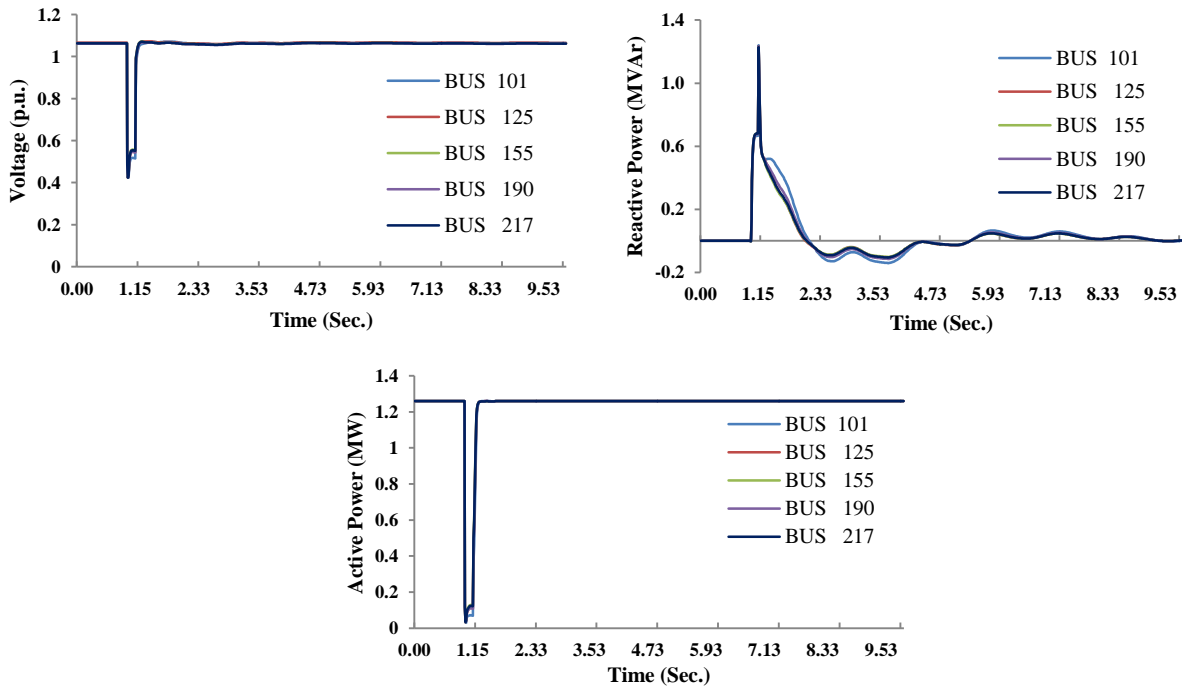


**Fig. 3.17. Full scale model response to disturbance event**

In full scale model, there are 117 generator buses and hence response shown in Fig. 3.17 are measured at arbitrarily chosen buses such that at least one bus must be very close to interconnection point and one bus must be at farthest end from interconnection point to take collection system impedance in account.

Fig. 3.18 shows the voltage response measured at POI in different cases under fault event. Root mean square (RMS) error for voltage measured at POI for one-machine, two-machine and five-machine reduced scale model are 0.06%, 0.28% and 0.357% respectively.

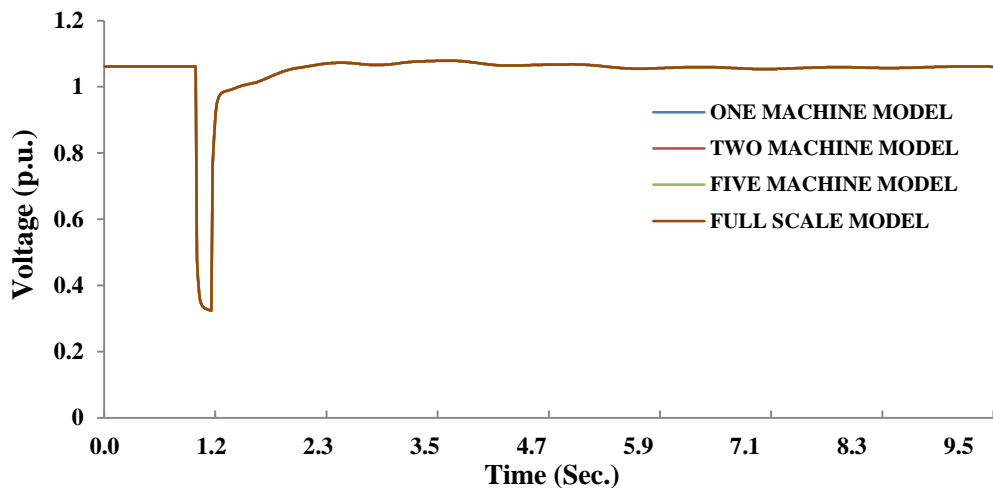


*Fig. 3.18. Voltage response measured at POI bus*

### 3.7. Case Study 2 – PV Plant VAR Capability with Inverters

PV plant reactive power support capability is always suspected by the transmission owners/utilities due to the fact that there is common misconception that PV plants are not able to provide reactive power support to the grid. Every utility has its own reactive power support requirements at POI to interconnect a plant which is mandated in Large Generator Interconnection Agreement (LGIA) and it varies from one utility to other. Most utility in western United States ask for +/- 0.95 power factor requirement at POI. These requirements must be met, either through

tap-changers, static capacitor bank or through dynamic VAR support devices. This study presents the reactive compensation analysis performed to determine the optimum capacitor bank size required to meet the large generator interconnection requirement (LGIA) at point of interconnection (POI) for a 250 MW solar PV plant. It has been shown in this study that with inverter VAR support, capacitor-bank size can be optimized to meet the grid interconnection requirements. The study is performed using GE PSLF v18.1. In order to meet the LGIA power factor requirement of +/- 0.95 at the POI, the results indicate that reactive power compensation is required at 100% plant generation level. A switched capacitor bank size of 24.0 MVAR is determined to meet this requirement. Data for plant under study is given in the section below.

### 3.7.1. Transmission Line (Gen-tie)

5.2 miles long, 954 kcmil drake conductor has been used as gen-tie. Transmission line has been modeled as single circuit line with no bundled conductors with positive sequence impedance data given in Table 7.

**Table 7. Plant Gen-tie Data**

Length =	5.2	mile			
$R_{pos} =$	0.089232	$\Omega/\text{mile}$	$R_{pos}$	0.0001856	p.u.
$X_{pos} =$	0.728691	$\Omega/\text{mile}$	$X_{Lpos}$	0.0015	p.u.
$X_{cpos} =$	170093	$\Omega/\text{mile}$	$B_{pos}$	0.0382	p.u.

### 3.7.2. Main Step-up Transformer

Plant has two main step-up transformers. The main step-up transformer has been modeled based on IEEE Std. 141-1993 [45]. The transformer taps have been modeled as a de-energized tap-changer. The parameters for the three winding Yyd step-up transformer are -

Rated power: 165/220/275 MVA

Open circuit voltage ratio: 525/34.5/19.92 kV

Short circuit impedance: 9.5% ( $\pm 7.5\%$  tolerance)

### 3.7.3. Solar Inverters and Pad-mounted transformers

The plant consists of one hundred sixty five pad-mounted transformers and associated PV modules. Each medium voltage pad-mounted transformer has two inverters with an output rating of 822.9 kVA at 50°C and operates to export a maximum of 767.9 kW with reactive power capacity of 0.93 leading to 0.93 lagging power factor at 100% output. Inverter specifications are given below in Table 8 and three winding inverter transformer data is given in Table 9.

**Table 8. Inverter specifications**

Inverter net capacity	822.9 kVA
Rated power factor	±0.93
Rated current	1344.6 A (on 360 V)
Number of Inverters	330

**Table 9. Medium Voltage pad-mounted transformer specifications**

Rated power	1600/800/800 kVA					
Open circuit voltage ratio	4.5/0.36/0.36 kV					
Short circuit impedance	H-Xa		H-Xb		Xa-Xb	
	% R	% X	% R	% X	% R	% X
	0.7	5.00	0.7	5.00	0.3	1.20
Number of Transformer units	165					

The inverters are modeled as 822.9 kVA solar PV generator with its real and reactive power varied to obtain various plant generation levels. These inverters are modeled assuming 0.93 leading to 0.93 lagging power factor at maximum power output level. The inverters are capable of operating at a power factor below 0.93 when the output power falls below 95%; the full reactive power capability of the inverters has been considered for this study.

### 3.7.4. Capacitor Bank Sizing

Load flow study cases were set up in PSLF with the inverters operating to generate 100% to 0% plant output with the POI voltage varied between +/- 5%. The study has been conducted using the full capability of the inverter based on the reactive power capability. The purpose of the

analysis is to ensure that the 250 MW plant is able to deliver to the point of interconnection reactive power at all output levels between 10% and 100% of nameplate capacity for a voltage range of +/-5%.

### **3.7.5. Lagging Generation Condition**

The solar plant reactive power consumption at various plant generation levels as determined is provided in Table 10 to Table 15. For the lagging case, it is observed that capacitive compensation is required when the plant generation level is between approximately 90% and 100% for both configurations.

**Table 10. Load flow study results with voltage at POI = 0.95 per unit (Lagging p.f. case)**

Voltage at POI BUS = 0.95 p.u.											
Plant Gen.	INVERTERS					POI			Required P.F. per LGIA	Required MVA <sub>r</sub> at POI to meet LGIA	Compensation Required
%	kW	kVA <sub>r</sub>	MW	MVA <sub>r</sub>	P.F.	MW	MVA <sub>r</sub>	P.F.			
Lagging Power Factor (Plant Producing VARs) with Capacitor Bank OFF											
100	767.9	295.8	253.4	97.63	0.93	250.12	60.74	0.97	0.95	82.210	NO
90	691.1	365.5	228.06	120.60	0.88	225.18	88.89	0.93	0.95	74.013	NO
80	614.3	365.5	202.72	120.60	0.86	200.31	95.07	0.90	0.95	65.839	NO
70	537.5	365.5	177.38	120.60	0.83	175.39	100.51	0.87	0.95	57.648	NO
60	460.7	365.5	152.04	120.60	0.78	150.41	105.21	0.82	0.95	49.437	NO
50	383.9	365.5	126.7	120.60	0.72	125.37	109.17	0.75	0.95	41.207	NO
40	307.2	365.5	101.36	120.60	0.64	100.28	112.41	0.67	0.95	32.960	NO
30	230.4	365.5	76.02	120.60	0.53	75.14	114.93	0.55	0.95	24.697	NO
20	153.6	365.5	50.68	120.60	0.39	49.93	116.72	0.39	0.95	16.411	NO
10	76.8	365.5	25.34	120.60	0.21	24.68	117.79	0.21	0.95	8.112	NO
0	0.0	0.0	0	0.00		0.00	5.75	0.00	0.95	0.000	NO
Lagging Power Factor (Plant Producing VARs) with Capacitor Bank ON											
100	767.9	295.8	253.4	97.63	0.93	250.15	83.03	0.95	0.95	82.220	YES

**Table 11. Load flow study results with voltage at POI = 0.95 per unit (Leading p.f. case)**

Voltage at POI BUS = 0.95 p.u.												
Plant Gen.	INVERTERS					POI				Required P.F. per LGIA	Required MVAR at POI to meet LGIA	Compensation Required
%	kW	kVAr	MW	MVAr	P.F.	MW	MVAr	P.F.				
Leading Power Factor (Plant Absorbing VARs) with Capacitor Bank OFF												
100	767.9	295.8	253.40	-97.63	0.93	249.13	-147.51	-0.86		-0.95	-81.89	NO
90	691.1	365.5	228.06	-120.60	0.88	224.07	-166.87	-0.80		-0.95	-73.65	NO
80	614.3	365.5	202.72	-120.60	0.86	199.40	-158.17	-0.78		-0.95	-65.54	NO
70	537.5	365.5	177.38	-120.60	0.83	174.64	-150.57	-0.76		-0.95	-57.40	NO
60	460.7	365.5	152.04	-120.60	0.78	149.81	-144.03	-0.72		-0.95	-49.24	NO
50	383.9	365.5	126.70	-120.60	0.72	124.89	-138.53	-0.67		-0.95	-41.05	NO
40	307.2	365.5	101.36	-120.60	0.64	99.89	-134.05	-0.60		-0.95	-32.83	NO
30	230.4	365.5	76.02	-120.60	0.53	74.82	-130.58	-0.50		-0.95	-24.59	NO
20	153.6	365.5	50.68	-120.60	0.39	49.67	-128.31	-0.36		-0.95	-16.33	NO
10	76.8	365.5	25.34	-120.60	0.21	24.44	-126.64	-0.19		-0.95	-8.03	NO
0	0.0	0.0	0.00	0.00		0.00	5.75	0.00		0.95	0.00	NO



**Table 12. Load flow study results with voltage at POI = 1.00 per unit (Lagging p.f. case)**

Voltage at POI BUS = 1.00 p.u.												
Plant Gen.	INVERTERS					POI				Required P.F. per LGIA	Required MVAR at POI to meet LGIA	Compensation Required
%	kW	kVAr	MW	MVAr	P.F.	MW	MVAr	P.F.				
Lagging Power Factor (Plant Producing VARs) with Capacitor Bank OFF												
100	767.9	295.8	253.40	97.63	0.93	250.41	65.18	0.97	0.95	82.306	YES	
90	691.1	365.5	228.06	120.60	0.88	225.43	92.77	0.92	0.95	74.095	NO	
80	614.3	365.5	202.72	120.60	0.86	200.52	98.41	0.90	0.95	65.908	NO	
70	537.5	365.5	177.38	120.60	0.83	175.56	103.36	0.86	0.95	57.704	NO	
60	460.7	365.5	152.04	120.60	0.78	150.55	107.66	0.81	0.95	49.483	NO	
50	383.9	365.5	126.70	120.60	0.72	125.49	111.27	0.75	0.95	41.247	NO	
40	307.2	365.5	101.36	120.60	0.64	100.37	114.23	0.66	0.95	32.990	NO	
30	230.4	365.5	76.02	120.60	0.53	75.21	116.53	0.54	0.95	24.720	NO	
20	153.6	365.5	50.68	120.60	0.39	50.00	118.17	0.39	0.95	16.434	NO	
10	76.8	365.5	25.34	120.60	0.21	24.73	119.14	0.20	0.95	8.128	NO	
0	0.0	0.0	0.00	0.00		0.00	6.36	0.00	0.95	0.000	NO	
Lagging Power Factor (Plant Producing VARs) with Capacitor Bank ON												
100	767.9	295.8	253.40	97.63	0.93	250.44	89.80	0.94	0.95	82.316	24MVAR	

**Table 13. Load flow study results with voltage at POI = 1.00 per unit (Leading p.f. case)**

Voltage at POI BUS = 1.00 p.u.											
Plant Gen.	INVERTERS					POI			Require d P.F. per LGIA	Required MVA <sub>r</sub> at POI to meet LGIA	Compensation Required
%	kW	kVA <sub>r</sub>	MW	MVA <sub>r</sub>	P.F.	MW	MVA <sub>r</sub>	P.F.			
Leading Power Factor (Plant Absorbing VARs) with Capacitor Bank OFF											
100	767.9	295.8	253.40	-97.63	0.93	249.62	-140.48	-0.87	-0.95	-82.05	NO
90	691.1	365.5	228.06	-120.60	0.88	224.55	-160.07	-0.81	-0.95	-73.81	NO
80	614.3	365.5	202.72	-120.60	0.86	199.79	-152.45	-0.79	-0.95	-65.67	NO
70	537.5	365.5	177.38	-120.60	0.83	174.96	-145.78	-0.77	-0.95	-57.51	NO
60	460.7	365.5	152.04	-120.60	0.78	150.07	-140.02	-0.73	-0.95	-49.33	NO
50	383.9	365.5	126.70	-120.60	0.72	125.10	-135.17	-0.68	-0.95	-41.12	NO
40	307.2	365.5	101.36	-120.60	0.64	100.06	-131.21	-0.61	-0.95	-32.89	NO
30	230.4	365.5	76.02	-120.60	0.53	74.96	-128.15	-0.50	-0.95	-24.64	NO
20	153.6	365.5	50.68	-120.60	0.39	49.79	-125.96	-0.37	-0.95	-16.37	NO
10	76.8	365.5	25.34	-120.60	0.21	24.55	-124.67	-0.19	-0.95	-8.07	NO
0	0.0	0.0	0.00	0.00		0.00	6.36	0.00	0.95	0.00	NO

**Table 14. Load flow study results with voltage at POI = 1.05 per unit (Lagging p.f. case)**

Voltage at POI BUS = 1.05 p.u.												
Plant Gen.	INVERTERS					POI				Required P.F. per LGIA	Required MVAR at POI to meet LGIA	Compensation Required
%	kW	kVAr	MW	MVAr	P.F.	MW	MVAr	P.F.				
Lagging Power Factor (Plant Producing VARs) with Capacitor Bank OFF												
100	767.9	295.8	253.4	97.63	0.93	250.67	69.16	0.96	0.95	82.391	YES	
90	691.1	365.5	228.06	120.60	0.88	225.64	96.29	0.92	0.95	74.164	NO	
80	614.3	365.5	202.72	120.60	0.86	200.70	101.45	0.89	0.95	65.967	NO	
70	537.5	365.5	177.38	120.60	0.83	175.71	106.00	0.86	0.95	57.753	NO	
60	460.7	365.5	152.04	120.60	0.78	150.67	109.91	0.81	0.95	49.523	NO	
50	383.9	365.5	126.7	120.60	0.72	125.59	113.22	0.74	0.95	41.279	NO	
40	307.2	365.5	101.36	120.60	0.64	100.46	115.94	0.65	0.95	33.020	NO	
30	230.4	365.5	76.02	120.60	0.53	75.28	118.05	0.54	0.95	24.743	NO	
20	153.6	365.5	50.68	120.60	0.39	50.05	119.55	0.39	0.95	16.451	NO	
10	76.8	365.5	25.34	120.60	0.21	24.78	120.46	0.20	0.95	8.145	NO	
0	0.0	0.0	0	0.00		0.00	7.01	0.00	0.95	0.000	NO	
Lagging Power Factor (Plant Producing VARs) with Capacitor Bank ON												
100	767.9	295.8	253.4	97.63	0.93	250.70	96.23	0.93	0.95	82.401	24MVAR	

**Table 15. Load flow study results with voltage at POI = 1.05 per unit (Leading p.f. case)**

Voltage at POI BUS = 1.00 p.u.											
Plant Gen.	INVERTERS					POI			Require d P.F. per LGIA	Required MVAr at POI to meet LGIA	Compensation Required
%	kW	kVAr	MW	MVAr	P.F.	MW	MVAr	P.F.			
Leading Power Factor (Plant Absorbing VARs) with Capacitor Bank OFF											
100	767.9	295.8	253.40	-97.63	0.93	250.03	-134.55	-0.88	-0.95	-82.18	NO
90	691.1	365.5	228.06	-120.60	0.88	224.93	-154.37	-0.82	-0.95	-73.93	NO
80	614.3	365.5	202.72	-120.60	0.86	200.11	-147.62	-0.80	-0.95	-65.77	NO
70	537.5	365.5	177.38	-120.60	0.83	175.23	-141.69	-0.78	-0.95	-57.60	NO
60	460.7	365.5	152.04	-120.60	0.78	150.28	-136.57	-0.74	-0.95	-49.39	NO
50	383.9	365.5	126.70	-120.60	0.72	125.27	-132.25	-0.69	-0.95	-41.17	NO
40	307.2	365.5	101.36	-120.60	0.64	100.20	-128.73	-0.61	-0.95	-32.93	NO
30	230.4	365.5	76.02	-120.60	0.53	75.07	-126.00	-0.51	-0.95	-24.67	NO
20	153.6	365.5	50.68	-120.60	0.39	49.88	-124.05	-0.37	-0.95	-16.39	NO
10	76.8	365.5	25.34	-120.60	0.21	24.63	-122.89	-0.20	-0.95	-8.10	NO
0	0.0	0.0	0.00	0.00		0.00	7.02	0.00	0.95	0.00	NO

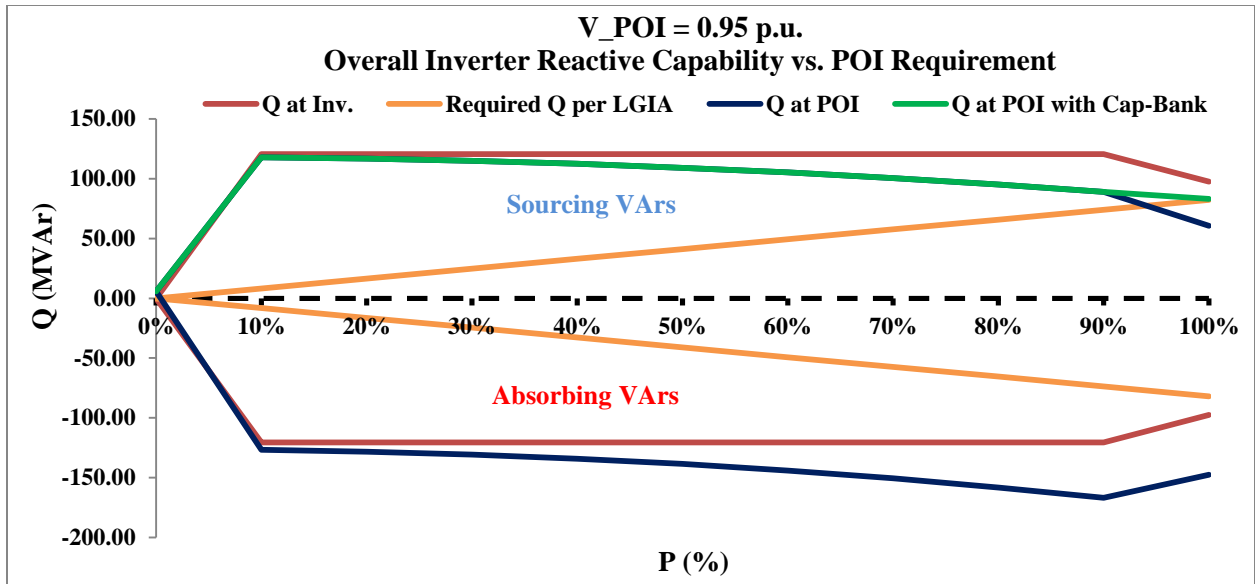


*Fig. 3.19. Plant reactive power capability at POI at 0.95 p.u. voltage*

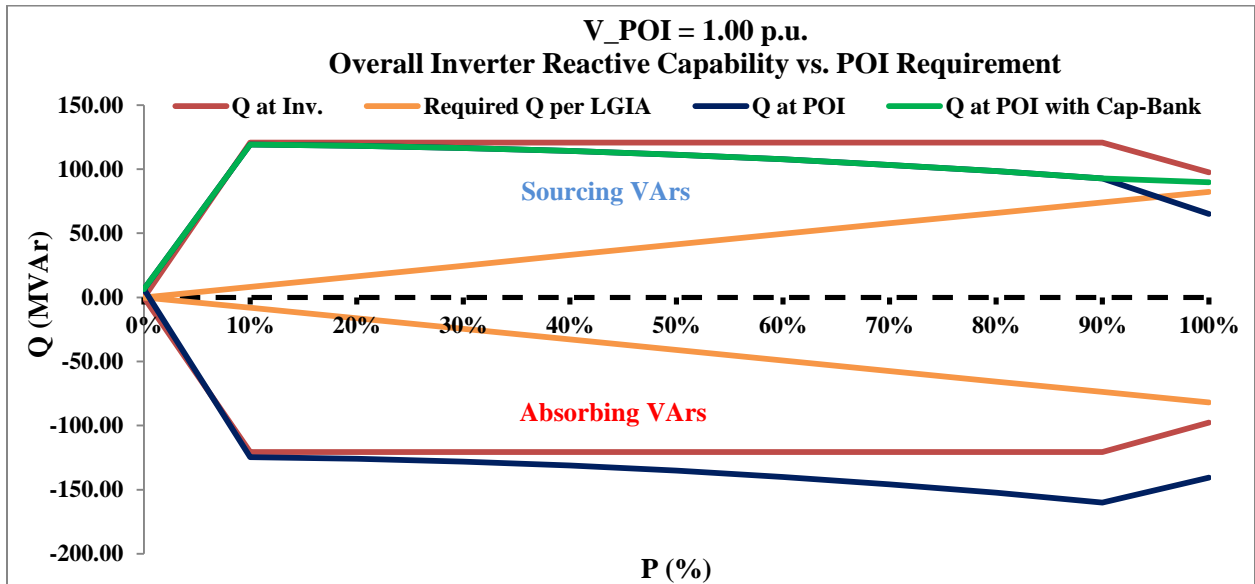


*Fig. 3.20. Plant reactive power capability at POI at 1.00 p.u. voltage*

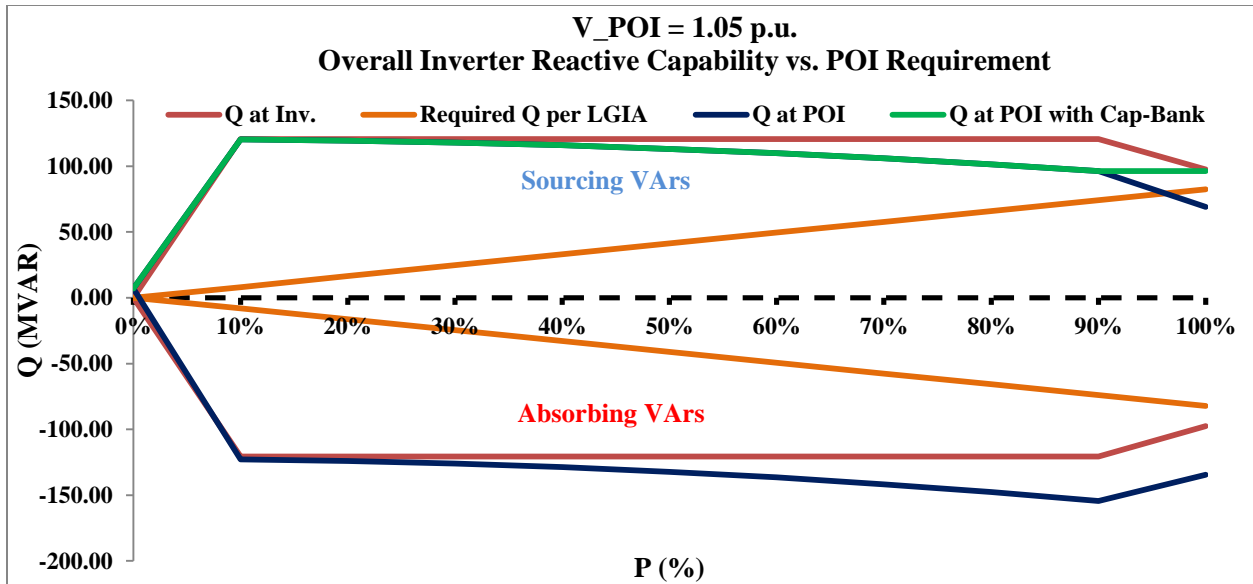


**Fig. 3.21. Plant reactive power capability at POI at 1.05 p.u. voltage**

As shown in Table 10 for the 100% (250 MW) plant output case the real power delivered per inverter is 767.9 kW which, according to the reactive power capability curve allows for a power factor of 0.93. Based on the results, a minimum capacitor size of 24 MVAR is needed at the 34.5 kV bus to meet the requirement for the lagging generation mode when the POI voltage is 95% of nominal. In the leading mode the inverters are able to collectively absorb sufficient reactive power to satisfy the LGIA requirements. The reactive power capability at the POI is provided with capacitor bank switched on and off in fig. 3.19 - 3.21.

**Conclusions**

- (1) From Case study 1, it is clear that in power system stability studies for planning and operation, a reduced scale solar PV plant model in a single machine form is adequate. RMS error calculated for measured voltage response is less than even 1% which is relatively small and hence can be neglected. This ensures the computational efficiency without losing any information about system behavior. Measured values of voltage, active power and reactive power during steady state runs for all scenarios and dynamic response measured at

point of interconnection clearly indicates that reduced order model can represent the complete PV plant in similar manner as a full scale model and hence can be used for both online (operation) and offline (stability) studies.

- (2) From case study 2, it can be concluded that a solar PV plant is capable of meeting grid reactive power interconnection requirements, if the inverters VAr capacity is utilized properly. Although in some cases, small capacitor banks may be required to meet these grid codes.

## Chapter 4

### PV PLANT DYNAMIC MODELING

#### Introduction

This chapter discusses in detail about the various PV plant dynamic models as evolved from one generation to other. In 2012, WECC released a guide for solar PV system dynamic simulation models [26]. This document is intended to serve as a specification for generic solar photovoltaic (PV) system positive-sequence dynamic models to be implemented by software developers and approved by the WECC Modeling and Validation Workgroup (MVWG) for use in bulk system dynamic simulations in accordance with NERC MOD standards. Solar PV model is still under development and testing phase, Electric Power Research Institute (EPRI) along with WECC is working on developing and testing solar PV models for positive sequence load flow and dynamic stability studies. Prior to release of any PV plant model for dynamic study of solar PV plants, plant owners used to submit user-written EPCL model files written in GE PSLF or Siemens PSSE to WECC data base. Those models are highly based on inverter technology and require specific code to simulate inverter response. These models are no more accepted by WECC. First generation of test models for solar PV named PV1G for generator converter model; PV1E for electrical control model was released in 2012 and are available in GE PSLF 18.1 and Siemens PSSE 30.0 tools. Second generation models (REGC\_A, REEC\_B, and REPC\_A) are not yet released in GE PSLF or Siemens PSSE versions, but for test purpose and model validation, beta version was provided by GE to complete this study. This chapter compares the results obtained for dynamic response of a 298 MW solar PV plant modeled using user-written EPCL code, using first generation PV plant models (PV1G, PV1E) and second generation PV plant models (REGC\_A, REEC\_B, REPC\_A).



## 4.1. First Generation PV Plant Dynamic Model

This section describes the general structure and functionalities associated with first generation of generic PV plant dynamic models. First Generation model has two components-

- Full Converter Generator / Converter Model (PV1G)
- Converter Control / Electrical Control Model (PV1E)

### 4.1.1. Full Converter Generator / Converter Model (PV1G)

As the name represents, PV1G, this model represents the equivalent of all converters (generator) available in a solar PV plant and provides the interface between the solar plant and the power network. Since this was the first generation of solar PV generator, therefore “1” represents its generation. The control block diagram is shown in fig. 4.1. Converter parameters are shown in Table 16.

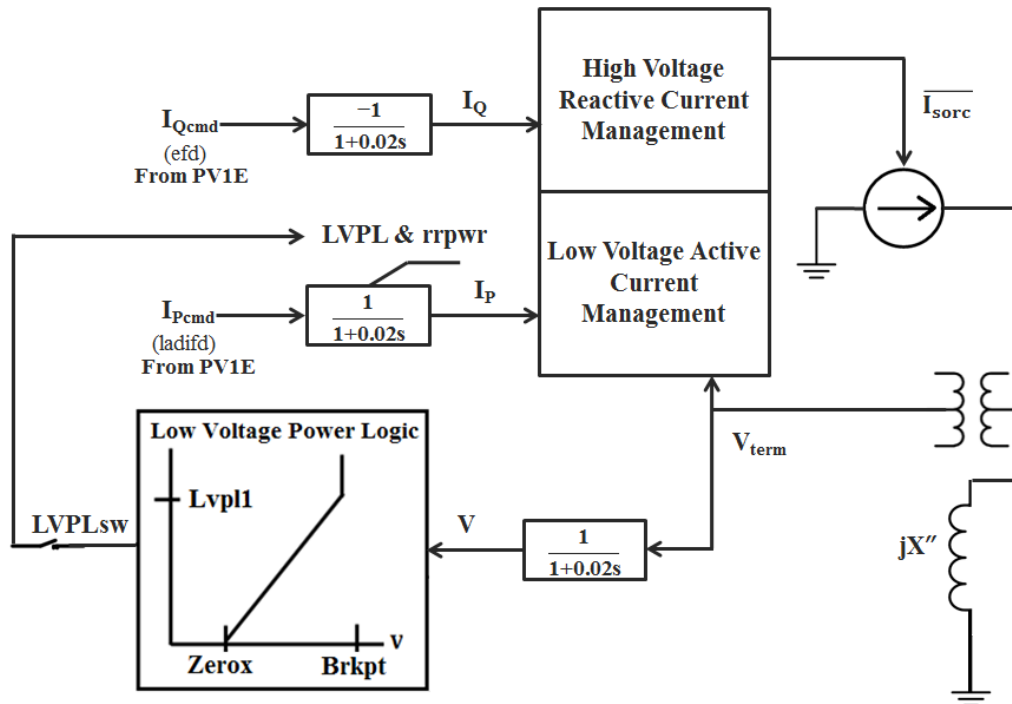


*Fig. 4.1. PV1G model block diagram [26]*

While invoking this model in dynamics data file, MVA base is specified as MVA equal to power output of the plant after the steady state simulation. All variable in Table 16 are in per

unit on the unit MVA base. PV1G model is a very simplistic representation of extremely complex and very fast inverter control system. The small time constants (0.02 seconds) provide a reasonable approximation to fast electronic control systems. PV1G model is connected in cascade and ahead of PV1E model. It provides active and reactive current command to the network. During voltage dip events, it is Low Voltage Power Logic (LVPL) circuit that allows for a controlled response of active current. It approximates the response of the inverter PLL controls during voltage dips. If “Lvplsw” is set to “0” the Low Voltage Power Logic is not used and the LVPL and Rrpwr limits are not applied.

**Table 16. PV1G variables description**

EPCL Variable	Default Data	Description
Lvplsw	1.0	Connect (1) / disconnect (0) Low voltage Power Logic Switch
Rrpwr	10.0	LVPL ramp rate limit, p.u.
Brkpt	0.9	LVPL characteristic breakpoint, p.u.
Zerox	0.4	LVPL characteristic zero crossing, p.u.
Lvpl1	1.22	LVPL Breakpoint, p.u.
Volim	1.2	Voltage limit used in high voltage reactive current management function, p.u.
Lvpnt1	0.8	High voltage point for low voltage active current management function, p.u.
Lvpnt0	0.4	Low voltage point for low voltage active current management function, p.u.
Iolim	-1.3	Current limit in the high voltage reactive current management function, p.u.
Khv	0.70	Acceleration factor used in the high voltage reactive current management function

Converters are current controlled devices and their performance is highly dependent on current thermal limits. High voltage reactive current management unit monitors the reactive current injected into the network. If the converter terminal voltage is exceeded beyond the set “Volim” value, High voltage reactive current management unit restricts the reactive current injection. The low voltage active current management unit reduces the active current linearly as a

function of converter terminal voltage during low voltage events and captures the characteristics of active power under any such event.

#### 4.1.2. Converter Control model (PV1E)

This is first generation of converter electrical control systems. This block determines the active and reactive power to be delivered to the PV1G model based on the plant load flow model initial conditions. The control block diagram is shown in Fig. 4.2.

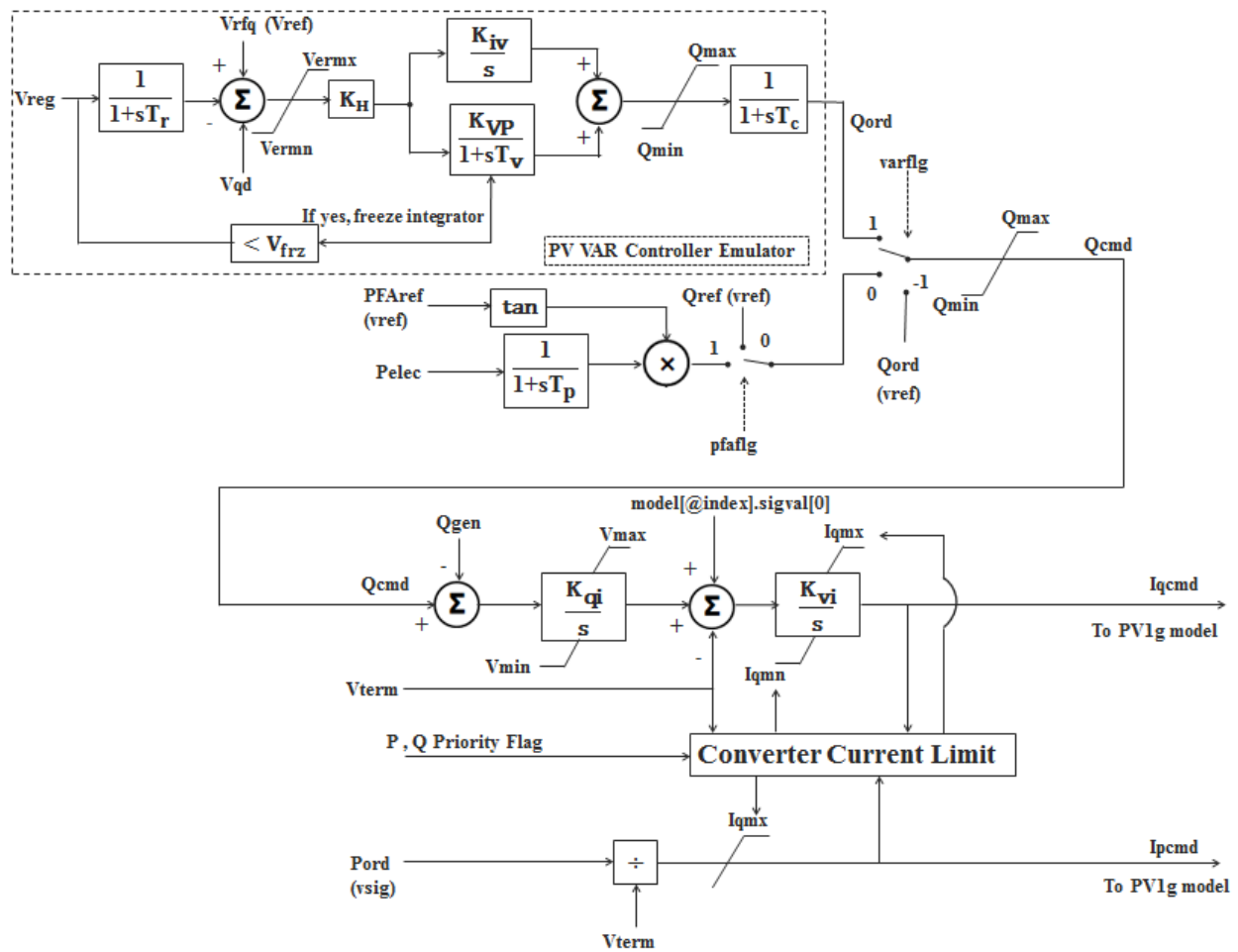


Fig. 4.2. PV1E model block diagram [26]

Detailed description of PV1E electrical control model parameters are shown in Table 17.

**Table 17. PVIE variables description**

EPCL Variable	Default Data	Description
Varflg	1	1 = Qord from PV plant VAR controller emulator; -1 = Qord from vref (i.e., separate model); 0 = constant
Kqi	0.1	Q control integral gain
Kvi	120	V control integral gain
Vmax	1.1	Maximum V at regulated bus (p.u.)
Vmin	0.9	Minimum V at regulated bus (p.u.)
Qmax	0.40	Maximum Q command (p.u.)
Qmin	-0.4	Minimum Q command (p.u.)
Tr	0.02	Voltage measurement lag, sec.
Tc	0.15	Lag time constant, sec.
Kpv	18.0	Regulator proportional gain
Kiv	5.0	Regulator integral gain
Pfaflg	0	1 = regulate power factor angle; 0 = regulate Q
Tv	0.05	Time constant in proportional path, sec.
Tpwr	0.05	Time constant in power measurement for PFA control (Tp), sec.
Iphl	1.24	Hard limit on real current, p.u.
Iqhl	1.25	Hard limit on reactive current, p.u.
Pqflag	0	0 = Q priority; 1 = P priority
Kdbr	10.0	Dynamic breaker resistor gain, p.u.
Ebst	0.2	Dynamic breaking resistor energy threshold, p.u.
Xc	0.0	Compensating reactance for voltage control p.u.
Kqd	0.0	Gain on Q Droop function
Tlpqd	0.0	Time constant in Q Droop function
Xqd	0.0	Compensating reactance for Q Droop function
Vermn	-0.1	Minimum limit on regulated bus voltage error, pu.
Vermx	0.1	Maximum limit on regulated bus voltage error, pu.
Vfrz	0.7	Voltage threshold to freeze integrators in PV plant VAR controller emulator voltage regulator, p.u.
Imaxtd	1.70	Maximum temperature dependent converter current limit

PV1E model includes a VAR control emulator that represents the effect of a centralized power plant controller. First generation of PV plant dynamic model does not implement full governor model for centralized plant controller. “Varflg” switch decides the Q-order, which should come from either a separate user written model via the `genbc[k].vref` signal (`varflg = -1`) or from the PV plant VAR controller emulator (`varflg = 1`). When a centralized plant controller is present in actual solar PV plant, it is possible to regulate voltage at a remote bus within plant or at inverter terminal voltage. This feature is implemented in PV1E model through VAR control emulator. With VAR control emulator, voltage at a remote bus (e.g. system interface) can be regulated by entering the bus identification as the second bus on the input record or generator terminal bus voltage can be regulated by omitting the second bus identification in dynamics data invocation. Centralized plant controller communicates with several inverters in a very small duration to vary their individual active and reactive power outputs. The time constant  $T_c$  in PV1E model reflects the delays associated with cycle time, communication delay, and filtering in the plant control. Q-controller integral gain “ $K_{qi}$ ” is an important parameter to obtain faster or slower system response during the post-disturbance period and it requires a parametric tuning as it depends on grid stiffness and converter control modes. The time constant of the Q-control loop is approximately equal to the equivalent reactance looking out from the plant terminals ( $= dV/dQ$ ) divided by  $K_{qi}$ ). Value of  $K_{qi}$  can be anywhere from 0.001 to 10.  $K_{qi} = 0.1$  is appropriate for a PV plant connected to a stiff system. For constant Q regulation (`varflg = pfaflg = 0`), the value of  $K_{qi}$  should be set to a very small number, e.g. 0.001 since this control is a slow reset. The default PV plant VAR controller emulator gains,  $K_{pv}$  and  $K_{iv}$ , are appropriate when the system short circuit capacity beyond the point of interconnection of the PV plant is 5 or more times the MW capacity of the PV plant. For weaker systems, these values should be reduced, e.g.

for  $SCC = 2$ ,  $K_{pv} = 13$  and  $K_{iv} = 2$  are recommended. The compensating reactance for voltage control,  $X_c$ , is used to synthesize a bus for regulating that is further into the power system than either the terminal bus or a remote bus. In actual practice PV plant do not regulate any far bus in the power system which do not lies within the plant. In case where, point of interconnection (POI) is far away from plant site (may be miles), then there may be substantial amount of voltage drop in the gen-tie, and hence this feature of line drop compensation can be implemented to compensate for reactive power/voltage droop. All parameters  $X_c$ ,  $K_{qd}$ ,  $T_{lpqd}$ , and  $X_{qd}$  are set to zero in all studies presented in this work.

## 4.2. Converter Control Modes

In this section PV1E model converter control modes are discussed.

### 4.2.1. Reactive Power Control Mode

In this model, Q-command comes from the load flow solution ( $Q_{cmd} = Q_{ref} = Q_{gen\_Loadflow}$ ) as shown in fig. 4.3. And both “Varflg” and “Pfaflg” are set to zero ( $Varflg=0$ ;  $Pfaflg =0$ ). This mode does not allow voltage regulation at either remote terminal or inverter terminal bus.

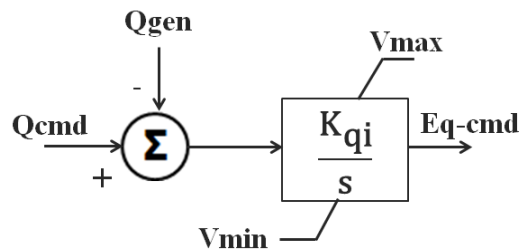


*Fig. 4.3. Reactive Power Control Mode*

### 4.2.2 Power Factor Control Mode

In this mode, “Varflg” is kept disabled ( $Varflg=0$ ) but “Pfaflg” is enabled ( $Pfaflg =1$ ). Reference power factor angle (PF<sub>Aref</sub>) is calculated from initial load flow solution based on  $P_{gen}$  and  $Q_{gen}$ . “PF<sub>Aref</sub>” and “ $P_{gen}$ ” is then used to determine reactive power command

“Qcmd” to PV1G model. Voltage regulation at either is not possible in this case also. Fig. 4.4 shows the model flag settings.

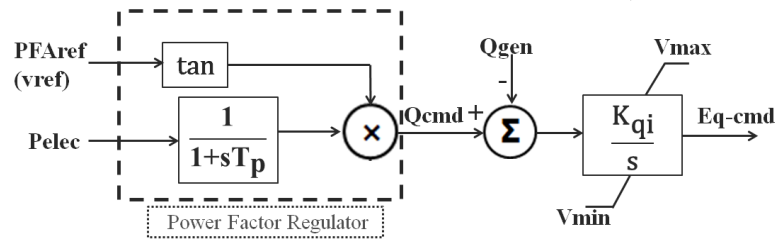


**Fig. 4.4. Power Factor Control Mode**

### 4.2.3. Plant Level Reactive Compensation

This mode sets and monitors the voltage at remote bus within plant to be equal to “Vrfq” which is defined initially in load flow solution. However, terminal voltage is still not regulated. To attain this, plant level VAR emulator is enabled by setting “Varflg=1” and Qcmd is derived from VAR emulator. Voltage controller integral gain “Kvi” is set to zero in this mode. Fig. 4.5 shows the model flag settings.

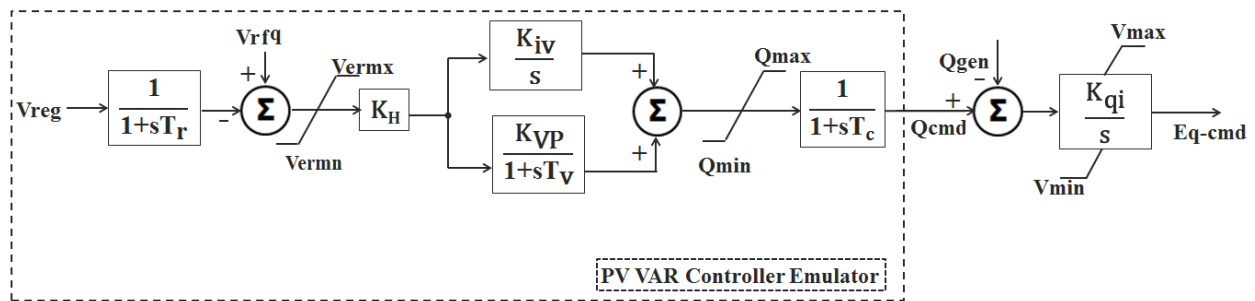


**Fig. 4.5. Plant Level Reactive Compensation Mode**

### 4.2.4. Voltage Control Emulation for Plant Level Reactive Compensation Mode

This mode brings together all features of plant level VAR emulator and converter control in practice and terminal voltage is controlled with faster control loop which provides good system response during fault events. In this mode “Varflg” is set to 1 which means that Qcmd is

derived from VAR emulator just like in previous case but “Kvi” is not set to “0”. Fig. 4.6 shows the model flag settings.

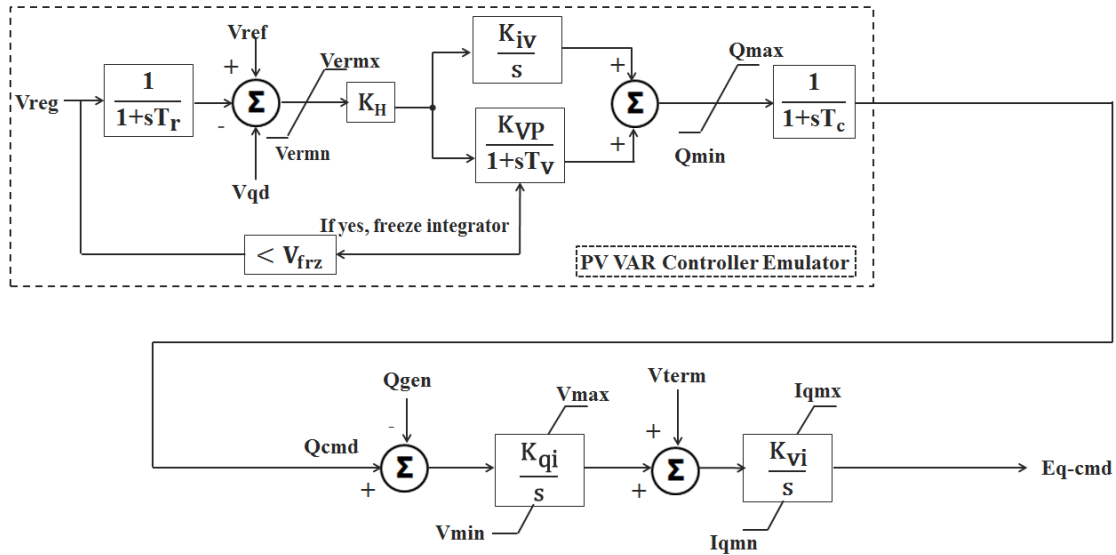


**Fig. 4.6. Voltage Control Emulation for Plant Level Reactive Compensation Mode**

### 4.3. Second Generation PV Plant Dynamic Models

Second generation solar PV plant dynamic model is under WECC approval and not available in GE PSLF or Siemens PSSE library yet. Beta version of these models is provided by GE for model validation purpose which is one of the objectives of this thesis. Second generation PV plant models are evolved from PV1G and PV1E models and are not very different from these, except that second generation models now includes a separate plant controller also known as Power Plant controller (PPC), which represents the centralized plant control emulator. A generalized model of central station PV system is shown in fig. 4.7. The overall model structure consists of a “generator” model (REGC\_A) to provide current injections into the network solution, an electrical control model (REEC\_B) for local active and reactive power control, and plant controller model (REPC\_A) to allow for plant-level active and reactive power control.



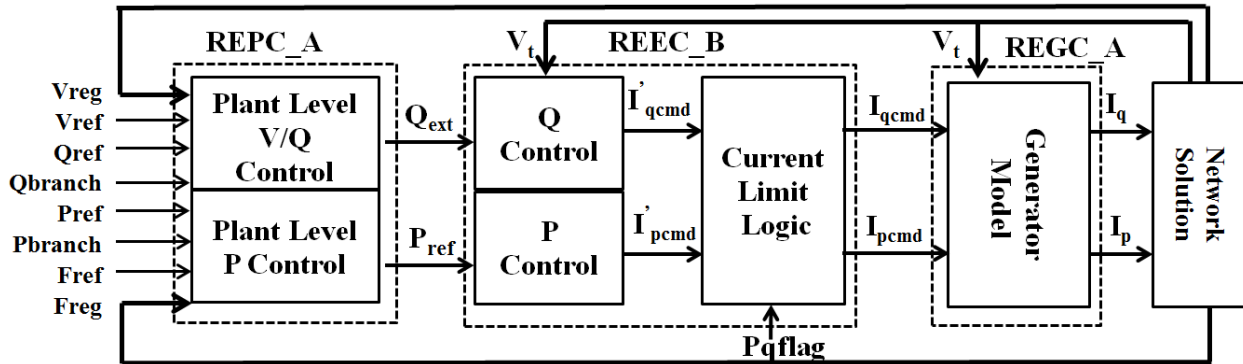


Fig. 4.7. Overall Model Structure for Central Station PV System [26]

### 4.3.1. Renewable Energy Generator Converter Model (REGC\_A)

The model is almost similar to PV1G model in all respects. It incorporates a high bandwidth current regulator that injects real and reactive components of inverter current into the external network during the network solution in response to real and reactive current commands from electrical controller model. Model block diagram is shown in fig. 4.8.

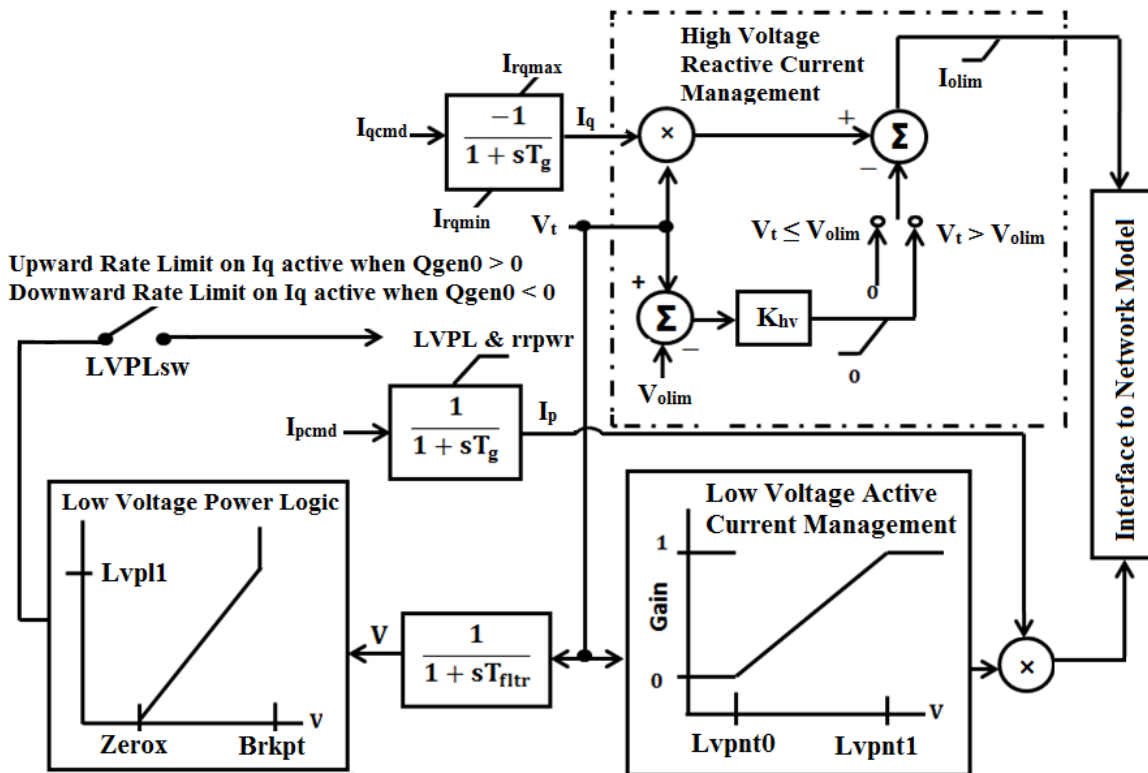


Fig. 4.8. REGC\_A Model Block Diagram [26]

### **4.3.2. Renewable Energy Electrical Controller Model (REEC\_B)**

Electrical controller model features two separate models within it – A local active power controller and a local reactive power controller. A prefix “Local” is added to ensure that this model represents only converter level active and reactive power control.

#### **4.3.2.1. Local Active Power Control (included in REEC\_B model)**

Active power control subsystem provides active current command to REGC\_A model. Active current command is subject to converter current limits based on thermal ratings, with user-selectable priority between active and reactive current through “pqflg”. REEC\_B model derives the active current command either from reference active power and the inverter terminal voltage determined as determined in load flow solution or, from plant controller model (REPC\_A), if it is present.

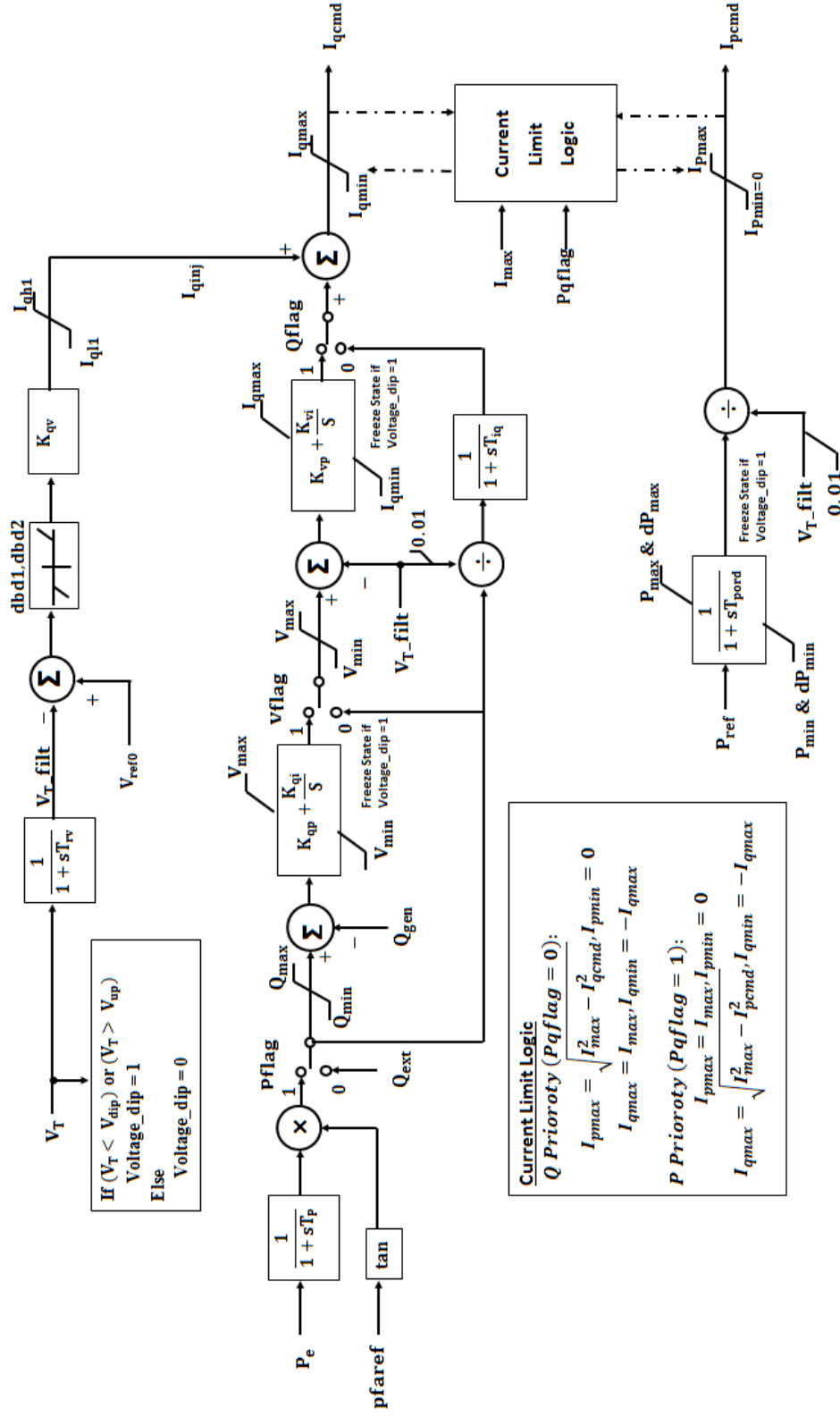
#### **4.3.2.2. Local Reactive Power Control (included in REEC\_B model)**

Reactive power control subsystem provides reactive current command to REGC\_A model. It is also subject to current limiting. The following control modes are accommodated –

- Constant power factor mode, based on the inverter power factor in load flow case
- Constant reactive power mode, based either on the inverter absolute reactive power in the solved load flow case or reactive power from power plant controller (if it is present).

Several switches with cascaded PI controllers to select between the proper control modes are modeled. These switches can bypass these PI regulators and directly derive a reactive current command from the inverter terminal voltage. Model block diagram in fig. 4.9 explain the complete model in detail.

Fig. 4.9. REEC\_B Model Block Diagram [26]



### 4.3.3. Renewable Energy Plant controller model (REPC\_A model)

This model represents centralized PV plant controller. Plant controller model (REPC\_A) is an optional model because not all solar PV plants are built with this centralized control unit. Power Plant Controller (PPC) is also termed as Smart Grid Interface (SGI), and provides plant-level control of active and/or reactive power. REPC\_A model block diagram is shown in fig. 4.10. This device communicates with several inverters in plant and commands them to vary their active and/or reactive power output within inverter kVA limits. REPC\_A model incorporates the following features –

- Remote bus located far away from plant can be regulated through closed loop voltage regulation with the provision of line drop compensation.
- Closed loop reactive power regulation on a user-designated branch within plant.
- Provides plant-level governor response derived from frequency deviation on the monitored bus.

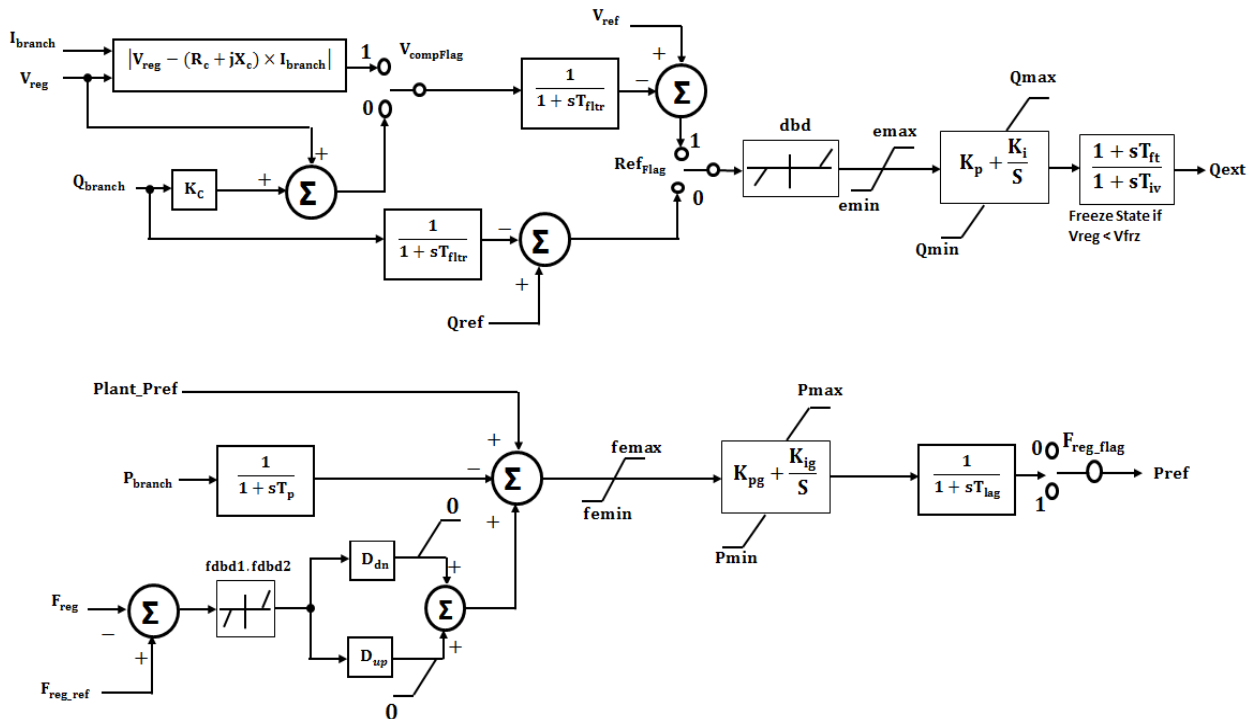


Fig. 4.10. REPC\_A Model Block Diagram [26]

#### 4.4. Active and Reactive Power Control Modes

With several user selectable switches in REGC\_A, REEC\_B and REPC\_A models there could be many possible combinations of operating modes for a solar PV plant model. Table 18 and 19, explains the models needed and the proper flag setting and/or input parameter settings for various active and reactive power control functionality.

**Table 18. Active Power Control Options**

Functionality	Model Needed	Freq_flag	Ddn	Dup
No governor response	REGC_A + REEC_B	0	N/A	N/A
Governor response with down regulation, only	REGC_A + REEC_B + REPC_A	1	> 0	0
Governor response with up and down regulation	REGC_A + REEC_B + REPC_A	1	> 0	> 0

**Table 19. Reactive Power Control Options**

Functionality	Models Needed	PfFlag	Vflag	Qflag	RefFlag
Constant local pf control	REGC_A + REEC_B	1	N/A	0	N/A
Constant local Q control	REGC_A + REEC_B	0	N/A	0	N/A
Local V control	REGC_A + REEC_B	0	0	1	N/A
Local coordinated V/Q control	REGC_A + REEC_B	0	1	1	N/A
Plant level Q control	REGC_A+REEC_B+ REPC_A	0	N/A	0	0
Plant level V control	REGC_A+REEC_B+ REPC_A	0	N/A	0	0
Plant level Q control+ local coordinated V/Q control	REGC_A+REEC_B+ REPC_A	0	1	1	0
Plant level V control + local coordinated V/Q control	REGC_A+REEC_B+ REPC_A	0	1	1	1

## **4.5. Case Study – Validation of First and Second Generation Generic Models**

Purpose of this case study is to compare and validate the user-written EPCL model, first generation model (PV1G & PV1E) and second generation model (REGC\_A, REEC\_B & REPC\_A) dynamic performance of a solar PV plant. To perform this study, a solar PV plant with active power output of 298 MW at POI is considered and positive sequence model is developed in PSLF. To validate these models against each other, dynamic response of each of the above mentioned models are compared for a bolted 3-phase LLLG fault at POI bus. Dynamics data file for each model is provided in Appendix-A.

### **4.5.1. System Description**

Test system load flow model comprises of 482 inverters each rated 630kW/700 kVA at 50°C. All inverters are modeled per WECC guidelines as discussed in previous chapter and are represented as one equivalent generator. System consists of 241 pad-mounted transformer medium voltage transformers with LV side rated for 324 V and HV side rated for 34.5 kV nominal voltages. Each pad mounted transformer is connected to two sets of PV inverters on LV side. PV plant under study is huge in size this is well clear from the fact that medium voltage collection system cable of 209669 feet (39.7 mile) is spread within the plant. Collection system equivalent impedance is calculated on 34.5 kV, 100 MVA base. This plant is connected to a 500 kV transmission line at the POI through a very short gen-tie of almost 500 feet. Two station transformers each rated 96/128/160 MVA step-up the voltage from 34.5 kV to 500 kV interconnection voltage level. In PSLF model these two station step-up transformers are represented as an equivalent single unit. Table 20, 21, 22, and 23 below provides the data for each electrical component of plant under study. A program is written in MATLAB to convert Gen-tie impedance data from  $\Omega$ /mile to per unit. This is provided in Appendix-B.

**Table 20. Inverter and pad mounted transformer data**

Transformer Data				
Transformer MVA Rating	1400	KVA		
Number of Transformer units installed	241			
Equivalent Transformer MVA Base	337.4	MVA		
High Side Voltage HV	34500	V	Delta	
Low side 1 Voltage LV X	324	V	Ungrounded Y	
Low side 2 Voltage LV Y	324	V	Ungrounded Y	
% Z @ 75°C, base kVA and Rated Voltage	5.5	%		
Positive Sequence Resistance and Reactance	%R	%X	Base kVA	
Primary to Secondary	1.0506	5.3987	1400	
Primary to Tertiary	1.0506	5.3987	1400	
Secondary to Tertiary	1.91	9.816	1400	
7 fixed tapes on HV windings +4/-2 at 2.5% per tap, De-energized tap changer				
Inverter Data				
Number of Inverters	482	Two inverters per transformer		
Power factor operating range of inverters	0.9	lag	0.9	lead
Name Plate Rating of Each Inverter	630	kW	700	kVA
MW Rating of generator in PSLF model @ 0.90 power factor	303.66	MW	337.4	MVA

**Table 21. Station step-up transformer data**

Station Transformer Data			
Rating in MVA (ONAN/ONAF1/ONAF2)	96	128	160
Nominal Voltage in kV (High/Low/Tertiary)	500	34.5	13.8
Winding Connection	Solidly Grounded Y	Solidly Grounded Y	Buried Delta
Positive Sequence Impedance (on 96MVA and 80°C)	9	%	
Exciting Current (100 % Voltage @ 96 MVA)	0.42	%	
No-Load Losses	92	kW	
Load Loss (I <sup>2</sup> R+Stray) at self-cooled rating at rated tap	157	kW	
Tap Changer on HV side(De-energized tap changer)	±2 × 2.5% taps		
Number of Transformer Units Installed	2		
Equivalent winding resistance on winding apparent power base (96 MVA) and winding voltage base	0.001635	p.u.	
Equivalent winding reactance on winding apparent power base (96 MVA) and winding voltage base	0.089985	p.u.	
Equivalent Magnetizing Susceptance	-0.004089	p.u.	

**Table 22. Collection system equivalent impedance**

Positive Sequence Impedance Data		
Beq=	0.059492546	p.u.
Req=	0.002135334	p.u.
Xeq=	0.014390011	p.u.

**Table 23. Gen-tie positive sequence Impedance data in p.u. on 100 MVA and 500 kV base**

Gen-tie Positive Sequence Impedance Data					
Line Length	0.0947	mile			
R <sub>pos</sub>	0.089232	Ω/mile	R <sub>pos</sub>	0.0000034	p.u.
X <sub>Lpos</sub>	0.728691	Ω/mile	X <sub>pos</sub>	0.0000276	p.u.
X <sub>cpos</sub>	170093	Ω/mile	B <sub>Cpos</sub>	0.0006959	p.u.

Table 24 shows the flag and other controller parameter setting for PV1G and REGC\_A model.

**Table 24. Parameter values for PV1G and REGC\_A for model simulation**

PV1G Model Parameters	Value	REGC_A Model Parameters	Value
Lvplsw	1	Lvplsw	1
Rrpwr	1.2	Rrpwr	1.2
Brkpt	0.9	Brkpt	0.9
Zerox	0.4	Zerox	0.9
Lvpl1	1.22	Lvpl1	1.22
Volim	1.1	Vtmax	1.1
Lvpnt1	0.1	Lvpnt1	0.1
Lvpnt0	0.05	Lvpnt0	0.05
Iolim	-1.3	qmin	-1.3
Khv	0.7	accel	0.7
		tg	0.02
		tfltr	0.02
		irqmax	99
		irqmin	-99
		xe	0

It is important to create correct load flow model for proper dynamic model initialization. If the load flow model is not initialized correctly, PSLF will display a warning during the



dynamics run. PSLF load flow model file for this test system is provided in Appendix-A. Table 25 shows the flag and other controller parameter setting for PV1E and REEC\_B model.

**Table 25. Parameter values for PV1E and REEC\_B in simulation model**

PV1E Model Parameters	Value	REEC_B Model Parameters	Value
mvab	337.4	mvab	337.4
Varflg	0	Vdip	0.9
Kqi	0.5	Vup	1.1
Kvi	120	trv	0.02
Vmax	1.1	dbd1	0
Vmin	0.9	dbd2	0
Qmax	0.66	kqv	0
Qmin	-0.66	iqh1	1
Tr	0.02	iq11	-1
Tc	0.2	vref0	0.7
Kpv	18	tp	0.05
Kiv	5	qmax	0.66
Pfaflg	1	qmin	-0.66
Fn	1	vmax	1.1
Tv	0.05	vmin	0.9
Tpwr	0.05	kqp	0
Iphl	1.1	kqi	10.072
Iqhl	1.1	kvp	10
Pqflag	0	kvi	60
Kdbr	10	tiq	0.02
Ebst	0.2	dpmax	99
Xc	0	dpmin	-99
Kqd	0	pmax	1
Tlpqd	0	pmin	0
Xqd	0	imax	1.1
Vermn	-0.1	tpord	0.02
Vermx	0.1	pfflag	1
Vfrz	0.7	vflag	1
Imaxtd	1.7	qflag	1
Viqlim	1.6	pqflag	0

All three test model (user-written EPCL code, PV1x and RExC) dynamics files are run for four seconds with reactive power priority. As a test stimulus, a bolted 3-phase LLLG fault is applied at point of interconnection Bus 99999 for duration of 9-cycles. Voltage, active power and reactive power are measured at equivalent inverter/ PV generator model. Pre-fault condition in all three models is kept same. Fig. 4.11 shows that, in all cases, voltage at equivalent inverter model terminals was 1.03 per unit.

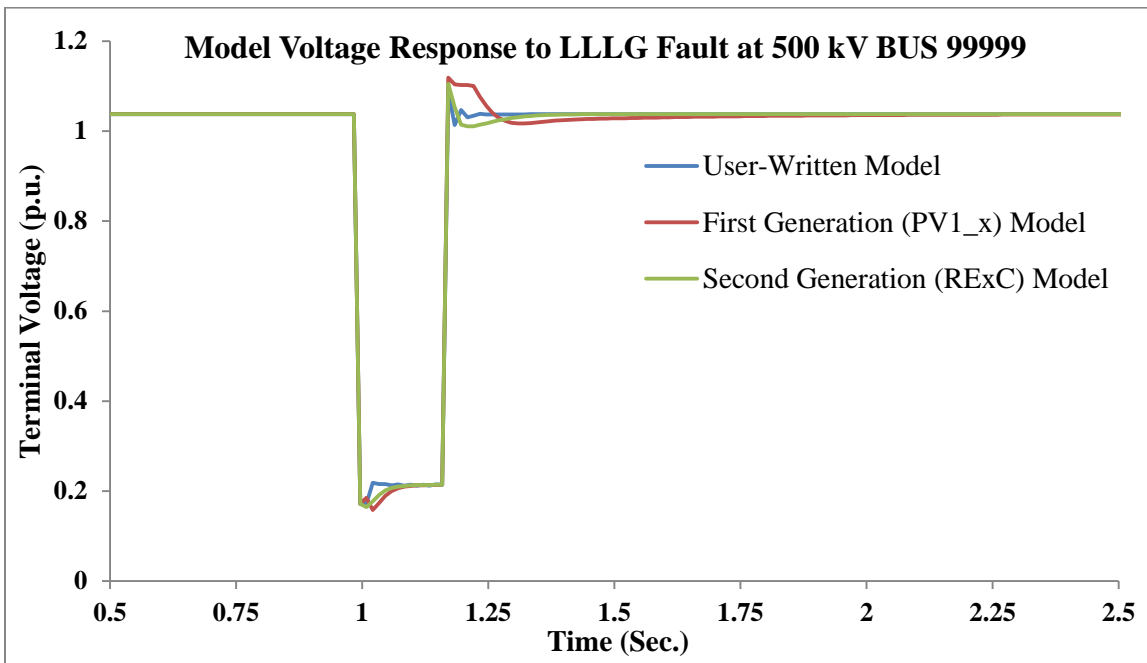


**Fig. 4.11. Voltage response of all three test models to 9-cycles LLLG fault**

When an external fault was applied, active power drops immediately to almost zero, but, the inverters did not tripped offline. Low voltage power logic steadily recovers the inverter from almost zero active power to full rated output as soon as the fault was cleared by protection devices. The low voltage active current management unit reduced the active current linearly as a function of converter terminal voltage as shown in fig. 4.12 during low voltage event. During voltage dip, Low Voltage Power Logic (LVPL) circuit allowed a controlled response of active current.

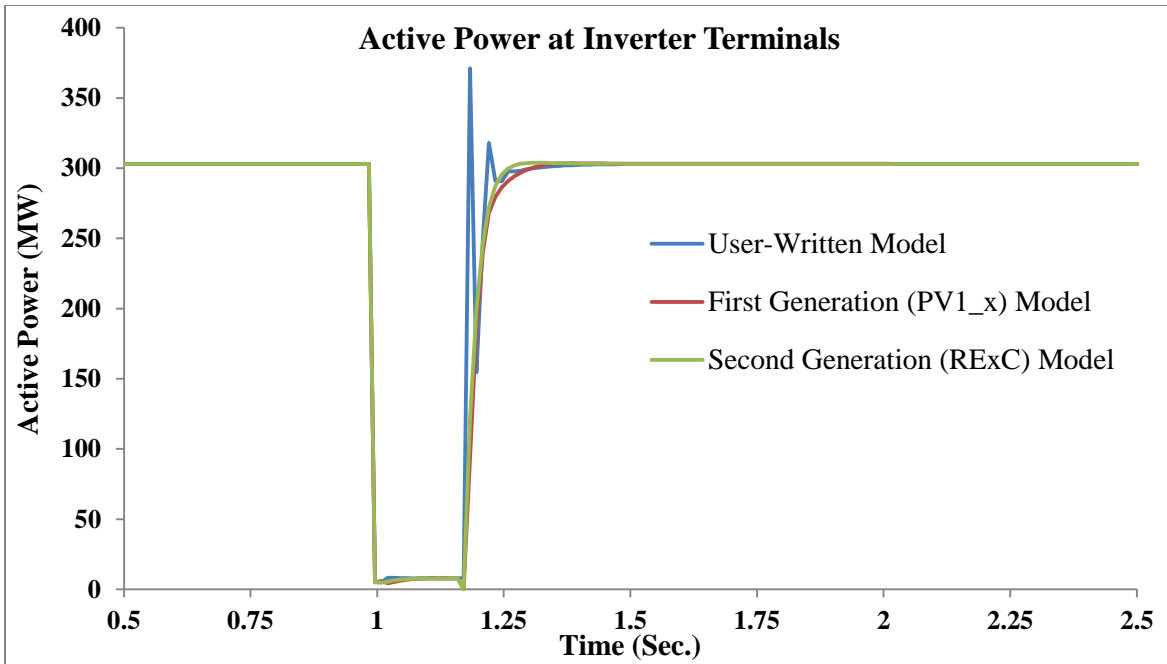


*Fig. 4.12. Active power at inverter terminals*

All models are implemented with Q-priority and local coordinated V/Q control with required flag settings.

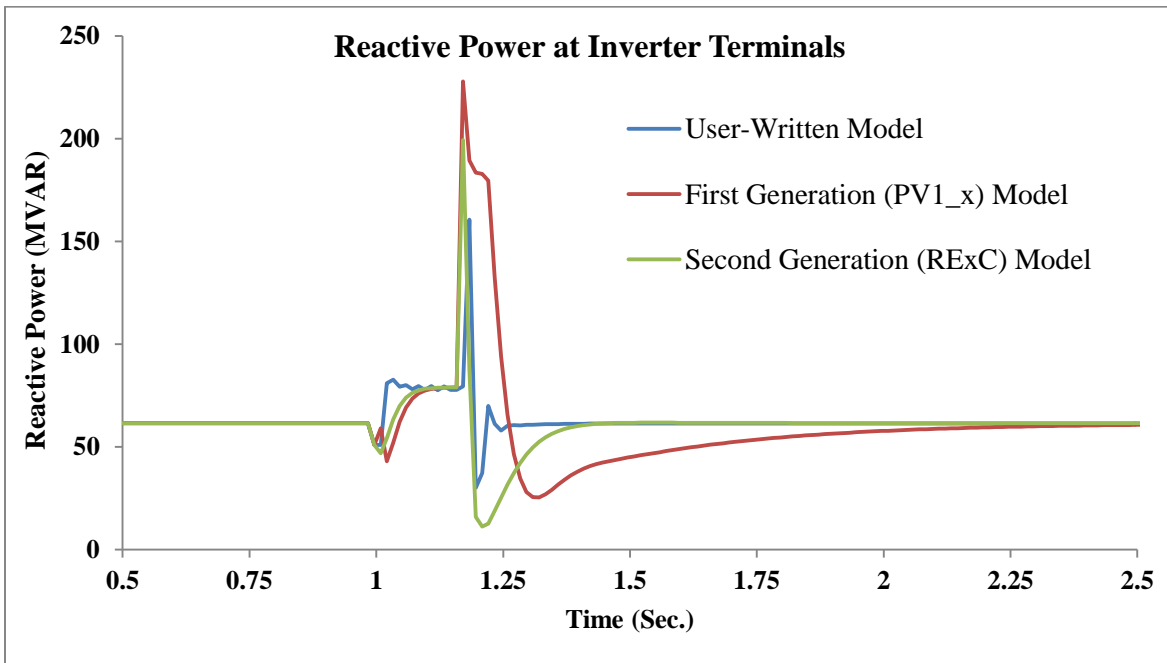


*Fig. 4.13. Reactive power response at inverter terminals*

Q-controller integral gain,  $K_{qi}$  is an important parameter to obtain faster or slower system response during the post-disturbance period. This is verified in fig.4.13, where it can be clearly seen that, since user-written model was implemented with  $K_{qi} = 100$ , therefore reactive power response during the post-fault period is extremely sharp. While in REEC\_B model  $K_{qi}$  was set 10.072 which gave it a little slower reactive power recovery. PV1E model implemented with  $K_{qi} = 0.5$ , apparently seems to have very sluggish reactive power recovery.

Significant spikes can be seen in active and reactive power plots upon inception and clearing of voltage dip. These spikes can be attributed to the fact that, the actual converter control system is of the order of kHz level and these simulations are performed on a positive sequence model where the integration time step is 4.167ms (1/4 cycle) for 60 Hz. Stability level model is unable to capture fast dynamics of the inverters during abrupt changes such as fault inception and clearing. However, actual control action is much faster (kHz) and so spike is much shorter in duration and likely much smaller in magnitude. In practice, some low-pass filters are also applied to remove high frequency noise in measured signals which also attenuates these spikes.

## **Conclusions**

With the above findings, where the first and second generation PV plant models proposed by WECC is validated against a user-written EPCL model for a particular inverter type, it has been proven that proposed plant models are fully capable of representing inverter behavior. Therefore generic plant models can suitably replace the EPCL models and reduce the complexity faced during the dynamic runs of a large power system with PV penetration.

## Chapter 5

### PROPOSED ALGORITHM AND ITS VALIDATION

#### Introduction

Performance and reliability of converter electrical controller and power plant controller models of solar PV plant solely depends on parameter tuning. Designing and tuning a proportional-integral (PI) controller appears to be theoretically instinctive, but it can be hard in practice, especially if multiple (and often conflicting) objectives such as short-transient and high-stability objectives are to be achieved. In practice, through multiple computer simulations, initial designs obtained need to be adjusted repetitively until the closed-loop system performance as desired is obtained. This led to the development of intelligent methods that can support engineers to obtain the best possible values of PI control parameters for the entire operating range or envelope.

This chapter proposes a novel hybrid method based on a classical Zeigler-Nichols (ZN) and adaptive Particle Swarm Optimization (PSO) technique to determine the converter controller (REEC\_B) and power plant controller (REPC\_A) optimal controller gains to meet system performance requirements. A new performance criterion in time domain is proposed to include the overshoot  $M_p$ , rise time  $t_r$ , settling time  $t_s$ , and steady-state error  $E_{ss}$ . Methodology proposed is discussed in detail with validation against real-time field captured data. A toolbox in MATLAB® 7.0 is developed to determine these controller gains. Obtained parameters are then imported into PSLF dynamic data file and validated for a 90 MW solar PV plant model to confirm the accuracy of estimated gains. REEC\_B controller gains are validated against the model response from EPRI WTGMV toolbox and REPC\_A model controller gains are validated against field measured plant data for a capacitor bank switching on medium voltage bus.

### 5.1. Performance Estimation of PI Controller

There are three most popular PI controller design methods that most commonly used in industrial practice. These methods are -

- Integrated Absolute Error (IAE)
- Integrated Squared Error (ISE)
- Integrated Time-weighted Squared Error (ITSE)

Reason for the popularity of these methods is that, it can be evaluated analytically in the frequency domain. In frequency domain, these performance criteria have their own advantages and disadvantages. For example, a disadvantage of the IAE and ISE criteria is that it can result in relatively small overshoot but a long settling time in the response, because the ISE performance criterion weights all errors equally independent of time. Although, Integrated Time-weighted Squared Error (ITSE) performance criterion can overcome the disadvantage of the ISE criterion, but its analytical formulas are intricate and onerous. The IAE, ISE, and ITSE performance criterion formulas are as follows:

$$\text{IAE} = \int_0^{\infty} |r(t) - y(t)| dt = \int_0^{\infty} |e(t)| dt \quad (24)$$

$$\text{ISE} = \int_0^{\infty} e^2(t) dt \quad (25)$$

$$\text{ITSE} = \int_0^{\infty} te^2(t) dt \quad (26)$$

Integrated squared error method is used as a performance measure for all the cases studied in this chapter.

### 5.2. Linearization of REGC\_A Model

In REGC\_A model active and reactive power is controlled by fast and high bandwidth regulators embedded in converter control. Inverter real and reactive currents are injected into external network in response to real and reactive current commands from high bandwidth current

regulator. Under transient conditions of severe voltage dips and relatively high system impedance, low voltage active current management unit performs a linear reduction of active current for terminal voltages below 0.8 per unit and approximates the response of the inverter phase locked loop (PLL) controls that results in controlled response of active current during and immediately after the voltage dips. Reactive current delivery remains high under these transient events to provide voltage support and short-circuit strength. For mathematical modeling and transfer function of the reactive component, the component must be linearized, which takes into account the major time constant and ignores the saturation and nonlinearities related to high voltage reactive current management block. The reasonable transfer function of these components may be represented as

$$\frac{I_q(s)}{I_{qcmd}(s)} = \frac{K_q}{1+T_g s} \quad (27)$$

Typical value of  $K_q$  is 1, and inverter current regulator lag time constant is very small, 0.02 seconds as mentioned in WECC solar PV dynamic model specification guide [26]. Generator model as implemented in MATLAB® Simulink is shown in fig. 5.1.

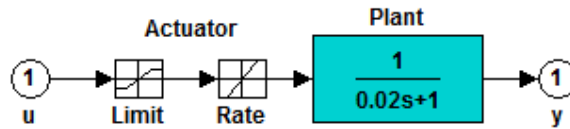


*Fig. 5.1. PV plant generator model in MATLAB Simulink*

### 5.3. Linearization of REEC\_B Model

Solar PV plant dynamic response during grid disturbance events are completely ruled by the converters. REEC\_B model has two modules: active power also called P-control and reactive power also called Q-control. Function of active power control subsystem is to provide active current command to the current injection model. This active current command is obtained from

reference active power and the voltage at inverter terminals. The reference active power is either taken as initial active power from the solved load flow case or from the plant controller model (REPC\_A) by enabling the pflag to 1 in REEC\_B model. Active current command always respects the apparent current limits. A user-settable “pqflag” option to choose between active and reactive current priority is implemented in the model. The reactive power control module delivers reactive current command to the current injection REGC\_A model. The gains  $K_{vp}$  and  $K_{vi}$  associated with voltage regulator are field adjustable and are tuned to meet performance objectives. Higher gain values result in better response to grid voltage disturbance, but there is a risk of instability because as the system deteriorates the closed-loop response gets faster. Q-controller integral gain  $K_{qi}$  is an important parameter to obtain faster or slower system response during the post-disturbance period and it requires a parametric tuning as it depends on grid stiffness and converter control modes.

If centralized power plant controller is absent, then reactive power is controlled by inverters local coordinated V/Q control. REEC\_B model can be realized with “pfflag” set to 1, Vflag set to 1 and Qflag set to 1. In this case net active power output and power factor at inverter terminals is used to calculate net reactive power input to Q-controller. Functional block diagram with above mentioned flag settings is shown in fig. 5.2 and model implementation in MATLAB® Simulink is shown in fig. 5.3.

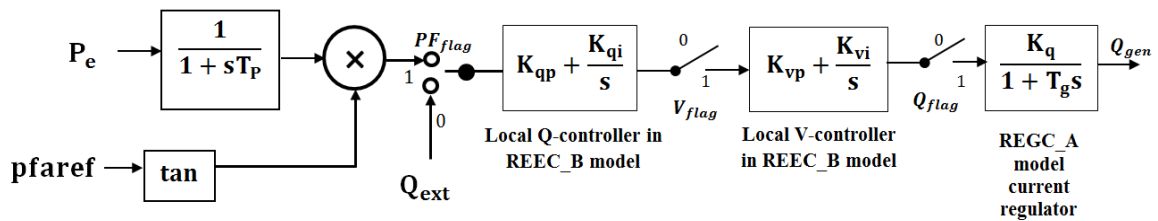


**Fig. 5.2. Simplified REGC\_A and REEC\_B with local V and Q-control loops**



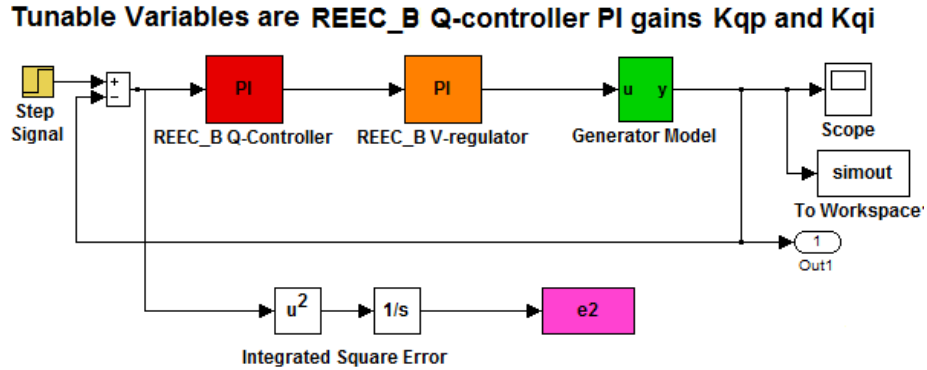


*Fig. 5.3. Plant model with REEC\_B block in MATLAB Simulink*

#### 5.4. Linearization of REPC\_A Model

The plant controller model REPC\_A is an optional model used when plant-level control of active and/or reactive power is desired. REPC\_A model has two separate loops, one for reactive power control and other for governor or active power control. In Q-control loop, if there are no monitored buses or monitored buses are absent in model invocation, then  $I_{branch}$ ,  $Q_{branch}$  and  $P_{branch}$  are set to zero, and  $P_{ref}$  is constant and is always equal to the initial values. In this mode of operation regulated bus voltage will be regulated, provided that  $V_{cmpflag}$  and  $Ref_{flag}$  are set to one. This would result in the simplified and linearized model for the Q-control loop by eliminating the non-linearity caused by dead-band block. To eliminate the effect of dead-band during tuning process, dead-band limits are set to zero. Fig. 5.4 shows block diagram of simplified REPC\_A block and fig.5.5 shows its MATLAB® Simulink implementation.

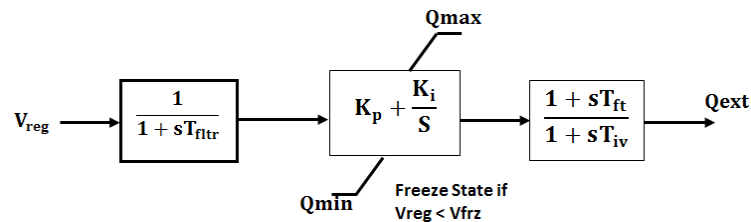


*Fig. 5.4. Simplified REPC\_A Q-Control model block diagram*

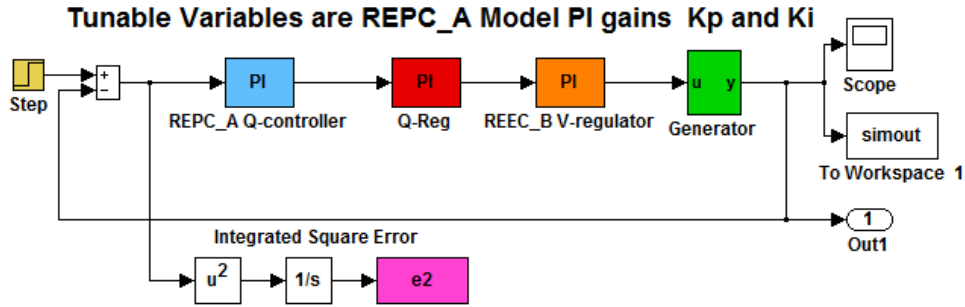


Fig. 5.5. Plant model with REPC\_A block in MATLAB Simulink

### 5.5. Complete Structure of Solar PV plant Q-Controller

Based on the reactive power control actions as described in chapter 4, and PV plant models linearization; an overall Q-controller model with plant level voltage control through REPC\_A model and local coordinated V/Q control through REEC\_B model can be represented in its most simplified form as shown in fig. 5.6 below.

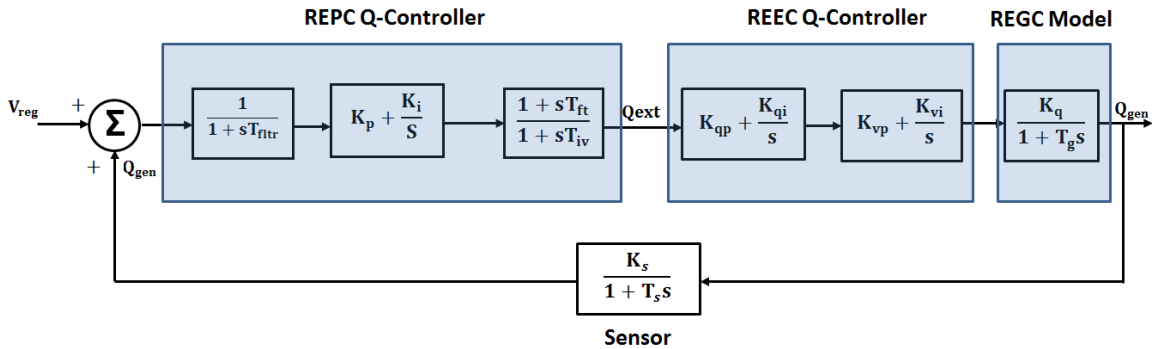


Fig. 5.6. Simplified overall solar PV plant Q-Control model block diagram

### 5.6. Overview of Particle Swarm Optimization (PSO) Technique

In 1995, Kennedy and Eberhart first introduced an evolutionary optimization technique called Particle Swarm Optimization method. The method is derived from the social theory of swarm such as fish schooling and bird flocking. It has been found robust in solving problems featuring nonlinearity and non-differentiability, multiple-optima, and high dimensionality

through adaptation [46]. It can be easily implemented, and has stable convergence characteristic with good computational efficiency.

Instead of using evolutionary operators to manipulate the particle (individual), like in other evolutionary computational algorithms, each particle in PSO flies in the search space with velocity which is adjusted dynamically according to particles own flying experience and its companions flying experience. Each particle in the swarm is treated as a volume-less entity in  $g$ -dimensional search space. Each particle keeps record of its flying path and remembers the coordinates in the solution space travelled so far, which are associated with the best solution also called as evaluating value, it has achieved so far in all moves. This value is called personal best or  $pbest$ . Each particle updates its  $pbest$  as soon as it reaches another optimal value lower or higher depending on that whether optimization problem is a minimization or maximization problem. Another value that is recorded by the particles is the overall best value, and its coordinates, obtained so far by any particle in the group. This is called the global best or  $gbest$ .

The PSO concept consists of, at each time step, changing the velocity of each particle toward its  $pbest$  and  $gbest$  locations. Fig. 5.7 shows the general concept of modification of search point by PSO.

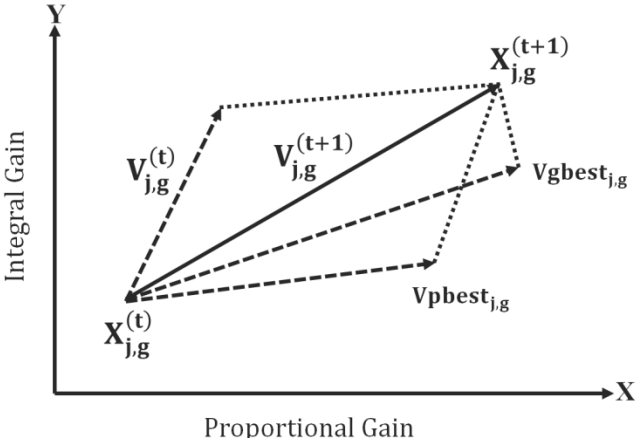


**Fig. 5.7. General Concept of modification of search point by PSO**

Acceleration is biased by a random numbers, with separate random numbers being generated for acceleration toward pbest and gbest locations. For example, the  $j^{\text{th}}$  particle is signified as  $x_j = (x_{j,1}, x_{j,2}, \dots x_{j,g})$  in the  $g$ -dimensional solution space. The set of best personal values attained so far by the  $j^{\text{th}}$  particle during its flying experience can be represented as  $pbest_j = (pbest_{j,1}, pbest_{j,2}, \dots pbest_{j,g})$ . The best particle among all of the particles in the group is represented by the  $gbest_g$ . The velocity of the  $j^{\text{th}}$  particle is represented by a vector as  $V_j = (V_{j,1}, V_{j,2}, \dots V_{j,g})$ . The modified or the updated velocity and position of each particle can be calculated using the current velocity and the distance from  $pbest_{j,g}$  to  $gbest_g$  as using (28) and (29) below-

$$V_{j,g}^{(t+1)} = \omega \cdot V_{j,g}^{(t)} + C_1 \text{rand} \left( pbest_{j,g} - x_{j,g}^{(t)} \right) + C_2 \text{rand} \left( gbest_g - x_{j,g}^{(t)} \right) \quad (28)$$

$$x_{j,g}^{(t+1)} = x_{j,g}^{(t)} + V_{j,g}^{(t+1)} \quad \forall j = 1, 2, \dots, n \text{ and } g = 1, 2, \dots, m \quad (29)$$

Where,

$n$  = number of particles in a group &  $m$  = number of members in a particle;

$t$  = number of iterations (generations);

$V_{j,g}^{(t)}$  = velocity of particle  $j$  at iteration  $t$ ,  $V_g^{\min} \leq V_{j,g}^{(t+1)} \leq V_g^{\max}$ ;

$\omega$  = Inertia weight factor;

$C_1, C_2$  = Acceleration constant;

rand = Random number between 0 and 1;

$x_{j,g}^{(t)}$  = Current position of particle  $j$ ;

$pbest_{j,g}$  = personal best of particle  $j$ ;

$gbest_g$  = global best of the group  $g$ .

PSO algorithm is initialized with a random seed in the very first iteration within the feasible solution search space. In context of PI controller gain estimation, one dimension of this search space represents proportional gain and other represents integral gain. Initial position of particles is decided randomly in this search area using  $\text{rand}()$  function, where the minimum and maximum limits of the search region are defined by the user. Also, since initially there is no personal record and global record of flying experience, therefore at first iteration, any point within the search region is defined as the personal and global best. During first iteration, particles own no velocity. Velocity and position for next iterations are then calculated using (28) and (29) and pbest and gbest are updated as the algorithm iterates.

### **5.6.1. Parameter Selection**

Since its origin, much work has been done to understand and develop the ideal parameters for PSO implementation. The goal was to develop an algorithm with an optimal balance between global exploration and exploitation of local maxima. Without any boundaries or limits on the velocity, particles could essentially fly out of the physically meaningful solution space. One approach at solving this problem is to simply enforce a maximum allowed velocity called  $V^{\max}$ . But the parameter  $V^{\max}$  requires a resolution, or fitness, with which solution space be examined between the current position and the target position. If  $V^{\max}$  is too high, particles might fly past worthy solutions. If  $V^{\max}$  is too small, particles may not reach out of the local optimal solutions. In many experiences with PSO,  $V^{\max}$  is often set at 10% - 20% of the dynamic range of the variable on each dimension of the search space [38].

The constant  $C_1$  called as self-constriction factor and  $C_2$  often called as social-constriction factor represent the weighting of the random acceleration terms that pull each particle towards the best possible solution [39]. Low values of these factors allow particles to travel far from the

goal before they can be pulled back within the actual target region. On the other hand, high values result in abrupt movement toward, or past, target regions. Hence, the acceleration constants  $C_1$  and  $C_2$  are both set as 2.

Various values of inertial weights have been suggested, attempting to strike a balance between global exploration and local exploitation. Larger inertial weights tend to encourage global exploration as a result of the particle being less moved by the pull of  $p_{best}$  and  $g_{best}$  instead preferring to fly nearer to its original direction. The analogy follows that it is more difficult to influence the heavy particles to deviate from their flight path. Conversely, a small inertial weight encourages local exploitation in that particles are rapidly pulled toward  $p_{best}$  and  $g_{best}$ . Realizing the importance of exploration early in the run, and the increasing importance of exploitation of maxima as the run progresses, it was suggested in literature [46] that varying the inertial weight linearly from 0.9 to 0.4 over the course of the run is most appropriate. Inertia weight  $\omega$  plays an important role in maintaining a balance between local and global exploration, Proper inertia weight could result in less iteration to find a sufficiently optimal solution. In general, the inertia weight  $\omega$  is set according to the following equation-

$$\omega = \omega_{\max} - \frac{\omega_{\max} - \omega_{\min}}{\text{iter}_{\max}} \times \text{iter} \quad (30)$$

Where  $\text{iter}_{\max}$  is the maximum number of iterations (generations), and  $\text{iter}$  is the current number of iterations. When applying this technique it is important to take care in choosing a reasonable number of iterations. If the maximum number of iterations is too large, the PSO may stagnate, waiting for the decrease in inertial weight to begin exploitation of the maxima. Likewise too few iterations could result in exploitation of local maxima before the swarm has had time to adequately explore the solution space and find the greater global maximum. Population size is another parameter that necessitates careful selection. Large populations, while

providing the most thorough exploration of the solution space, come at the cost of more fitness evaluations and computation time. For the PSO, it has been found that relatively small population sizes can sufficiently explore a solution space while avoiding excessive fitness evaluations. Parametric studies have found that a population size 20 particles have been effective for solving engineering problems.

### 5.6.2. Fitness Function Definition

Performance criterion in time-domain used to evaluate the PI controller in this work is explained here. In time-domain performance criteria, it is important to understand that a decent value of parameters ( $K_p$  and  $K_i$ ) combination can return a good system step response. The time-domain performance criteria include rise time ( $t_r$ ), settling time ( $t_s$ ), maximum overshoot ( $M_p$ ), and steady-state error ( $E_{ss}$ ). A new performance criterion, in time domain, can be defined as -

$$\min_{K:\text{stabilizing}} W(K) = (1 - e^{-\beta}) \cdot (M_p + E_{ss}) + e^{-\beta} \cdot (t_s - t_r) \quad (31)$$

where  $K$  is  $[K_p, K_i]$ , and  $\beta$  is the weighting factor.

Weighting factor  $\beta$  is an important parameter to satisfy the controller design requirements. It requires some trade-off between different performance measures. For example, value of  $\beta$  larger than 0.7 can reduce maximum overshoot and steady-state error, but to reduce rise time and settling time,  $\beta$  should be less than 0.7.

Fitness function is therefore a kind of evaluation value of each particle in the group. The fitness function  $f$  is defined as the inverse of time-domain performance criterion  $W(K)$ . It implies that a smaller of  $W(K)$  would indicate higher evaluation or fitness of each individual particle.

$$f = \frac{1}{W(K)} \quad (32)$$

### 5.6.3. PSO flowchart to determine controller gain values

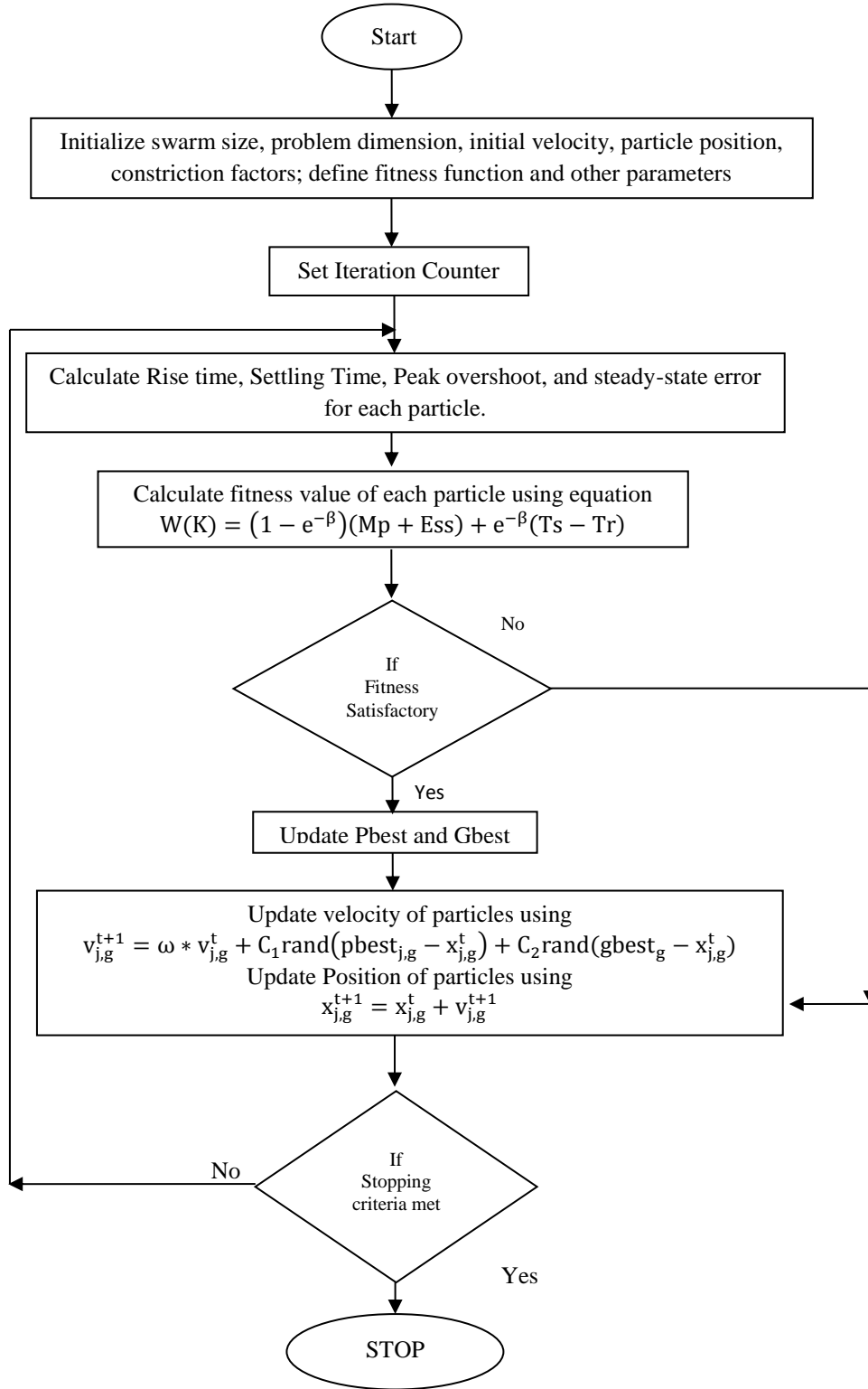


**Fig. 5.8. Algorithm for PSO method**



## 5.7. Algorithm for Proposed ZN-PSO Method

In this work, a hybrid method using PSO algorithm in conjunction with classical Zeigler-Nichols method is proposed to determine the unknown controller gains of solar PV plant dynamics model. Zeigler-Nichols method is used at the first place to determine REEC\_B model local V-controller gains ( $K_{vp}$  and  $K_{vi}$ ). The PSO algorithm is mainly utilized to determine local Q-controller gains ( $K_{qp}$  and  $K_{qi}$ ) of REEC\_B model and, reactive power control loop gains ( $K_p$  and  $K_i$ ) of REPC\_A model. A simplified flow model of the proposed methodology is shown in fig. 5.9. Step-by-step process is discussed in section 5.7.1 - 5.7.4. MATLAB code for ZN-PSO method is given in Appendix-C.

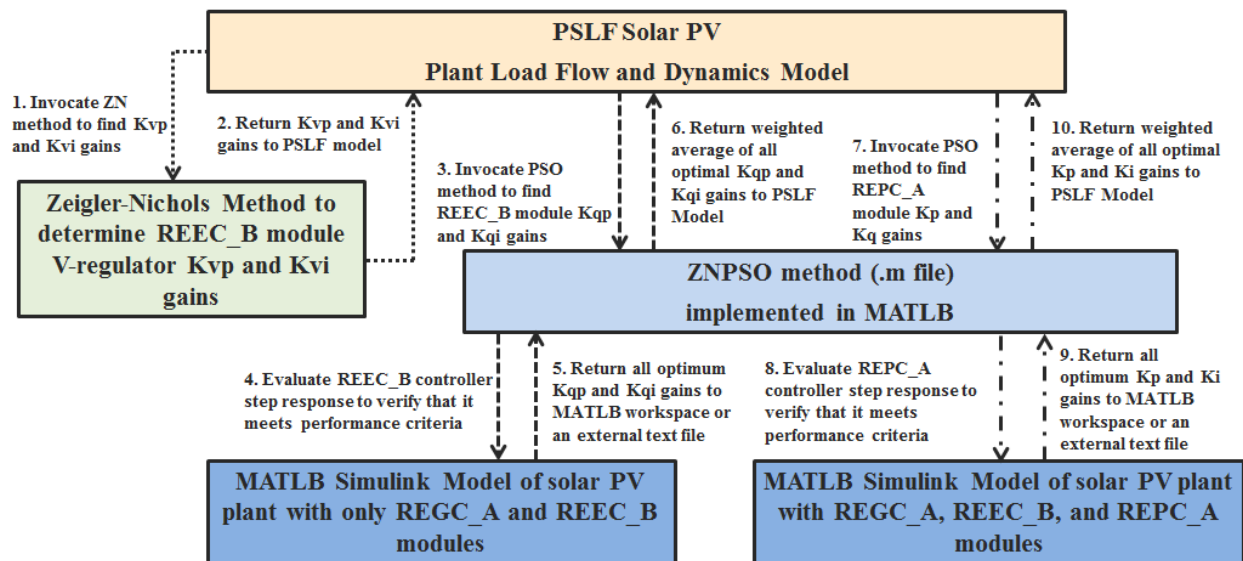


*Fig. 5.9. Work flow model of proposed methodology*

### 5.7.1. STEP A (Setting up GE PSLF model)

1. Create load flow (.sav file) and dynamic model (.dyd file) of solar PV plant in PSLF with REGC\_A (PV Generator Model), REEC\_B (Electrical Controller Model) and REPC\_A (Power Plant Controller Model). Initialize all steady state parameters properly.

- Initially, keep Power Plant Controller (REPC\_A) disabled in PSLF dynamic model and tune voltage regulator using Zeigler-Nichols method. While tuning the voltage regulator gain values ( $K_{vp}$  and  $K_{vi}$ ),  $K_{qp}$  and  $K_{qi}$  should be set to zero “0” in REEC\_B model.

### 5.7.2. STEP B (Finding Voltage Regulator Gains in REEC\_B model)

- Set  $K_{vi} = 0$ . Run dynamic simulation and gradually increase  $K_{vp}$  starting from zero until it reaches ultimate gain  $K_u$  at which the output of the loop starts to oscillate. Note the ultimate gain  $K_u$  and the oscillation period  $P_u$ .
- Calculate the integral ( $K_{vi}$ ) and proportional ( $K_{vp}$ ) gains by Zeigler-Nichols Method using the following Table 26.

*Table 26. ZN controller gain calculation table*

Controller Type	$K_{vp}$	$K_{vi}$
Proportional	$0.5K_u$	-
Proportional-Integral	$0.45K_u$	$1.2K_{vp}/P_u$
Proportional-Integral-Derivative	$0.60K_u$	$2K_{vp}/P_u$

### 5.7.3. STEP C (Finding Q-Regulator Gains in REEC\_B model)

- Now, model PV generator as first-order system having a time constant of 0.02 seconds and REEC\_B V-regulator modeled as PI-controller with gain values ( $K_{vp}$  and  $K_{vi}$ ) as obtained above in MATLAB Simulink®. Q-regulator is modeled as PI-controller with unknown gain values  $K_{qp}$  and  $K_{qi}$ .
- Run ZNPSO.m program with proper parameter initialization, like swarm population, iteration counts, constriction factor and inertia weights. Set desired controller evaluation parameters, like maximum allowed overshoot, steady-state error, rise time and settling time.

7. Store all  $K_{qp}$  and  $K_{qi}$  gain values that meet the desired controller evaluation parameters, like maximum allowed overshoot, steady-state error, rise time and settling time in data\_REEC.txt file at the program termination.
8. Calculate weighted average of  $K_{qp}$  and  $K_{qi}$  values and test it in PSLF dynamic program by applying a LLLG fault at POI.

#### **5.7.4. STEP D (Finding Power Plant Controller PPC Gains in REPC\_A model)**

9. Now input the Q-regulator gains values as obtained above in PI-controller for reactive power and model PPC as another PI-controller with unknown gains in MATLAB Simulink® model.
10. Rerun ZNPSO.m and collect all possible sets of  $K_p$  and  $K_i$  gain that satisfies the desired controller evaluation parameters in data\_REPC.txt file. Calculate weighted average of  $K_p$  and  $K_i$  values.
11. Now enable the REPC\_A model in PSLF dynamic model and set “pfflag” to “0” in REEC\_A model because reactive power command for all inverters will now be sent by centralized power plant controller.
12. Calculate the lag-time constant for lag compensator in REPC\_A model as  $T_{fv} = \frac{K_p}{K_i}$ .
13. Test the system performance by running dynamic tests in PSLF on complete plant model with all controllers enabled.

#### **5.8.1. Case Study 1 – REEC\_B model controller gain tuning with proposed algorithm**

This section describes a real-time problem faced by every interconnecting PV facility and a solution to it based on the proposed algorithm. This case study explains how the proposed algorithm can be efficiently used to determine the optimal controller gains for PV plant REEC\_B model without performing a factory test.

EPRI has developed a tool called Wind Turbine Generator Model Validation [27] version1.0 (WTGM V1.0) that can be used to fit controller parameters and/or validate generic model for wind plants. Since solar PV plant models are derived from wind generator type 4 full converter models, WTGM V1.0 tool is also used by interconnecting facilities/utilities for solar PV plant model validation just by disabling the turbine model (WTGT\_A). A general flowchart of model validation and/or controller tuning using WTGM V1.0 tool is shown in fig. 5.10.

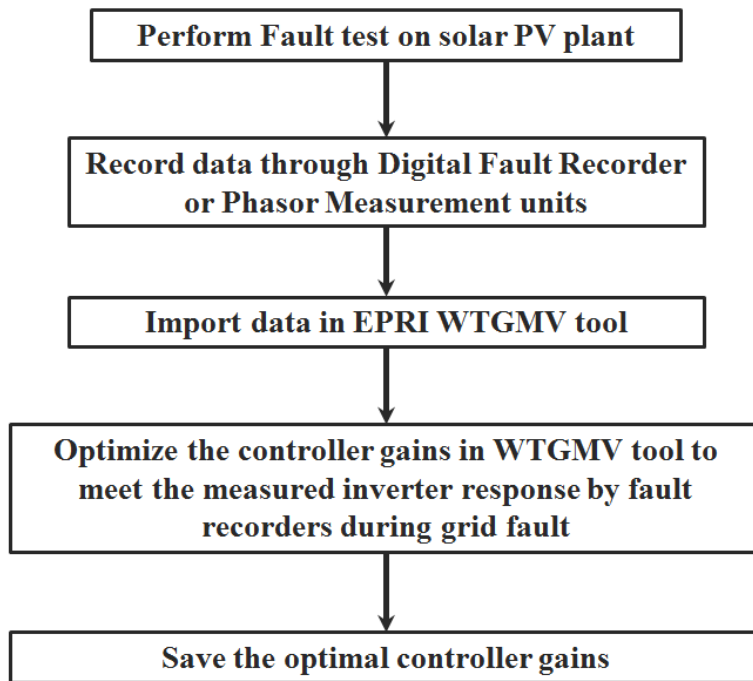


***Fig. 5.10. WTGM V1 model validation process***

In this tool, validation is achieved based on measured field data from a digital fault recorder (DFR) or phasor measurement unit (PMU) located at wind turbine generators WTG, or through factory test data provided by turbine manufacturer. This tool requires the data acquisition at converter/inverter terminals for a fault or voltage-depression event on the grid. Model validation requires positive sequence data recorded at a sampling rate of at least 30-60 samples per second. Such field tests are difficult to carry out by inverter manufactures to obtain

this field data. On the other hand, WECC requires all interconnection facilities to provide PV plant equivalent generator model (inverter model) data in generic format i.e. REGC\_A and REEC\_B model format.

Inverter manufactures usually provides WECC format data for a small laboratory test PV plant model and not for actual PV plant facility. Several model parameters are highly dependent on actual plant design, collection system impedance, plant MVA rating, grid short-circuit strength etc. For example time constant of Q-control loop depends on equivalent reactance looking out from the plant terminals ( $=dV/dQ$ ) divided by Q-control loop integral gain  $K_{qi}$ . Similarly, power plant controller PI gain values depend on system short circuit capacity beyond the point of interconnection. Therefore it is important to model the complete plant model and perform dynamic stability study on it. Upon request, manufacturers provide a detailed user-written EPCL model of their inverter, which unfortunately is not accepted by WECC anymore.

This left the interconnection facilities with only one option, that is, to use EPCL code to simulate their plant model in PSLF or PSSE, and import the measured response for a grid-fault into WTGM V1.0 tool and tune REEC\_B model until they hit the correct gain values. This is a cumbersome and time taking process which sometime takes weeks to complete the solar PV plant dynamics model in WECC approved format. Fig. 5.11 shows this model validation process.

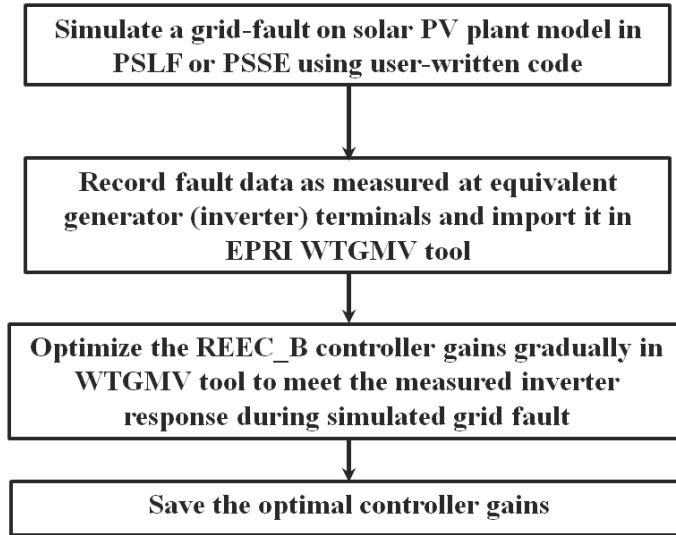


*Fig. 5.11. WTGMV model validation using user-written inverter model*

Proposed ZN-PSO method can provide a better alternative to this validation process, which neither requires data from field tests, nor the user written model file from inverter manufacturer. This method is already described in Section 5.7 of this chapter. If the PV plant does not have a centralized power plant controller then only Steps A, B and C are to be followed to determine the REEC\_B model PI gains. Fig. 5.12 illustrates the flow for parameter estimation.

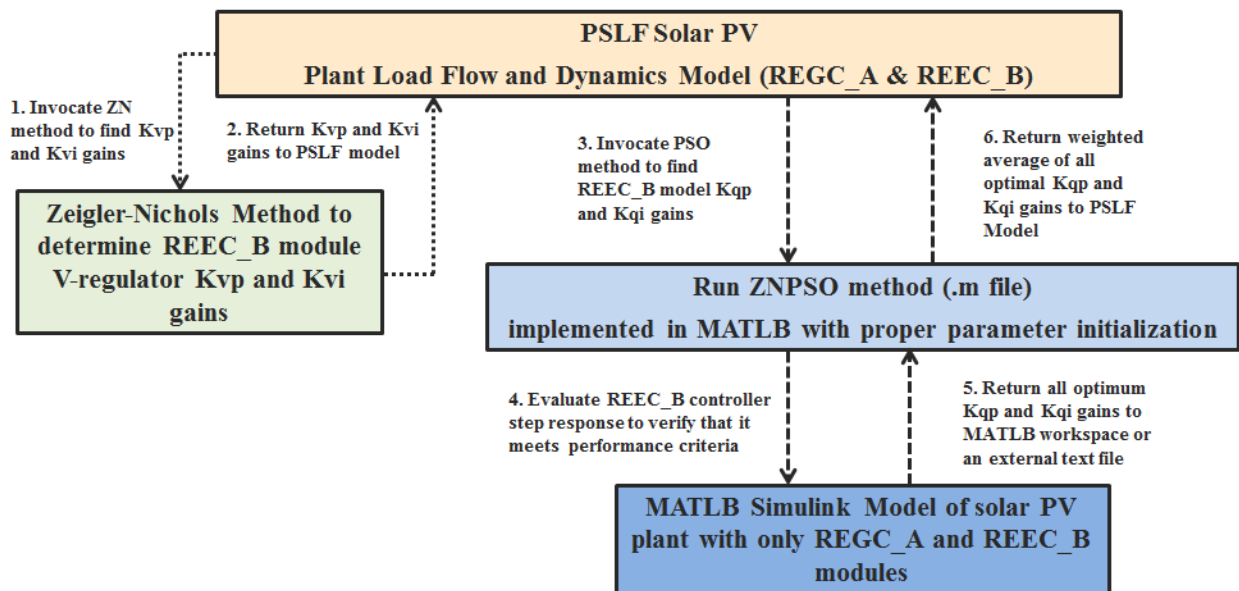


*Fig. 5.12. ZN-PSO method to find V and Q-controller gains in REEC\_B model*

To validate the performance accuracy and efficiency of ZN-PSO method, to find REEC\_B model controller gains, a 90 MW PV plant test model is developed and simulated. Plant steady state and dynamics model is developed in PSLF v18.1. Fig. 5.13 shows the equivalent load flow model of this 90 MW solar PV plant. Plant is shown connected to a 500 kV bus, operated at 1.05 per unit voltage. Grid side is modeled as an infinite generator with  $r_a = 0.0002$  and  $l_{ppd} = 0.0072$  per unit.

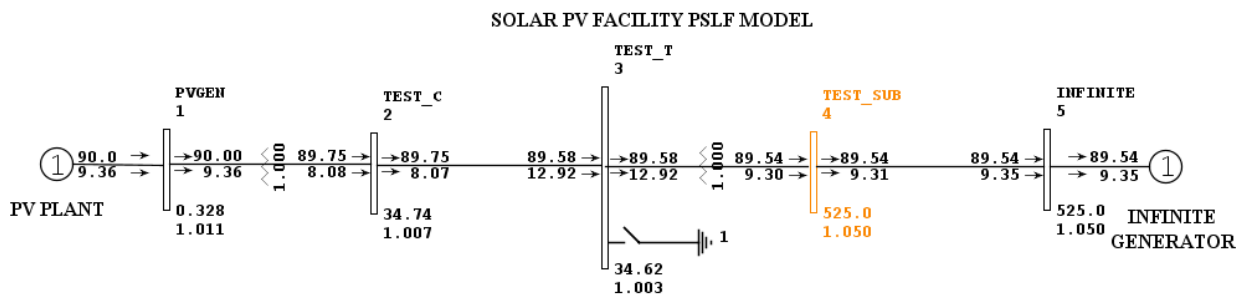


**Fig. 5.13. PSLF load flow model of PV plant under test**

Two test cases are developed to validate the proposed methodology - In the first case above shown plant model is simulated for 18 cycles LLLG fault at infinite bus # 5 with user-written inverter model (EPCL model) and procedure shown in fig. 5.11 above is followed to determine the correct controller gains. In the second case, same plant model is again simulated for 18 cycles LLLG fault at bus # 5 but with second generation WECC generic (REGC\_A & REEC\_B) dynamic models and procedure shown in fig. 5.12 for ZN-PSO method is followed to find the controller gains. Value of V-controller ( $K_{vp}$  and  $K_{vi}$ ) and Q-controller ( $K_{qp}$  and  $K_{qi}$ ) gains as obtained from both methods are compared to validate the accuracy of ZN-PSO method. In both models, voltage dips are recognized when the voltage drops below 90% of the previous minute average voltage. The voltage dip is assumed to be cleared when the voltage rises above 95% of this reference voltage. During grid faults which are seen as voltage dips at the grid

interconnection point of the inverter, reactive current must be contributed to support the voltage according to current grid codes as shown in fig.5.14.

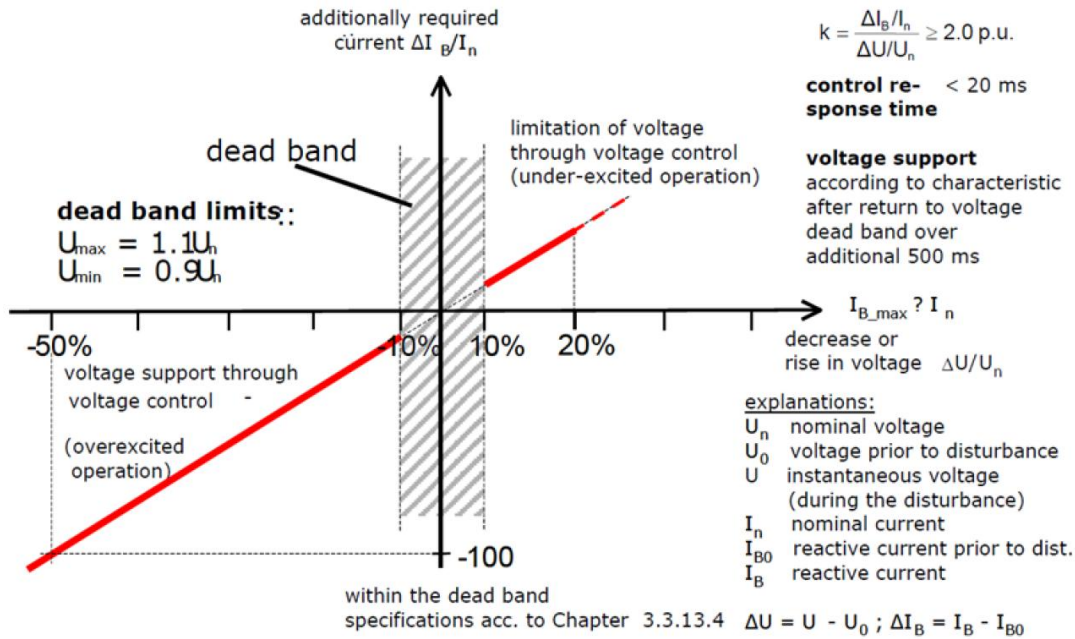


Fig. 5.14. Voltage support during grid fault according to grid codes

Fig. 5.15 shows the input data for case with user-written model.

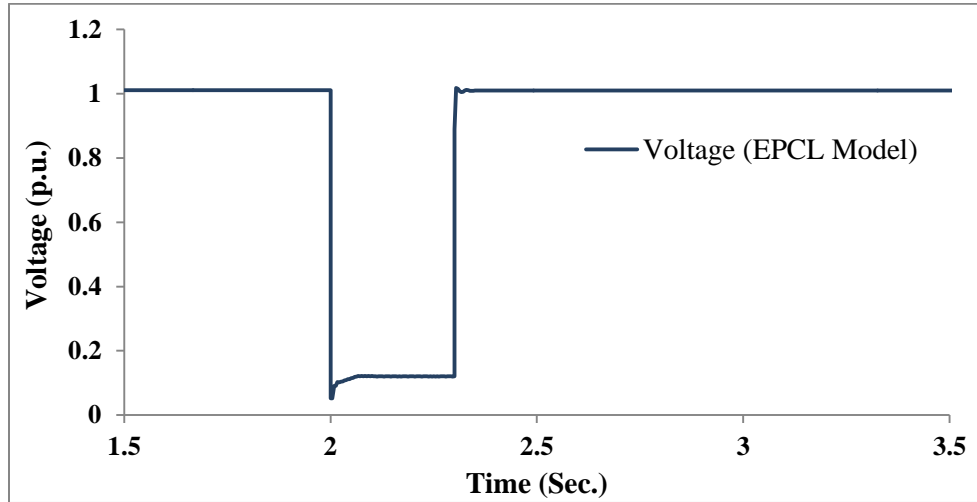
```

/* Input parameters:
/* rsrc = source resistance, pu (0.0)
/* xsrc = source reactance, pu (0.0)
/* vratio = PV array Voc to Vmp voltage ratio (1.2)
/* Iratio = PV array Isc to Imp current ratio (1.1)
/* Tdc = inverter dc cap bank time constant, sec (0.010)
/* Ilim = inverter ac current limit, pu (1.10)
/* Kpdc = dc voltage regulator proportional gain (2.0)
/* Kidc = dc voltage regulator integral gain (20.0)
/* MOD = mode of operation (0 =power factor control, 1= reactive power control)
/* PFLGmin = minimum overexcited power factor (0.93)
/* PFLDmin = minimum underexcited power factor (0.93)
/* OV1L = overvoltage trip point #1, pu (1.20)
/* OV1T = overvoltage delay #1, sec (0.10)
/* OV2L = overvoltage trip point #2, pu (1.10)
/* OV2T = overvoltage delay #2, sec (1.00)
/* OV3L = overvoltage trip point #3, pu (1.10)
/* OV3T = overvoltage delay #3, sec (2.00)
/* UV1L = undervoltage trip point #1, pu (0.05)
/* UV1T = undervoltage delay #1, sec (0.15)
/* UV2L = undervoltage trip point #2, pu (0.75)
/* UV2T = undervoltage delay #2, sec (1.10)
/* UV3L = undervoltage trip point #3, pu (0.90)
/* UV3T = undervoltage delay #3, sec (3.00)
/* OF1L = overfrequency trip point #1, pu (62.2)
/* OF1T = overfrequency delay #1, sec (1.00)
/* OF2L = overfrequency trip point #2, pu (61.5)
/* OF2T = overfrequency delay #2, sec (30.00)
/* UF1L = underfrequency trip point #1, pu (57.8)
/* UF1T = underfrequency delay #1, sec (1.00)
/* UF2L = underfrequency trip point #2, pu (58.5)
/* UF2T = underfrequency delay #2, sec (30.00)
  
```

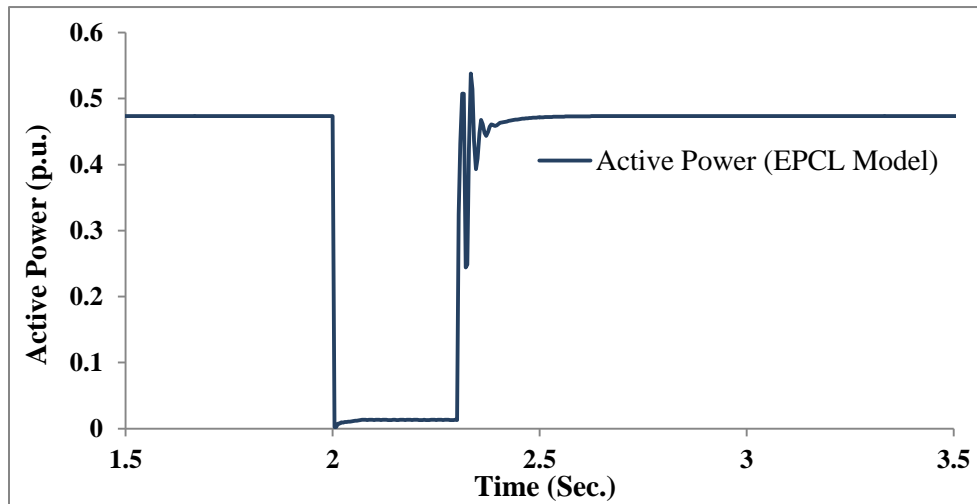
Fig. 5.15. Dynamic data input parameters of EPCL model



When this EPCL model is simulated for a LLLG grid fault at bus # 5, responses shown in fig. 5.16 – fig. 5.18 are obtained for voltage, active power and reactive power respectively at inverter terminals.

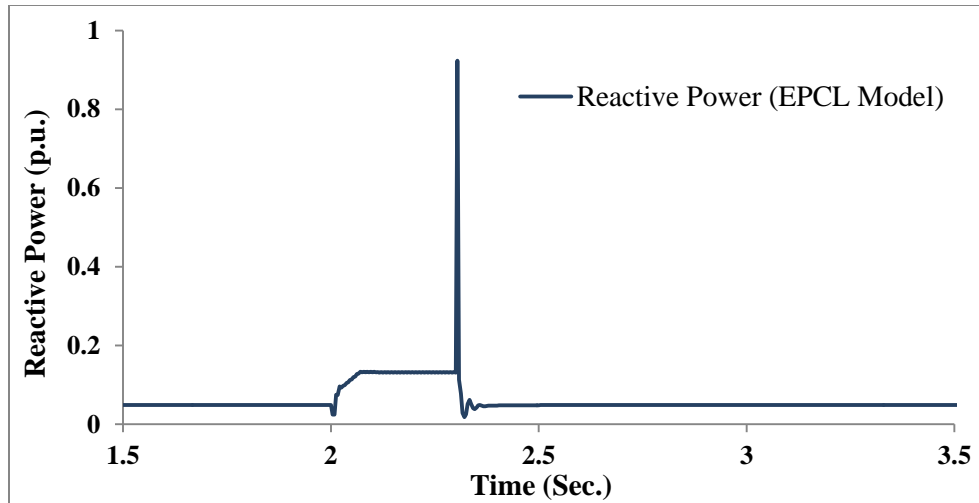


**Fig. 5.16. Voltage at inverter terminal in response to 18cycles LLLG grid fault**



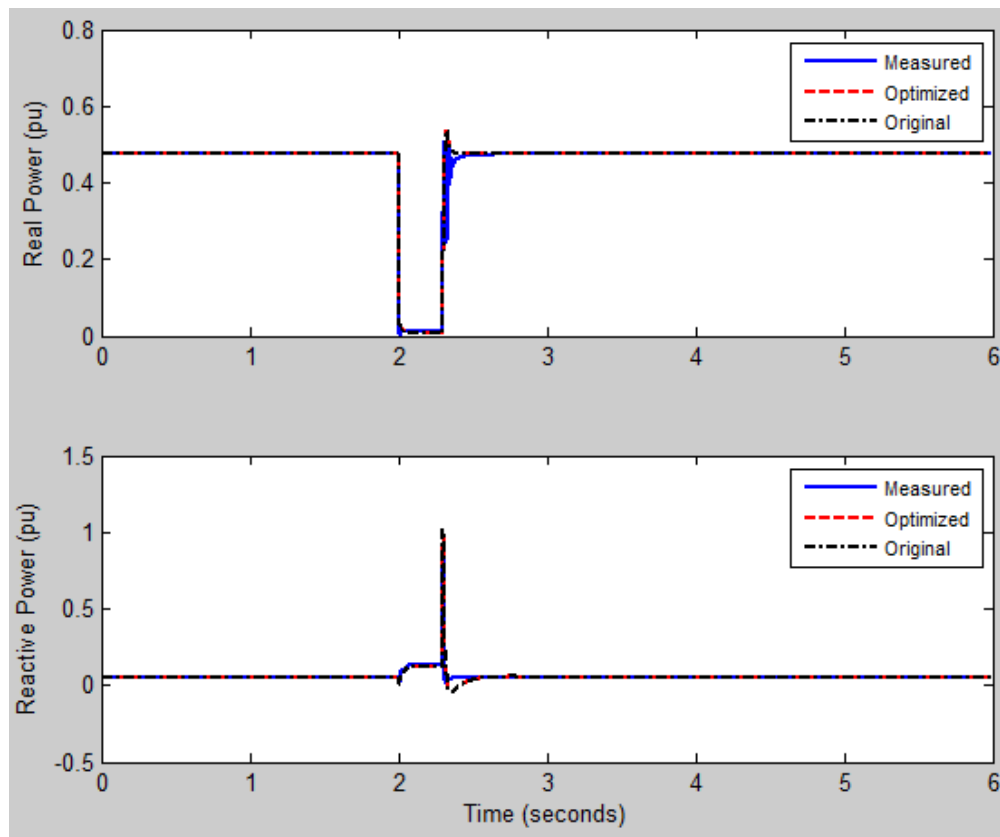
**Fig. 5.17. Active Power at inverter terminal in response to 18cycles LLLG grid fault**

These measured responses at a sampling rate of 240 samples per second are stored in a “data\_EPCL.txt” text file in the order such that first column represents time, second, third and fourth column corresponds to P, Q and V in per unit respectively.



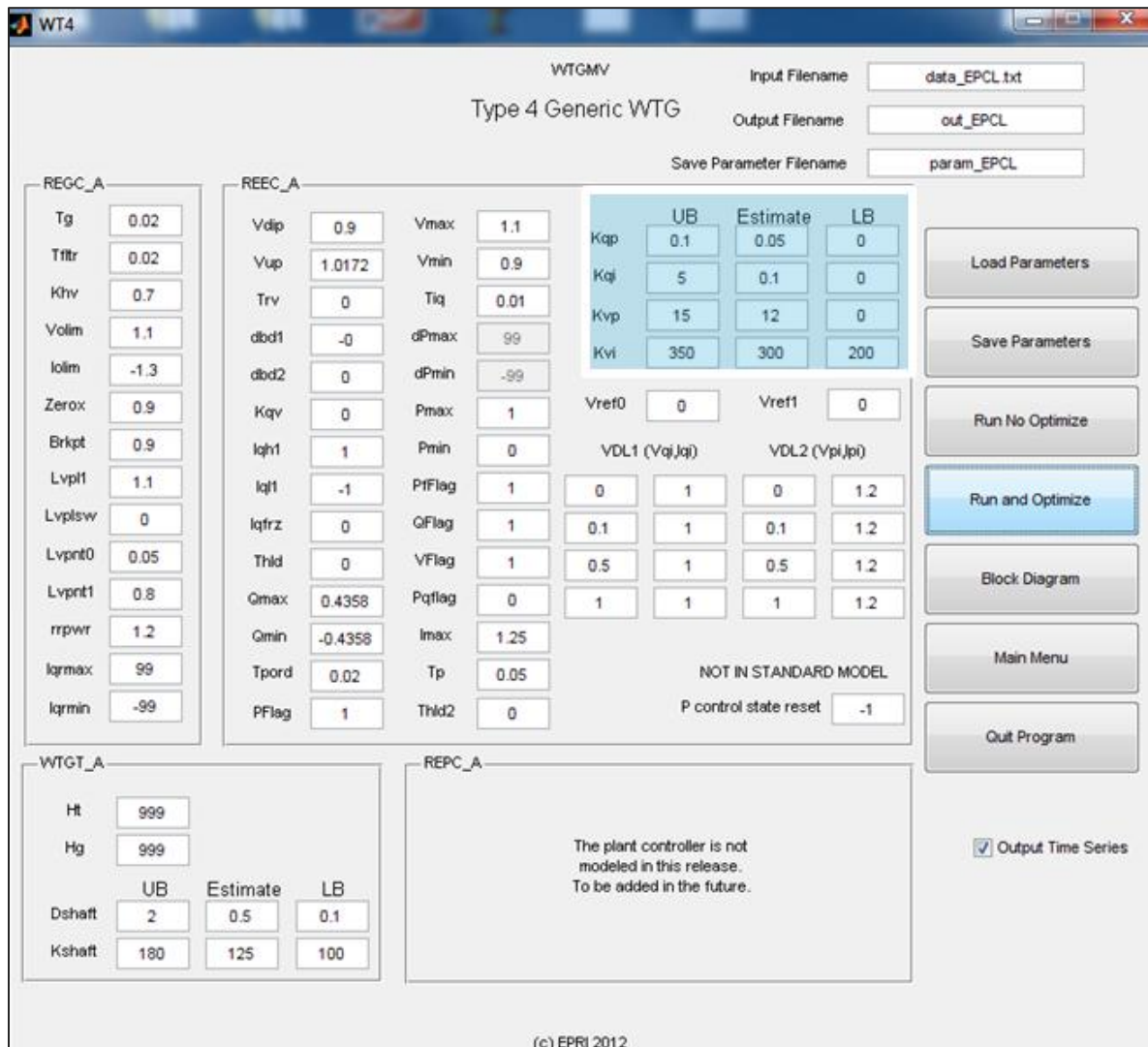
**Fig. 5.18. Reactive power at inverter terminal in response to 18cycles LLLG grid fault**

Fig. 5.19 shows the measured and optimized response based on optimal controller gains using WTGMV tool.



**Fig. 5.19. Measured and optimized response for EPCL model in WTGMV tool**

Fig. 5.20 shows the input window for WTGMV tool, where the section inside blue box shows the input parameters for Q-controller and V-controller gains. It asks for the lower and upper bound of the controller gains as an input. Estimated controller gains are regressively modified by hit and trial method until approximate values of controller gains at which optimized and measured responses shows a good match is obtained. Optimal values for  $K_{qp}$ ,  $K_{vp}$ ,  $K_{qi}$  and  $K_{vi}$  corresponding to response shown in fig. 5.19 as obtained for EPCL model from this validation process are shown in Table 27.



**Fig. 5.20. WTGMV parameters input window with EPCL model variables**

**Table 27. Estimated optimal gain values for using WTGMV tool**

Gain	Estimated Value
$K_{vp}$	12
$K_{vi}$	300
$K_{qp}$	0.05
$K_{qi}$	0.1

Now we will determine these controller gains using ZN-PSO method by following the procedure shown in fig. 5.12 for the same PV plant, and will compare the new gain values against the values obtained from WTGMV tool. To do this, same load flow model as shown in fig. 5.13 is run with dynamic data file in WECC generic format. Fig. 5.21 shows the input dynamic data file for WECC generic format. Detailed dynamic data (.dyd) is provided in Appendix-D.

```
# dynamics data written Fri Dec 27 18:33:23 2013
# from saved case filename [C:\Users\sachin\Desktop\PSLWork\model.dyd]
# title
# MODEL FOR 90MW Solar PV PLANT WITH REGC_A and REEC_B models
# prepared by SACHIN SONI
lodrep
#
models
# REGC_A AND REEC_B MODEL PARAMETERS
#-----
regc_a      1 "PVGEN"    0.32 "1" : #9 mva=90.000 "lvp1sw" 0.000000 "rrpwr"
1.2000 "brkpt" 0.900000 "zerox" 0.900000 "lvpl1" 1.100 "vtmax" 1.1000 "lvpnt1"
0.800000 "lvpnt0" 0.050000 "qmin" -1.3000 "accel" 0.700000 "tg" 0.02000 "tfltr"
0.020000 "iqrmax" 99.0000 "iqrmin" -99.0000 "xe" 0.0

reec_b      1 "PVGEN"    0.32 "1" : #9 mva=90.000 "vdip" 0.9000 "vup" 1.0172
"trv" 0.00 "dbd1" 0.000000 "dbd2" -0.000000 "kqv" 0.0000 "igh1" 1.0000 "iq11" -1.00
"vref0" 0.0000 "tp" 0.0500000 "qmax" 0.4358 "qmin" -0.4358 "vmax" 1.1000 "vmin"
0.900000 "kqp" 0.000 "kqi" 0.000 "kvp" 15.00 "kvi" 0.000 "tiq" 0.020000 "dpmax"
99.0000 "dpmin" -99.0000 "pmax" 1.000000 "pmin" 0.0 "imax" 1.1 "tpord" 0.020000
"pfflag" 1.000000 "vflag" 1.000000 "qflag" 1.0 "pqflag" 0.000000

gencls      5 "INFINITE" "500.00" "1" : #9 mva=1000.0000 "h" 999.0000 "d"
0.0000 "ra" 0.0002 "lppd" 0.0072 "rcomp" 0.0000 "xcomp" 0.0000 "accel" 0.0000
```

**Fig. 5.21. Dynamic data input parameters for WECC generic format**

As first step, the gain values for PI voltage regulator ( $K_{vp}$  and  $K_{vi}$ ) of REEC\_B model are tuned using Zeigler-Nichols method. While tuning the voltage regulator, gains for Q-controller  $K_{qp}$  and  $K_{qi}$  are set to zero. Also,  $K_{vi}$  is set to 0. During dynamic runs  $K_{vp}$  is increased until it reaches ultimate gain  $K_u$  at which the reactive power output of the plant starts

to oscillate at a constant time period. It is illustrated in fig. 5.22 that how, on increasing Kvp from 15 to 28 resulted in oscillations in plant reactive power output.

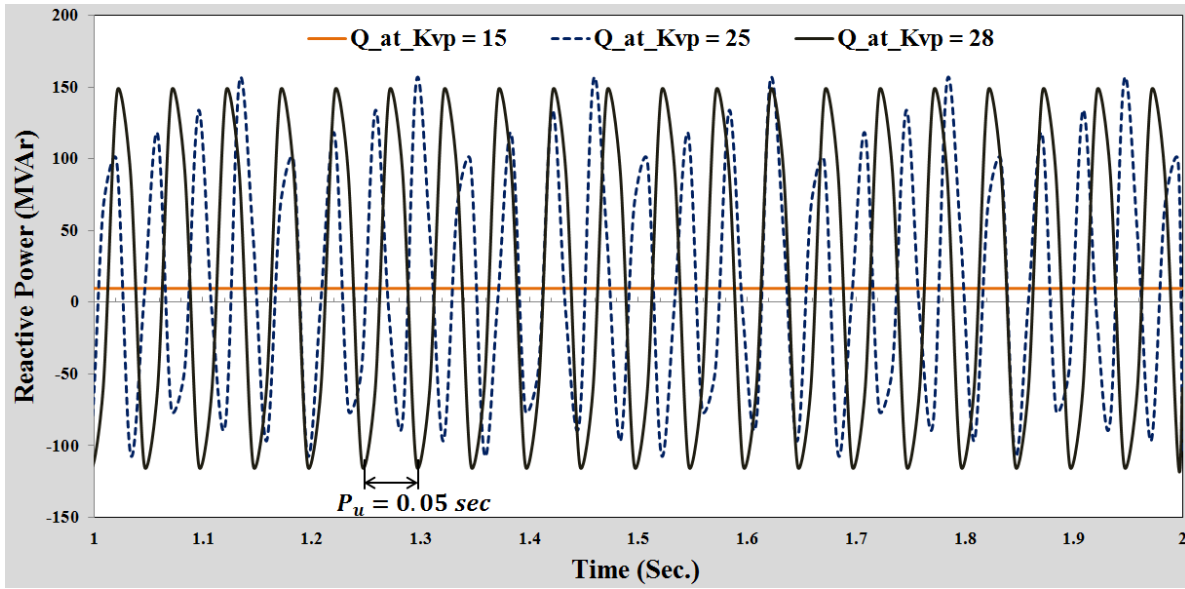


**Fig. 5.22. Reactive power output at different Kvp gains**

From fig. 5.22, it can be seen that plant reactive power output starts to oscillates with a constant time period of  $P_u = 0.05$  sec at  $K_{vp} = 28$ . This  $K_{vp}$  is therefore the ultimate gain and equals  $K_u$ . Now from Table 26 we can obtain actual  $K_{vp}$  which is,  $K_{vp} = 0.45 \times K_u = 12.6$  and  $K_{vi} = 1.2K_{vp}/P_u = 302.4$ . Now, solar PV plant model and PSO algorithm implemented in MATLAB, imports  $K_{vp}$  and  $K_{vi}$  as input to PI voltage regulator and run optimization algorithm to find optimal  $K_{qp}$  and  $K_{qi}$  gains. PSO algorithm is initialized with parameter settings as shown in Table 28.

**Table 28. PSO parameter settings**

PSO Parameters	Description	Value
$C_1, C_2$	Constriction Factors	2
t	Number of iterations	20
$\omega$	Inertia weight	0.9 -0.4
n	Number of particles	20
m	Number of members in a particle	2

ZNPSO.m file initializes these parameters and tries to determine optimal  $K_{qp}$  and  $K_{qi}$  gains in the solution search space. Fig. 5.23 shows the optimal gain search process conducted by the PSO algorithm after 10 and 15 iterations. It can be seen that the particle tends to converge toward a global optimal solution as the iteration passes by.

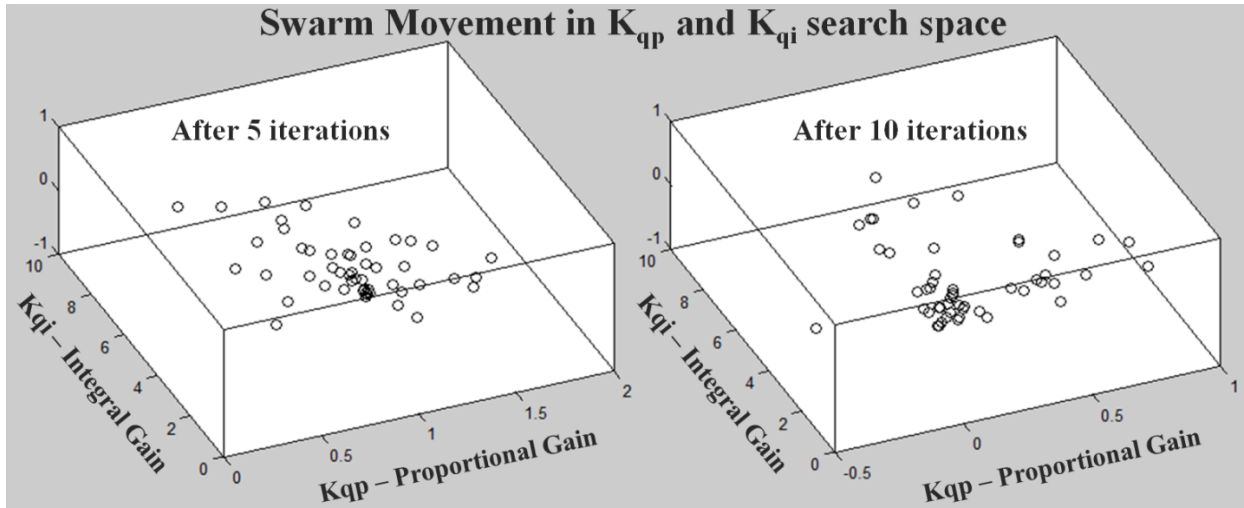


**Fig. 5.23. Search process in two-dimensional  $K_{qp}$ - $K_{qi}$  solution space**

Each particle yields a possible solution set of  $K_{qp}$  and  $K_{qi}$  gains. These values are then passed to Simulink PV plant model using MATLAB callback function and step response of the PV plant is tested for each solution set. To decide whether a solution combination is good or bad performance criteria  $W(k)$  in time domain mentioned in equation (31) is used. All solution sets of  $K_{qp}$  and  $K_{qi}$  that minimizes this performance criterion and meets the requirements mentioned in Table 29 are selected as good solution.

**Table 29. Time domain performance criteria measures**

Description	Desired value
Peak Overshoot ( $M_p$ )	< 0.4
Steady state error ( $E_{ss}$ )	0.005
Settling time ( $t_s$ )	0.1 second
Rise time ( $t_r$ )	0.05 second

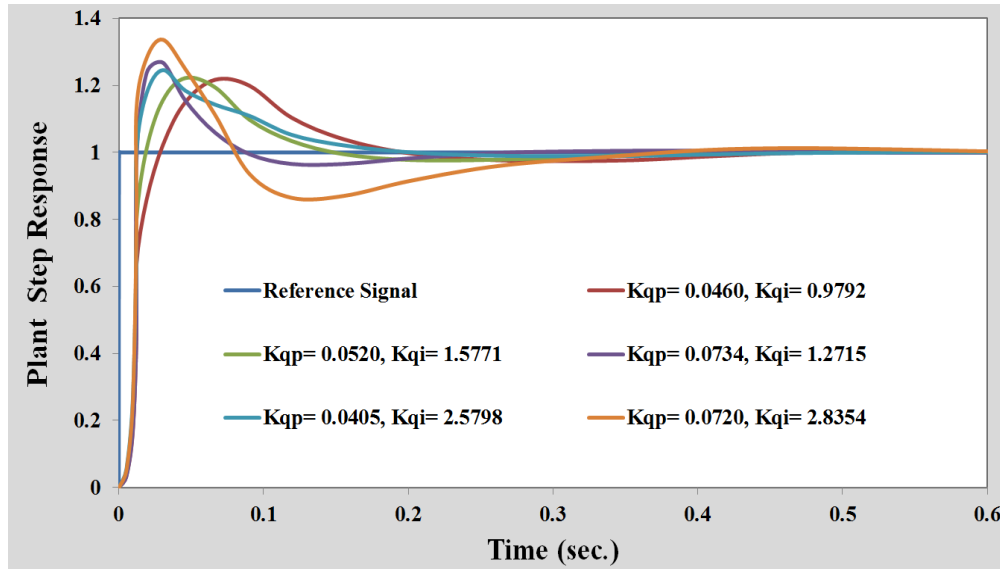


**Fig. 5.24. PV plant step response at different  $K_{qp}$  and  $K_{qi}$  gains**

Fig. 5.24 shows the step response of the solar PV plant at different  $K_{qp}$  and  $K_{qi}$  gain combinations. Each particle returns a set of  $K_{qp}$  and  $K_{qi}$  solution which is stored in MATLAB workspace and a separate text file at the end of iteration run. Fig. 5.25 shows the  $K_{qp}$  and  $K_{qi}$  controller gains obtained for iteration during program run.

```

Good Set of Values for Controller Gains is Kp= 0.0520, Ki= 1.5771
ans =
Mp = 0.2219, Ess = 0.0000, Tr = 0.0497, Ts = 0.0560
ans =
Good Set of Values for Controller Gains is Kp= 0.0734, Ki= 1.2715
ans =
Mp = 0.1636, Ess = 0.0000, Tr = 0.0292, Ts = 0.0526
ans =
Good Set of Values for Controller Gains is Kp= 0.0405, Ki= 2.5798
ans =
Mp = 0.3463, Ess = 0.0000, Tr = 0.0443, Ts = 0.0506
ans =
Good Set of Values for Controller Gains is Kp= 0.0460, Ki= 0.9792
ans =
Mp = 0.2164, Ess = 0.0001, Tr = 0.0687, Ts = 0.0749
ans =
Good Set of Values for Controller Gains is Kp= 0.0720, Ki= 2.8354
ans =
Mp = 0.2134, Ess = -0.0000, Tr = 0.0306, Ts = 0.0541
ans =
Good Set of Values for Controller Gains is Kp= 0.0617, Ki= 1.7148
ans =
Mp = 0.1869, Ess = 0.0000, Tr = 0.0441, Ts = 0.0503
ans =
Good Set of Values for Controller Gains is Kp= 0.0310, Ki= 1.3922

```

**Fig. 5.25. Different  $K_{qp}$  and  $K_{qi}$  gains at any iteration**

Fig.5.25 clearly indicates the effect of significant randomness in value of proportional and integral gains as obtained by proposed method. All particles have not converged to one

single optimum gain combination. It could be considered as a drawback of heuristic optimization methods. This makes it difficult to decide which value should be chosen as best gain combination. To mitigate this randomness, a weighted average method based on (33) to determine final Kqp and Kqi gains is used which nullifies the effect of scattered solutions.

$$\bar{K} = \frac{\sum_{i=1}^n f_i K_i}{\sum_{i=1}^n f_i} \quad (33)$$

Where  $f_i$  = fitness weight based on performance criteria given in (32)

$K_i$  = gain value

$n$  = number of solutions

Therefore, solutions with a high weight contribute more to the weighted mean than do elements with a low weight.

Based on the weighted mean,  $K_{qp} = 0.0440$  and  $K_{qi} = 2.1806$  is obtained for the above test system. Table 30 provides the gain values for both voltage regulator and Q-controller of REEC\_B model using ZNPSO method.

**Table 30. Estimated optimal gain values using ZNPSO method**

Gain	Estimated Value
$K_{vp}$	12.6
$K_{vi}$	302.4
$K_{qp}$	0.0440
$K_{qi}$	2.1806

To validate these controller gains, 90 MW solar PV plant model prepared in WECC generic dynamic data format with gain values as calculated above is simulated with LLLG grid fault at bus # 5, and the plant response i.e. voltage, active power and reactive at inverter terminals is compared with EPCL model. Fig. 5.26 – 5.28 shows the plots for both EPCL and generic model to compare their response side by side.



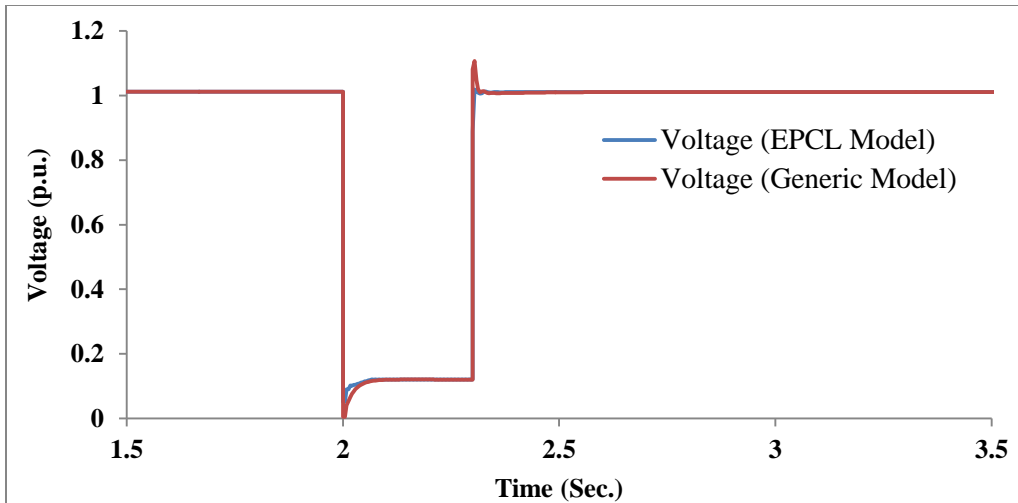


**Fig. 5.26. Voltage dips at inverter terminals during LLLG fault at POI**

It can be seen in fig. 5.26 and fig. 5.27, that when a three phase LLLG fault is applied at interconnection point in both models, reactive current is contributed to support the voltage. The inverter set-points, as determined by the active and reactive power controllers (or the voltage support during dips section), are subject to limiting to prevent damage to the inverter, this values is set to 1.25 per unit in both cases. Also, reactive current is set to have priority over active current when the total current magnitude approaches its limits in both cases.

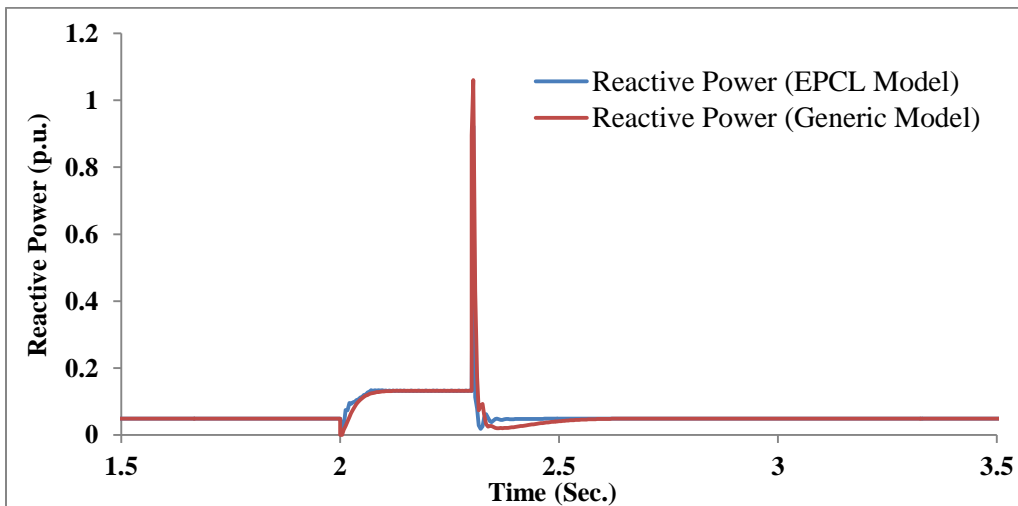


**Fig. 5.27. Reactive power contribution to support voltage during LLLG fault at POI**

Both cases are simulated with maximum and minimum reactive power inverter limits as,  $Q_{max} = 0.4358$  and  $Q_{min} = -0.4358$  per unit on PV generator equivalent MVA base. Active power output in normal operation and during not too deep voltage dips is held constant by a simple PI controller but in this case the voltage has fallen below 0.2 per unit, therefore at this low voltage event active power output at inverter terminal drops to almost zero as shown in fig. 5.28.

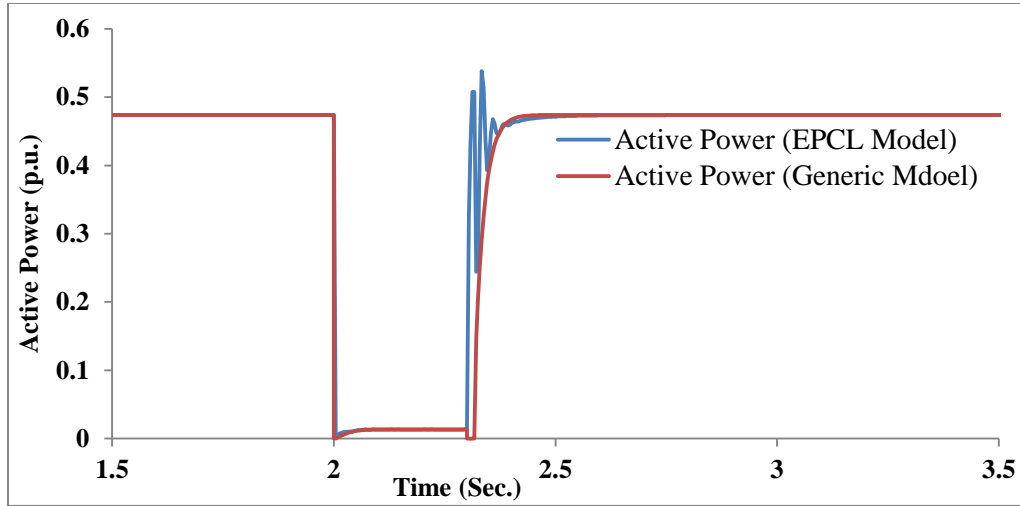


*Fig. 5.28. Active power dip during LLLG fault at POI*

Table 31 compares the controller gains obtained by WTGMV tool and ZNPSO method.

*Table 31. Estimated optimal gain values by WTGMV and ZNPSO method*

Gain	Estimated Value by WTGMV Tool	Estimated Value by ZNPSO method
$K_{vp}$	12.0	12.6
$K_{vi}$	300	302.4
$K_{qp}$	0.05	0.0440
$K_{qi}$	0.1	2.1806

Values looks to be close enough and the plant response to grid fault using either method gave almost similar response. This proves that proposed method can be used to accurately tune REEC\_B model voltage regulator and Q-controller gains in a short time span. ZN-PSO does not apply hit and trial method which could save man-hours and provide accurate gain values.

### 5.8.2. Case Study 2 – REPC\_A model validation against field measured data

Reactive power capability and response characteristics are an important consideration in system studies. A variety of reactive power control modes can be implemented in a PV power plant depending on plant size. Large scale solar PV power plants typically control voltage at the point of interconnection. Smaller plants are typically operated in power factor control mode. During a dynamic event, the reactive power response is the net result of fast inverter response and slower supervisory control by the centralized power plant controller. Once the REEC\_B model gain values are determined, REPC\_A model is enabled to provide the reactive power command to inverter controls by setting pfflag to zero in REEC\_B model (see fig. 4.9). This allows the REPC\_A model to send Q-command to inverters. Inverters and power plant controller then coordinate with each other to control voltage at POI by maintain the required VAr flow within the plant. Fig. 5.29 shows trajectory and movement of swarms in  $K_p$  and  $K_i$  search space.

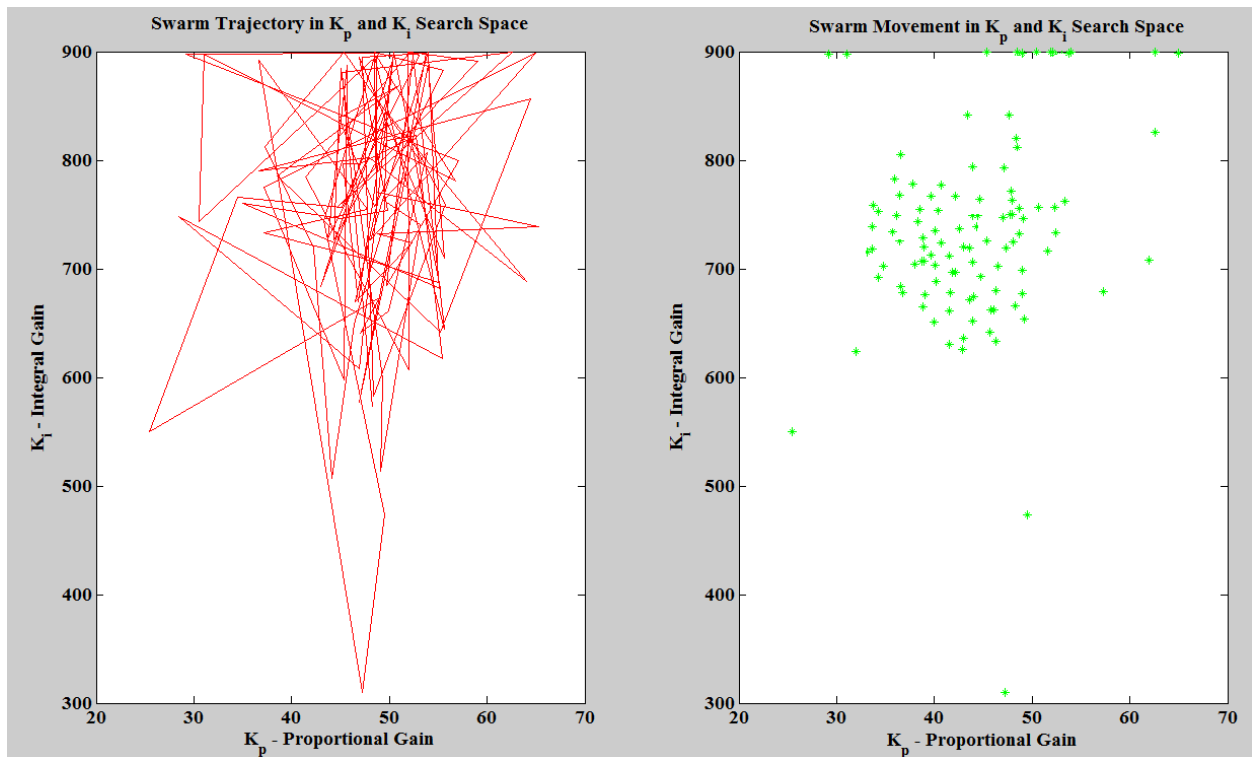


*Fig. 5.29. Swarm trajectory and movement in  $K_p$  and  $K_i$  search space*

Method to determine controller gains using ZNPSO algorithm is already explained. Fig. 5.29 shows that swarm converges to a narrow region in  $K_p$  and  $K_i$  search space to find most optimal controller gains. Steps listed in section-D of ZNPSO algorithm when followed, resulted in weighted average gain value of  $K_p = 33.6$  and  $K_i = 792.06$  for REPC\_A model reactive controller loop.

To validate that calculated  $K_p$  and  $K_i$  values are good enough to capture supervisory level plant response, a simulation model of solar PV plant with REPC\_A model enabled is simulated and, the simulation results are compared with field measured data of an actual solar PV plant operating at a curtailed active power output of only 90 MW. Data logged in SCADA (Supervisory Control and Data Acquisition) system for a 12 MVAR capacitor bank switching event on 34.5 kV medium voltage collection system bus is used to validate the plant model. System load flow (.epc) and dynamic data (.dyd) is provided in Appendix-D.

A 12 MVAR capacitor located at the 34.5kV collector bus is turned online as an external stimulus. Fig. 5.30 illustrates that, when the capacitor bank is engaged at  $t = 0$  seconds relative time, power plant controller sends control signals to each individual inverter to immediately address this switching event. Eventually inverters reactive power contribution to the plant drops, in fact inverters mode of operation changes from lagging to leading i.e., inverters start absorbing reactive power to control the voltage at regulated bus. Both, field measured reactive power command ( $Q_{cmd\_actual}$ ) and simulated model command ( $Q_{cmd\_simulation}$ ) are shown. Initial quick response by inverters which took almost 100ms, followed by dominance of power plant controller in the order of seconds, to maintain post-disturbance stability can be clearly seen in fig. 5.30.

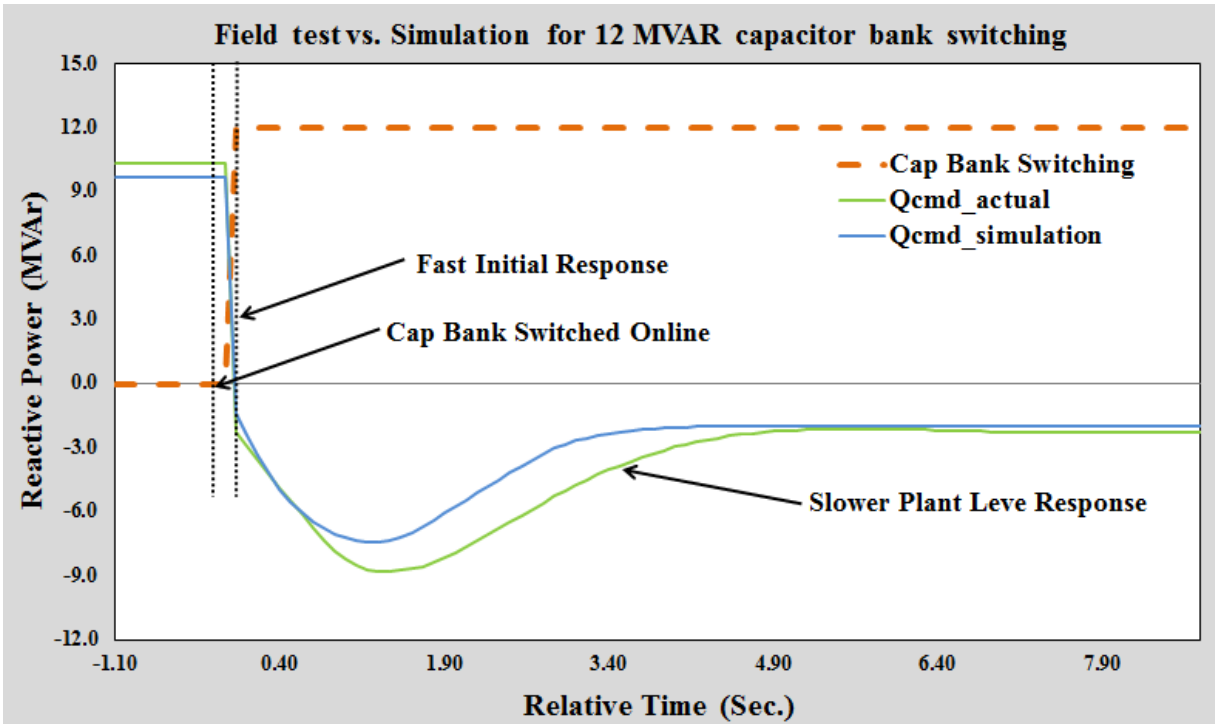


Fig. 5.30. Commanded reactive power ( $Q_{cmd}$ ) – field test vs. simulation

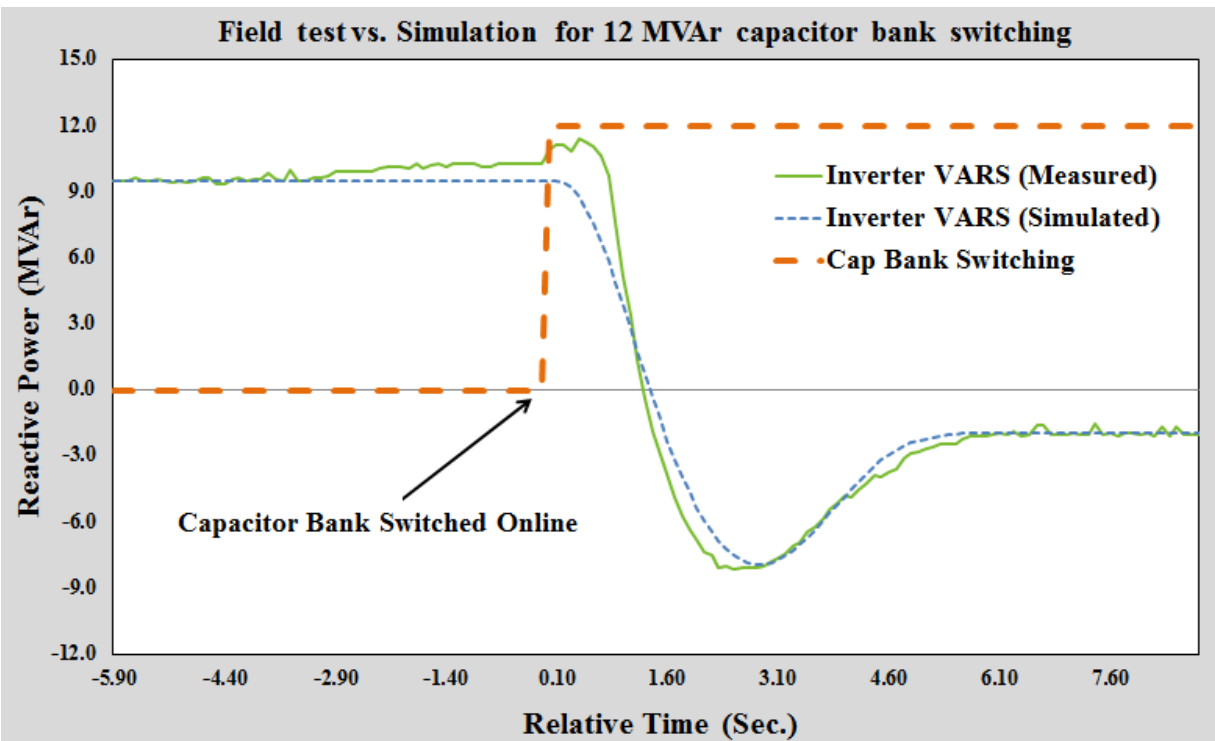


Fig. 5.31. Inverter reactive power contribution during 12 MVAR capacitor engagement test

Fig. 5.31 illustrates that the simulation model performance adequately mimics actual plant behavior. The response matches closely, with a difference immediately following the switching operation which could be attributed to the lower sampling rate in the field measurement than in PSLF simulation.

### **Conclusions**

Proposed ZNPSO algorithm is discussed in detail and validated. As first validation step, results obtained for REEC\_B model tuning are compared with those obtained from EPRI WTGMV tool. Results showed a good match against each other. To further validate the acceptability of proposed algorithm, REPC\_A model parameters were determined and field results were compared with the simulation model. Both tests were successful and have proven the authenticity of proposed algorithm.

## Chapter 6

### CONCLUSIONS AND FUTURE WORK

#### Conclusions

Comparison of full scale model with reduced order model concluded that for planning and operation, a reduced scale solar PV plant model in a single machine form is good enough. Computational efficiency without losing any system information is established. From PV plant VAR study it is concluded that solar PV plants are capable of meeting grid reactive power interconnection requirements, if the inverters VAR capacity is utilized properly. First and second generation PV plant models proposed by WECC is validated against user-written model and it has been proven that WECC proposed plant model are fully capable of representing inverter behavior. Proposed ZNPSO algorithm is discussed in detail and validated. Computer simulation plant model is validated against field measured data. Validation results demonstrate that, the proposed algorithm is performing well to determine controller gains within the region of interest. Also, it concluded that developed PV plant models are adequate enough to capture PV plant dynamics.

#### Future work

Power plant controller active power control loop (governor model) needs a validation against field measurement. Also, electrical control model needs to be tested with other flag settings like when Vflag and Qflag are set to 0.

## REFERENCES

- [1]. R. Gelman, S. Gossett, S. Buchanan, "2011 Renewable Energy Data book," Energy Efficiency and Renewable Energy, US Department of Energy, DOE/GO-102012-3598, Revised February 2013  
[Online] Available: <http://www.nrel.gov/docs/fy13osti/54909.pdf>.
- [2]. Annual Energy Review 2011, US Energy Information Administration, DOE/EIA-0384 (2011), September 2012.  
[Online] Available: <http://www.eia.gov/totalenergy/data/annual/pdf/aer.pdf>.
- [3]. Standard Models for Variable Generation, NERC Special Report, May 2010  
[Online] Available:  
<http://www.nerc.com/files/Standards%20Models%20for%20Variable%20Generation.pdf>
- [4]. O Wasynczuk, N. A. Anwah, "Modeling and dynamic performance of a self-commutated photovoltaic inverter system," IEEE Power Engineering Review, Vol.9, No. 9, 1989, pp. 33-34.
- [5]. O Wasynczuk, "Modeling and dynamic performance of a line-commutated photovoltaic inverter system," IEEE Power Engineering Review, Vol.9, No. 9, 1989, pp. 35-36.
- [6]. L. Wang, Y. H. Lin, "Dynamic stability analysis of photovoltaic array connected to a large utility grid," IEEE Power Engineering Society Winter Meeting, Vol. 1, 2000, pp. 476-480.
- [7]. K.H. Hussein, I. Muta, T.Hoshino, M.Osakada, "Maximum photovoltaic power tracking: an algorithm for rapidly changing atmospheric conditions," IEEE Journal on Generation, Transmission, Distribution, vol. 42, Issue 1, 1995, pp. 59-64.
- [8]. M Calais, H. Hinz, "A ripple-based maximum power point tracking algorithm for a single-phase grid-connected photovoltaic system," Solar energy Vol. 63, No. 5, pp. 277-282, 1998.
- [9]. C. Hua, J. Lin, C. Shen, "Implementation of DSP-controlled photovoltaic system with peak power tracking," IEEE Transactions on Industrial Electronics, Vol. 45, No.1, February 1998, pp. 99-106.
- [10]. Y.T.Tan, D.Kirschen, N. Jenkins, "A model for PV generation suitable for stability analysis," IEEE Transactions on Energy Conversion, Vol. 19, No.4, December 2004, pp.748-755.



- [11]. J.Y.Astic, A.Bihain, M.Jerosolimski, "A mixed adams-BDF variable step size algorithm to simulate transient and long term phenomena in power systems," IEEE Transactions on Power Systems, Vol.9, No.2, May 1994, pp. 929-935.
- [12]. M.C.D. Piazza, M.Pucci, A. Ragusa, G Vitale, "A grid-connected system based on a real time PV emulator: design and experimental set-up," IECON 2010 36<sup>th</sup> Annual conference on IEEE Industrial Electronics Society, 2010, pp. 3237-3243.
- [13]. R.G.Wandhare, V.Agarwal, "Advanced control scheme and operating modes for large capacity centralized PV-grid systems to overcome penetration issues," 37<sup>th</sup> IEEE Photovoltaic Specialist Conference (PVSC), 2011, pp. 2466-2471.
- [14]. High gain DC/DC converter for the grid integration of large-scale PV systems, IEEE International Symposium on Industrial Electronics, (ISIE), 2012, pp. 1011-1016.
- [15]. H.Choi, M.Ciobotaru, V.G.Agelidis, H.Wang, Y.Peng, Z.Yang, "Analyzing the key technologies of large-scale application of PV grid-connected systems," IEEE International Conference on Power System Technology, 2010, pp.1-4.
- [16]. R.A.Walling, K.Clark, "Grid support functions implemented in utility-scale PV systems," IEEE PES Transmission and Distribution Conference and Exposition, 2010, pp. 1-5.
- [17]. IEEE standards for interconnecting distributed resources with electric power systems, IEEE 1547.
- [18]. G.Islam, A. Al-durra, S.M.Muyeen, J.Tamura, "Low voltage ride through capability enhancement of grid connected large scale photovoltaic system," 37<sup>th</sup> Annual conference on IEEE Industrial Electronics society, 2011, pp. 884-889.
- [19]. EPRI guide on Generic models and model validation for wind and solar PV generation: Technical update. Product ID: 1021763, December 2011.  
[Online] Available:  
<http://www.epri.com/abstracts/pages/productabstract.aspx?ProductID=00000000001021763>
- [20]. EPRI guide on Wind and solar PV modeling and model validation: Technical update. Product ID: 1025475, November 2012.  
[Online] Available:  
<http://www.epri.com/abstracts/Pages/ProductAbstract.aspx?ProductId=00000000001025475>
- [21]. M.Asmine, J.Brochu, J.Fortmann, R.Gagnon, Y.Kazachkov, C.E. Langlois, C.Larose, E.Muljadi, J.MacDowell, P.Pourbeik, S.A.Seman, K.Wiens, "Model validation for wind turbine generator models," IEEE Transactions on Power Systems, Vol. 26, No. 3, August 2011, pp. 1769-1782.

- [22]. K.Clark, R.A.Walling, N.W. Miller, “Solar photovoltaic (PV) plant models in PSLF,” IEEE Power and Energy Society General Meeting, 2011, pp. 1-5.
- [23]. K.Clark, N. W. Miller, R.Walling, “Modeling of GE solar photovoltaic plants for grid studies,” April 2010
- [24]. A.Ellis, M.Behnke, C.Baker, “PV system modeling for grid planning studies,” 37<sup>th</sup> IEEE Photovoltaic Specialists Conference (PVSC), 2011, pp. 2589-2593.
- [25]. WECC PV plant power flow modeling guide, August 2010.  
[Online] Available:  
<http://www.wecc.biz/library/WECC%20Documents/Documents%20for%20Generators/Generator%20Testing%20Program/WECCPVPlantPowerFlowModelingGuide.pdf>
- [26]. WECC REMTF Generic solar photovoltaic system dynamic simulation model specification, September 2012.  
[Online] Available:  
<https://www.wecc.biz/committees/StandingCommittees/PCC/TSS/MVWG/REMTF/Materials%20Discussed%20at%20November%2056%202012%20REMTF%20Meet/WECC%20Solar%20PV%20Dynamic%20Model%20Specification%20-%20September%202012.pdf>
- [27]. Wind Turbine Generator Model Validation (WTGMV) software user’s manual: Version 1.0 EPRI, Palo Alto, CA: 2011, Product ID # 1024346.
- [28]. K.J.Astrom, P.Albertos, J.Quevedo, “PID Control,” Automatica Journal of Control Engineering Practice 9 (2001) pp.1159-1161.
- [29]. K.H.Ang, G.Chong, Y.Li, “PID Control system analysis, design, and technology,” IEEE Transactions on Control Systems Technology, Vol. 13, No. 4, July 2005, pp. 559-576.
- [30]. PID Controllers: Theory, Design, and Tuning. K.Astrom and T.Hagglund, 2<sup>nd</sup> Edition. 1995.
- [31]. J.G.Ziegler and N.B.Nichols, “Reprint of Optimum settings for automatic controllers,” Transactions of the A.S.M.E. November, 1942, pp. 759-765. Rochester, NY.
- [32]. K.J.Astrom, C.C.Hang, P.Persson, W.K.Ho, “Towards intelligent PID control,” Automatica, Vol. 28, No.1, pp. 1-9, 1992.
- [33]. W.K.Ho, K.W.Lim, WXu, “Optimal gain phase margin tuning for PID Controllers,” Control Engineering Practice, Vol. 34, No. 8, pp. 1009-1014, 1998.
- [34]. P.Wang, D.P.Kwok, “Optimal design of PID process controllers based on genetic algorithm,” Control Engineering Practice, Vol 2, No. 4, pp 641-648, 1994.

- [35]. V.Mukherjee, S.P.Ghoshal, "Intelligent particle swarm optimized fuzzy PID controller for AVR system," Elsevier, Electric Power System Research 77 (2007) 1689-1698, January 2007.
- [36]. M. Zamani, M. K.Ghartemani, N.Sadati, M.Parniani, "Design of fractional order PID controller for an AVR using particle swarm optimization," Elsevier, Control engineering practice, 17 (2009) 1380-1387., 2009.
- [37]. Z.Yachen and H.Yueming, "On PID controllers based on simulated annealing algorithm," Proceeding of the 27<sup>th</sup> Chinese Control Conference, July 16-18, 2008, China.
- [38]. Z.L.Gaing, "A particle swarm optimization approach for optimum design of PID controller in AVR system," IEEE Transactions on Energy Conversion, Vol. 19, No.2, June 2004.
- [39]. W.Lei, K.Qi, X.Hui, W.Qidi, "A modified adaptive particle swarm optimization algorithm," IEEE International Conference on Industrial Technology, 2005, pp. 209-214.
- [40]. A.Jalilvand, A.Kimiyaghalam, A.Ashouri, M.Mahdavi, "Advanced particle swarm optimization-based PID controller parameters tuning," IEEE International Multitopic Conference, 2008, pp. 429-435.
- [41]. B.Zhao, C.X.Guo, Y.J.Cao, "An improved particle swarm optimization algorithm for optimal reactive power dispatch," IEEE Power and Energy Society General Meeting, 2005, pp. 272-279.
- [42]. W.Xin, L.Ran, W.Yanghua, P.Yong, Q.Bin, "Self-tuning PID controller with variable parameters based on particle swarm optimization," IEEE International conference on Intelligent System Design and Engineering Applications, 2013, pp. 1264-1267.
- [43]. T.Athay, R.Podmore, S.Virman, "A practical method for the direct analysis of transient stability," IEEE Transactions on Power Apparatus and Systems, Vol.98, No.2, April 1979.
- [44]. M.A.Pai, "Energy function analysis for power system stability": Kluwer Academic Publishers 1989.
- [45]. IEEE Std 141-1993, IEEE recommended practice for electric power distribution for industrial plants, December 1993.
- [46]. R.C. Eberhart and Y.Shi, "Comparing inertia weights and constriction factors in particle swarm optimization," IEEE proceedings of the 2000 congress on Evolutionary Computation, pp. 84-88.
- [47]. R. Ayyanar, "Renewable Electric Energy Systems, EEE 598," Lecture Notes, Fall 2012.

APPENDIX-A

FIRST GENERATION MODEL DYNAMIC DATA FOR CASE STUDY

```

# dynamics data written Sat Apr 13 17:50:39 2013
# from saved case filename [C:\Users\c005540\Desktop\PSLFwork\PVx_model.dyd]
lodrep
#
# area 1 [UNKNOWN1          ]
#
models
gencls 99999 "INFINITE" " 500.00 "1 " : #9 mva=999.0000 "h" 999.0000 "d" 0.0000 "ra"
0.0002 "lppd" 0.0072 "rcomp" 0.0000 "xcomp" 0.0000 "accel" 0.0000
vmetr 99999 "INFINITE" " 500.00 "1 " : #9 "tf" 0.0
fmetr 99999 "INFINITE" " 500.00 "1 " : #9 "tf" 0.0
#
# area 99 [UNKNOWN2        ]
#
models
pv1g 99401 "TEST_G1" " 0.32 "1 " : #9 mva=337.4000 "lvplsw" 0.0 "rrpwr" 1.2000
"brkpt" 0.900000 "zerox" 0.900000 "lvpl1" 1.1000 "volim" 1.1000 "lvpnt1" 0.100000 "lvpnt0"
0.050000 "iolim" -1.3000 "khv" 0.7
pv1e 99401 "TEST_G1" " 0.32 "1 " : #9 "varflg" 0.0 "kqi" 0.500 "kvi" 120.00 "vmax"
1.1000 "vmin" 0.900000 "qmax" 0.66000 "qmin" -0.66000 "tr" 0.020000 "tc" 0.200000 "kpV"
18.0000 "kiv" 5.0000 "pfaflg" 1.000000 "fn" 1.000000 "tv" 0.050000 "tpwr" 0.050000 "iph1"
1.1000 "iqhl" 1.1000 "pqflag" 0.0 "xc" 0.0 "kqd" 0.0 "tlpqd" 0.0 "xqd" 0.0 "vermn" -0.100000
"vermx" 0.100000 "vfrz" 0.700000 "imaxtd" 1.1000 "viqlim" 1.6000
vmetr 99101 "TEST_02" " 34.50 "1 " : #9 "tf" 0.0
vmetr 99301 "TEST_03" " 34.50 "1 " : #9 "tf" 0.0
fmetr 99401 "TEST_G1" " 0.32 "1 " : #9 "tf" 0.0
list of out of service models
#
# template for PSLF dynamic models
#
# gencls : h d ra lppd rcomp xcomp accel
# vmetr : tf
# fmetr : tf
# pv1g : lvplsw rrpwr brkpt zerox lvpl1 volim lvpnt1 lvpnt0 iolim khv
# pv1e : varflg kqi kvi vmax vmin qmax qmin tr tc kpV kiv pfaflg fn tv tpwr iph1 iqhl pqflag xc
kqd tlpqd xqd vermn vermx vfrz imaxtd viqlim

```

SECOND GENERATION MODEL DYNAMICS DATA FOR CASE STUDY

```

# dynamics data written Mon Apr 15 22:09:42 2013
# from saved case filename [C:\Users\c005540\Desktop\PSLFwork\RExC_WECC_model.dyd]
lodrep
#
# area 1 [UNKNOWN1          ]
#
models
gencls 99999 "INFINITE" " 500.00 "1 " : #9 mva=999.0000 "h" 999.0000 "d" 0.0000 "ra"
0.0002 "lppd" 0.0072 "rcomp" 0.0000 "xcomp" 0.0000 "accel" 0.0000
vmetr 99999 "INFINITE" " 500.00 "1 " : #9 "tf" 0.0
fmetr 99999 "INFINITE" " 500.00 "1 " : #9 "tf" 0.0
#
# area 99 [UNKNOWN2        ]
#
models
regc_a 99401 " TEST_G1    " 0.32 "1 " : #9 mva=337.4000 "lvplsw" 0.000000 "rrpwr"
1.2000 "brkpt" 0.900000 "zerox" 0.900000 "lvpl1" 1.100 "vtmax" 1.1000 "lvpnt1" 0.100000
"lvpnt0" 0.050000 "qmin" -1.3000 "accel" 0.700000 "tg" 0.02000 "tfltr" 0.020000 "iqrmax"
99.0000 "iqrmin" -99.0000 "xe" 0.0

reec_b 99401 " TEST_G1    " 0.32 "1 " : #9 mva=337.4000 "vdip" 0.9000 "vup" 1.1000
"trv" 0.00 "dbd1" 0.000000 "dbd2" -0.000000 "kqv" 0.0000 "iqh1" 1.00 "iq11" -1.00 "vref0"
0.7000 "tp" 0.0500000 "qmax" 0.660 "qmin" -0.660 "vmax" 1.1000 "vmin" 0.900000 "kqp"
0.00 "kqi" 10.07206 "kvp" 10.0 "kvi" 60.00 "tiq" 0.020000 "dpmax" 99.0000 "dpmin" -99.0000
"pmax" 1.000000 "pmin" 0.0 "imax" 1.100 "tpord" 0.020000 "pfflag" 1.000000 "vflag"
1.000000 "qflag" 1.0 "pqflag" 0.000000

vmetr 99101 " TEST_02    " 34.50 "1 " : #9 "tf" 0.0
vmetr 99301 " TEST_03    " 34.50 "1 " : #9 "tf" 0.0
fmetr 99401 " TEST_G1    " 0.32 "1 " : #9 "tf" 0.0

```

PSLF MODEL LOAD FLOW DATA FOR CASE STUDY IN SECTION 4.5

```

# history file date Wed Apr 10 11:54:04 2013
# present file date Wed Apr 10 11:58:33 2013
# Version 18.1_00
title
!
solution parameters
tap 1 tcu1 enabled/disabled
phas 1 ps enabled/disabled
area 1 area enabled/disabled
svd 1 svd enabled/disabled
dctap 1 dc enabled/disabled
gcd 0 gcd enabled/disabled
jump 0.00029 jumper threshold
toler 0.1000 newton tolerance
sbase 100.0000 system mva base
!
bus data [ 5]          ty vsched volt angle ar zone vmax vmin date_in date_out pid L
own st latitude longitude island sdmon vmax1 vmin1 dvmax
 99001 "TEST_01      " 500.0000 : 1 1.00000 1.000003 0.00482 99 999 1.0500 0.9500
400101 391231 0 0 0 0.00000 0.00000 0 0.00000 0.00000 0.00000
 99101 " TEST_02      " 34.5000 : 1 1.01500 1.008084 4.52212 99 999 1.0500 0.9500
400101 391231 0 0 0 0.00000 0.00000 0 0.00000 0.00000 0.00000
 99301 " TEST_03      " 34.5000 : 1 1.00000 1.020386 6.87137 99 999 1.0500 0.9500
400101 391231 0 0 0 0.00000 0.00000 0 0.00000 0.00000 0.00000
 99401 " TEST_G1      " 0.3240 : 2 1.00000 1.037975 9.39193 99 999 1.0500 0.9500
400101 391231 0 0 0 0.00000 0.00000 0 0.00000 0.00000 0.00000
 99999 "INFINITE     " 500.0000 : 0 1.00000 1.000000 0.00021 1 1 1.0500 0.9500 400101
391231 0 0 0 0.00000 0.00000 0 0.00000 0.00000 0.00000
branch data [ 2]          ck se -----long_id_----- st resist react
charge rate1 rate2 rate3 rate4 aloss lngth
 99101 "TEST_02      " 34.50 99301 "TEST_03      " 34.50 "1 " 1 "          ": 1
0.002135 0.014390 0.026256 337.4 337.4 337.4 337.4 0.000 0.0 /
 0 0 0.000000 0.000000 0.000000 400101 391231 0 1 0 0.0 0.0 0.0 0.0 0 1.000
0 0.000 0 0.000 0 0.000 0 0.000 0 0.000 0 0.000 0 0.000 0 0
 99999 "INFINITE     " 500.00 99001 "TEST_01      " 500.00 "1 " 1 "          ": 1
0.000000 0.000027 0.000695 337.4 337.4 337.4 337.4 0.000 0.0 /
 0 0 0.000000 0.000000 0.000000 400101 391231 0 1 0 0.0 0.0 0.0 0.0 0 1.000
0 0.000 0 0.000 0 0.000 0 0.000 0 0.000 0 0.000 0 0.000 0 0
transformer data [ 2]          ck -----long_id_----- st ty --no---
reg_name          zt int          tert          ar zone tbase ps_r ps_x pt_r
pt_x ts_r ts_x
 99001 "TEST_01      " 500.00 99101 "TEST_02      " 34.50 "1 " "          ": 1
1 0 "          " 0.00 0 0 "          " 0.00 0 "          " 0.00 99 999 337.399994
1.635000e-003 9.000000e-002 0.000000e+000 0.000000e+000 0.000000e+000 0.000000e+000 /

```



```

525.000000 34.500000 0.000000 0.000000 0.000000e+000 -4.090000e-003 337.4 337.4
337.4 337.4 0.000 1.500000 0.510000 1.500000 0.510000 0.000000 1.000000 0.952300
1.000000 1.000000 400101 391231 0 1 0.0 0.0 0.0 0.0 /
0 1.000 0 0.000 0 0.000 0 0.000 0 0.000 0 0.000 0 0.000 0 /
0.000000 0.000000 0.000000 0.000000 0.0 0.0 0.0 0.0 0.0 0.0 0.000 0.000 0 0
0 0.0000 0.0000 0
99301 " TEST_03 " 34.50 99401 " TEST_G1 " 0.32 "1 " " " : 1 1
0 " " 0.00 0 0 " " 0.00 0 " " 0.00 99 999 337.399994
1.050600e-002 5.400000e-002 0.000000e+000 0.000000e+000 0.000000e+000 0.000000e+000 /
34.500000 0.324000 0.000000 0.000000 0.000000e+000 0.000000e+000 337.4 337.4 337.4
337.4 0.000 1.500000 0.510000 1.500000 0.510000 0.000000 1.000000 1.000000 1.000000
1.000000 400101 391231 0 1 0.0 0.0 0.0 0.0 /
0 1.000 0 0.000 0 0.000 0 0.000 0 0.000 0 0.000 0 0.000 0 /
0.000000 0.000000 0.000000 0.000000 0.0 0.0 0.0 0.0 0.0 0.0 0.000 0.000 0 0
0 0.0000 0.0000 0
generator data [ 2] id -----long_id----- st ---no-- reg_name prf qrf
ar zone pgen pmax pmin qgen qmax qmin mbase cmp_r cmp_x gen_r gen_x
hbus tbus date_in date_out pid N
99999 "INFINITE " 500.00 "1 " " " : 1 99999 "INFINITE " 500.00
1.000000 1.000000 1 1 -297.909180 999.000000 -999.000000 -12.398713 999.000000 -
999.000000 999.0000 0.000 0.000 0.000 0.007 0 " " 0.00 0 " " 0.00
400101 391231 0 1 /
0.0000 0.0000 1.0000 0 1.000 0 0.000 0 0.000 0 0.000 0 0.000 0 0.000 0 0.000
0 0 0 0 0 0 0 999.0 0 0 0.000000
99401 " TEST_G1 " 0.32 "1 " " " : 1 99101 " TEST_02 " 34.50
1.000000 1.000000 99 999 302.999786 0.000000 0.000000 61.526466 61.526699 -
61.526699 337.4000 0.000 0.000 0.000 1000000.000 0 " " 0.00 0 " " 0.00
400101 391231 0 1 /
0.0000 0.0000 1.0000 0 1.000 0 0.000 0 0.000 0 0.000 0 0.000 0 0.000 0 0.000
0 0 0 0 0 31 0 0.0 0 0 0.000000
svd data [ 1] id -----long_id----- st ty --no--- reg_name ar zone
g b min_c max_c vband bmin bmax date_in date_out pid N own part1 own part2 own
part3 own part4 M st
99101 " TEST_02 " 34.50 "1 " " " : 0 1 99101 " TEST_02 " 34.50
0 0 0.000000 0.362823 0.000000 0.840000 0.000000 0.000000 1.680000 400101
391231 0 0 0.0000 0 0.0000 0 0.0000 /
2 0.280000 2 0.140000 0 0.000000 0 0.000000 0 0.000000 0 0.000000 0 0.000000
0 0.000000 0 0.000000 0 0.000000 0
end
#

```

## APPENDIX-B

MATLAB SUBROUTINE TO CONVERT GEN-TIE DATA TO PER UNIT

```

clc
clear
format compact
ch=1;
while ch~=0
length=input('Line Length in miles=');
Rpos=input('Positive sequence Resistance(ohms/mile) =');
Xpos=input('Positive sequence Reactance(ohms/mile) =');
Xcpos=input('Positive sequence Capacitive Reactance(ohms/mile) =');

z=Rpos+j*Xpos;
y=0+j*(1/Xcpos);
B=imag(y);
Zc=sqrt(z/y);
gamma=sqrt(z*y);
Z_prime=Zc*sinh(gamma*length);
Y_prime=(2/Zc)*tanh(gamma*length/2);

Rprime=real(Z_prime);
Xprime=imag(Z_prime);
Gprime=real(Y_prime);
Bprime=imag(Y_prime);

Vbase=input('Base Voltage in kV=');
Sbase=input('Base MVA=');
Zbase=(Vbase^2)/Sbase;
Ybase=1/Zbase;
Bbase=Ybase;
R_p_u=Rprime/Zbase
X_p_u=Xprime/Zbase
G_p_u=Gprime/Ybase
B_p_u=(Bprime/2)/Ybase
disp('Do you want to make another calculation?')
ch=input('If YES Press 1, To Exit press 0: ');
end

```

## APPENDIX-C

### MATLAB SUBROUTINE FOR ZNPSO ALGORITHM

```

% Tuning of Solar PV model PI controller using ZNPSO
% Written by Sachin Soni
%
% Initialization
clear
clc
format compact
diary('data_REEC.txt')
% diary('data_REPC.txt')
n = 50;      % Maximum number of particles
itern = 10;  % Maximum number of iterations
m = 2;      % Dimension of the problem Kp and Ki
c1 =1.49;   % Acceleration constant C1
c2 =1.49;   % Acceleration constant C2
w =0.9;     % PSO Inertia
wmax=0.9; wmin=0.4; % Min-Max inertia range
fitness=0*ones(n, itern); % Initial fitness initialization Vector
R1 = rand(m, n); % Random number "R1" initialization
R2 = rand(m, n); % Random number "R2" initialization
current_fitness =0*ones(n,1);

%-----%
%   initializing swarm velocities and position %
%-----%
%Rmax=10;Rmin=0.0001; % Range for Initialization of Kp and Ki %
%current_position = 10*(rand(m, n));
%current_position = Rmin+((Rmax-Rmin)*(rand(m, n)));
Rmax_p=1;Rmin_p=0.001; % Range for Initialization of Kp and Ki %
Rmax_i=10;Rmin_i=1.00;
%current_position = 10*(rand(m, n));
current_position(1,:) = Rmin_p+((Rmax_p-Rmin_p)*(rand(1, n)));
current_position(2,:) = Rmin_i+((Rmax_i-Rmin_i)*(rand(1, n)));
current_position=[current_position(1,:);current_position(2,:)];
velocity = 0.3*randn(m, n) ;
local_best_position = current_position ;

%-----%
%   Evaluate initial population %
%-----%

for i = 1:n
    current_fitness(i) = znpsoc(current_position(:,i));
end

local_best_fitness = current_fitness ;
[global_best_fitness,g] = min(local_best_fitness) ;

```

```

for i=1:n
    globl_best_position(:,i) = local_best_position(:,g) ;
end

%-----%
% VELOCITY UPDATE %
%-----%

velocity=w*velocity+c1*(R1.*(local_best_position-current_position))+
c2*(R2.*(globl_best_position-current_position));

%-----%
% UPDATING SWARM POSITION %
%-----%

current_position = current_position + velocity ;

%-----%
% MAIN LOOP %
%-----%

%% Main Loop
iter = 0 ; % Iterations' counter
while ( iter < itern)
iter = iter + 1;
w=wmax-((wmax-wmin)*iter/n);
for i = 1:n
current_fitness(i) = znpsoc(current_position(:,i)) ;
end

for i = 1 : n
    if current_fitness(i) < local_best_fitness(i)
        local_best_fitness(i) = current_fitness(i);
        local_best_position(:,i) = current_position(:,i);
    end
end
[current_global_best_fitness,g] = min(local_best_fitness);

if current_global_best_fitness < global_best_fitness
    global_best_fitness = current_global_best_fitness;

    for i=1:n

```







## SUBROUTINE FOR FITNESS FUNCTION EVALUATION

```

function F = znps0(pid)
    % Track the output of optimizer to a signal of 1

    Kp = pid(1);
    Ki = pid(2);
    Kd = 0;

    % Compute function value
    simopt = simset('solver','ode45','SrcWorkspace','Current','DstWorkspace','Current'); %
Initialize sim options
[tout,xout,yout] = sim('optsim1',[0 1],simopt);
% Compute Rise Time
for i=1:length(ScopeData)
    if yout(i)>=0.1
        Tr1=tout(i);
        break
    else
        Tr1=0;
    end
end
for i=1:length(ScopeData)
    if yout(i)>=0.9
        Tr2=tout(i);
        break
    else
        Tr2=0;
    end
end
Tr=Tr2-Tr1;    % Rise Time

% Compute Settling-time
for i=1:length(ScopeData)
    if ((yout(end)-yout(i))<0.02)
        Ts=tout(i);
        break
    end
end

e=yout-1 ;    % compute the error
Ess=1-yout(end); % Compute Steady-State Error
Mp=max(yout)-1; % Compute System Overshoot
if ((Ess <=0.005) && (Mp<0.4) && (Tr>0) && (Kp>0) && (Ki>0))
    sprintf('Good Set of Values for Controller Gains is Kp= %3.4f, Ki= %3.4f',
pid(1),pid(2))

```

```
    sprintf('Mp = %3.4f, Ess = %3.4f, Tr = %3.4f, Ts = %3.4f', Mp, Ess, Tr, Ts)
end

beta=0.7;
%F=e2*beta+Mp*alpha;
F=(1-e2^(-beta))*(Mp+Ess)+(e2^-beta)*(Ts-Tr);
Eval_Value=1/F;
end
```

APPENDIX-D

REGC\_A AND REEC\_B MODEL PARAMETERS

```

# dynamics data written Fri Dec 27 18:33:23 2013
# from saved case filename [C:\Users\sachin\Desktop\PSLFwork\model.dyd]
# title
# MODEL FOR 90MW Solar PV PLANT WITH REGC_A and REEC_B models
# prepared by SACHIN SONI
lodrep
#
models
# REGC_A AND REEC_B MODEL PARAMETERS
#-----
regc_a    1 "PVGEN"  0.32 "1" : #9 mva=90.000 "lvplsw" 0.000000 "rrpwr" 1.2000 "brkpt"
0.900000 "zerox" 0.900000 "lvpl1" 1.100 "vtmax" 1.1000 "lvpnt1" 0.800000 "lvpnt0"
0.050000 "qmin" -1.3000 "accel" 0.700000 "tg" 0.02000 "tfltr" 0.020000 "iqrmax" 99.0000
"iqrmin" -99.0000 "xe" 0.0
reec_b    1 " PVGEN "  0.32 "1" : #9 mva=90.000 "vdip" 0.9000 "vup" 1.0172 "trv" 0.00
"dbd1" 0.000000 "dbd2" -0.00000 "kqv" 0.0000 "iqh1" 1.0000 "iq11" -1.00 "vref0" 0.0000 "tp"
0.0500000 "qmax" 0.4358 "qmin" -0.4358 "vmax" 1.1000 "vmin" 0.900000 "kqp" 0.0440 "kqi"
2.1806 "kvp" 12.60 "kvi" 302.40 "tiq" 0.020000 "dpmax" 99.0000 "dpmin" -99.0000 "pmax"
1.000000 "pmin" 0.0 "imax" 1.1 "tpord" 0.020000 "pfflag" 1.000000 "vflag" 1.000000 "qflag"
1.0 "pqflag" 0.000000
gencls    5 "INFINITE" 500.00 "1" : #9 mva=1000.0000 "h" 999.0000 "d" 0.0000 "ra"
0.0002 "lppd" 0.0072 "rcomp" 0.0000 "xcomp" 0.0000 "accel" 0.0000
# MEASURING INSTRUMENTS
#-----
vmetr     3 " TEST_T    " 34.50 "1" : #9 "tf" 0.0
vmetr     4 " TEST_SUB  " 500.00 "1" : #9 "tf" 0.0
imetr     3 " TEST_T    " 34.50 "1" 4 " TEST_SUB" 500 "1" 1 : #9 "tf" 0.0
imetr     4 " TEST_SUB  " 500.50 "1" 5 " TEST_SUB" 500 "1" 1 : #9 "tf" 0.0
fmetr     4 " TEST_SUB  " 500.00 "1" : #9 "tf" 0.0

```

```

# dynamics data written Sun Dec 29 00:15:21 2013
# from saved case filename [C:\Users\sachin\Desktop\PSLFwork\model1.dyd]
# title
# MODEL FOR 90MW Solar PV PLANT WITH REGC_A, REEC_B and REPC_A models
# prepared by SACHIN SONI
Lodrep
#
models
# REGC_A, REEC_B and REPC_A MODEL PARAMETERS
#-----
regc_a    1 " PVGEN " 0.32 "1" : #9 mva=90.000 "lvplsw" 0.000000 "rrpwr" 1.2000
"brkpt" 0.900000 "zerox" 0.900000 "lvpl1" 1.100 "vtmax" 1.1000 "lvpnt1" 0.800000 "lvpnt0"
0.050000 "qmin" -1.3000 "accel" 0.700000 "tg" 0.02000 "tfltr" 0.020000 "iqrmax" 99.0000
"iqrmin" -99.0000 "xe" 0.0
reec_b    1 " PVGEN " 0.32 "1" : #9 mva=90.000 "vdip" 0.9000 "vup" 1.0172 "trv" 0.00
"dbd1" 0.000000 "dbd2" -0.00000 "kqv" 0.0000 "iqh1" 1.0000 "iq11" -1.00 "vref0" 0.0000 "tp"
0.0500000 "qmax" 0.4358 "qmin" -0.4358 "vmax" 1.1000 "vmin" 0.900000 "kqp" 0.0440 "kqi"
2.1806 "kvp" 12.60 "kvi" 302.40 "tiq" 0.020000 "dpmax" 99.0000 "dpmin" -99.0000 "pmax"
1.000000 "pmin" 0.0 "imax" 1.1 "tpord" 0.020000 "pfflag" 0.000000 "vflag" 1.000000 "qflag"
1.0 "pqflag" 0.000000
repc_a    1 " PVGEN " 0.32 "1" 4 "TEST_SUB" 500.00 : #9 mva=90.000 "tfltr" 0.8 "kp"
33.6094 "ki" 792.0652 "tft" 0.000 "tfv" 0.0424 "refflg" 1.0000 "vfrz" 0.700 "rc" 0.0000 "xc"
0.0000 "kc" 1.0000 "vcmpflg" 1.0000 "emax" 0.1000 "emin" -0.1000 "dbd" 0.0000 "qmax"
0.4358 "qmin" -0.4358 "kpg" 10.0000 "kig" 0.1000 "tp" 0.02 "fdbd1" -0.0000 "fdbd2" 0.0000
"femax" 0.1000 "femin" -0.1000 "pmax" 1.000 "pmin" 0.000 "tlag" 0.0200 "ddn" 0.0000 "dup"
0.0000 "frqflg" 0.0000
gencls    5 "INFINITE " 500.00 "1" : #9 mva=1000.0000 "h" 999.0000 "d" 0.0000 "ra"
0.0002 "lppd" 0.0072 "rcomp" 0.0000 "xcomp" 0.0000 "accel" 0.0000
# MEASURING INSTRUMENTS
#-----
vmetr     3 "TEST_T " 34.50 "1 " : #9 "tf" 0.0
vmetr     4 " TEST_SUB " 500.00 "1 " : #9 "tf" 0.0
imetr     3 " TEST_T " 34.50 "1 " 4 " TEST_SUB" 500 "1" 1 : #9 "tf" 0.0
imetr     4 " TEST_SUB " 500.50 "1 " 5 " TEST_SUB" 500 "1" 1 : #9 "tf" 0.0
fmetr     4 " TEST_SUB " 500.00 "1 " : #9 "tf" 0.0

```

Sachin Soni

Master of Science Thesis

Required revisions

1. In places where plots of dynamic response are required:

Revise time scales to focus on the active part of the events. For example figure 4.11 does not need to show the full second of leading and the last two seconds of trailing steady operation.

Reduce the thickness of the plot lines so that the different traces in the figures are clearly visible and distinguishable from one another

This applies to figures 4.11-13 5.17-19 5.2-28 3-18

The adjustment of plot line thickness could also be applied to figures 3.14-17

2. On pages 105,106 the statement that "there is randomness, though very small" must be corrected. It must be recognized that there is a very significant variation in the values "discovered" for  $K_{qi}$  and commentary must address this fact.
3. In reference to the PSE method - it must be stated how the PSO population is initialized:  
for example -
  - x vector is seeded with random values within the feasible range
  - pbest and qbest are seeded with random values and this leads to random initial values of velocities
4. It should be stated explicitly that the order of the x vector in the PSO, as used, is two and that the members are estimates of the controller proportional and integral gains

To: G. Karady, V. Vittal  
From: J. Undrill

I have reviewed the changes made by Mr. Soni in his thesis, which is attached. I find them acceptable and I agree that the requirement for revisions has been met.

J. Undrill  
17 April 2014